Abstract book

15th Biometal

AUGUST 21 TO 27, 2023

Grand Hôtel San Michele, Cetraro, CS, Italy

BIODEGRADABLE METALS

15th Biometal

AUGUST 21 TO 27, 2023

Grand Hôtel San Michele, Cetraro, CS, Italy

Symposium Co – chairs:

Diego Mantovani
Laval University, Canada

Yufeng Zheng
Peking University, China

Frank Witte
Berlin Charité, Germany

Mark Staiger
University of Catenbury, New Zeland

Abstract book committee:

Vinicius Sales
Laval University, Canada

Jasmine Lebleu
Conferium

Masoud Shekargoftar
Laval University, Canada

Maria Laura Gatto
Università Politecnica delle Marche, Italy

Quang Nguyen Cao
Laval University, Canada

Abdelhakim Cherqaoui
Laval University, Canada

UNIVERSITÉ LAVAL

Conferium
Conferences . Events . Service

innosys
Medical and Smart Solution

KeAi
CHINESE ROOTS GLOBAL IMPACT

CHARITÉ
UNIVERSITÄTSMEDIZIN BERLIN

UC UNIVERSITY OF CANTERBURY
Te Whare Wānanga o Waitaha
CHRISTCHURCH NEW ZEALAND

PEKING UNIVERSITY 1898

TÜV SÜD

Informations about the abstract book, please contact: video5@ulaval.ca

Workshop

Tuesday, August 22nd, 2023

additive manufacturing anatomical magnesium alloy prosthesis for repairing periarticular fractures: from animal experiments to clinical studies

Yun Tian[1], Bingchuan Liu[1],Zhengguang Wang[1],Chaoxin Wang[1], Peng Wen[2], Yufeng Zheng[3]

[1] Department of Orthopedics, Peking University Third Hospital, Beijing, China.[2]Department of Mechanical Engineering, Tsinghua University, Beijing. [3]Department of Materials Science and Engineering, Peking University, Beijing

INTRODUCTION: Periarticular fractures with bone defects are common and complicated diseases. Additive manufacturing of magnesium alloy prostheses (AMMAP) provides the feasibility of realizing bone defect prostheses with personalized and degradable functions. In this study, we observed the efficacy of AMMAP from in vivo tests to clinical trials of human periarticular bone defect repair.

METHODS: (1) Diamond units were adopted to design porous scaffolds in anatomical morphology matching. Improving corrosion resistance of AMMAP by high-temperature oxidation. (2) 45 Male New Zealand white rabbits 6-month-old were enrolled. Design a model for repairing femoral condylar bone defects and fill it with AMMAP for repair. (3) Patients with periarticular fractures and bone defects were enrolled in the study, and AMMAP were used for internal support combined with titanium plate fixation to repair the fracture and bone defects.

RESULTS: High temperature oxidation treatment can enhance the corrosion resistance of AMMAP. In the repair of the defect model of rabbit femoral condylar, the internal supported magnesium alloy prosthesis and titanium plate support work together to achieve fracture healing. Without the fixation screw penetrating the prosthesis, the prosthesis can maintain a support time of more than 3 months. In the study of 15 patients with human periarticular bone defects, all patients achieved bone healing. Hydrogen can be seen to precipitate in soft tissues, increasing local swelling in the early stages, and hydrogen can be absorbed after about 2 months. Magnesium alloy prostheses can maintain a support time of over 2 months.

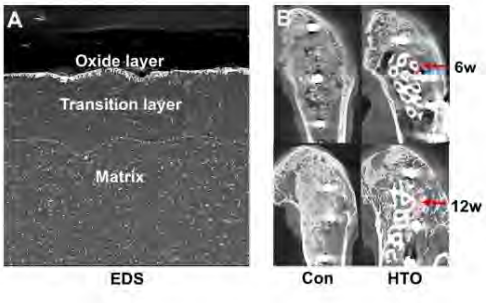

Fig. 1: Improving corrosion resistance of AMMAP in vivo after high temperature oxidation treatment:(A) Characterization at the cross sections after high temperature oxidation treatment. (B) Micro-CT scanning at 6 and 12 weeks after surgery showed the degradation of implantation restoration with bone regeneration.

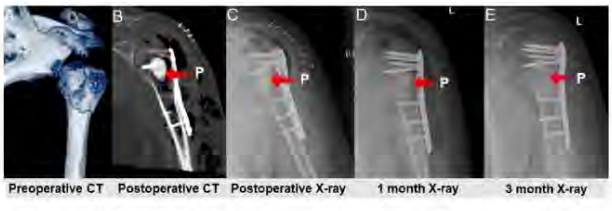

Fig. 2: AMMAP for the treatment of proximal humeral fractures.(A) Preoperative 3D CT reconstruction. (B) Postoperative CT scans.(C) Postoperative X-ray image (1st day).(D) Postoperative X-ray image (1st month).(E) Postoperative X-ray image (3th month).

DISCUSSION & CONCLUSIONS: Periarticular fractures and bone defects are complex injuries, and the previous plate tension band fixation model has shortcomings in biomechanics. The use of AMMAP can achieve longitudinal conduction at the center of the fracture area, which is more in line with the mechanical conduction characteristics of bone structure. Magnesium alloy porous prostheses can provide overall joint mechanical support for the repair of joint structures throughout the whole bone healing cycle. In summary, AMMAP internal support has good application prospects.

REFERENCES: [1] Jinge Liu, Bingchun Liu, Shuyuan Min, et al. Biodegradable magnesium alloy WE43 porous scaffolds fabricated by laser powder bed fusion for orthopedic applications: Process optimization, in vitro and in vivo investigation, *Bioactive Materials*. 2022. [3] Shuyuan Min, Chaoxin Wang, Bingchuan Liu, et al. The biological properties of 3d-printed degradable magnesium alloy WE43 porous scaffolds via the oxidative heat strategy, *International Journal of Bioprinting*. 2023.

15th Biometal
AUGUST 21 TO 27, 2023
Grand Hôtel San Michele, Cetraro, CS, Italy

Post-Pandemic Challenges in Biomaterial Research at KIST: Navigating the Path Forward

Chris Hyung-Seop Han[1,2,*]

[1] *Center for Biomaterials, Korea Insititute of Science and Technology (KIST), Republic of Korea*
[2] *Divison of Bio-Medical Science & Technology, KIST School, Republic of Korea*

ABSTRACT: This talk will shed light on the dynamic landscape of post-pandemic biomaterial research at KIST, emphasizing the challenges and opportunities that lie ahead. By addressing these challenges head-on and fostering interdisciplinary collaboration, KIST is poised to drive innovation and contribute significantly to the advancement of biomaterials that will shape the future of healthcare in a post-pandemic world.

OVERVIEW: The global COVID-19 pandemic has brought to light the critical importance of advancing biomaterial research to address emerging healthcare challenges. This abstract explores the post-pandemic landscape of biomaterial research at the Korea Institute of Science and Technology (KIST) and outlines the key challenges that researchers face in this rapidly evolving field.

In the wake of the pandemic, biomaterial research has taken on renewed significance, as it underpins critical areas such as vaccine development, diagnostic tools, and therapeutic interventions. Researchers at KIST have been at the forefront of these efforts, employing innovative strategies to design and engineer biomaterials that can meet the demands of the changing healthcare landscape.

This talk delves into the multifaceted challenges that biomaterial researchers at KIST must now address. These challenges encompass both scientific and translational aspects, including the need for accelerated development of adaptable biomaterial platforms, the optimization of drug delivery systems, and the integration of artificial intelligence and data-driven approaches into biomaterial design. Additionally, ethical and regulatory considerations gain prominence as new biomaterial solutions emerge, requiring a balance between rapid deployment and comprehensive safety assessment.

Furthermore, the talk will highlight the collaborative nature of post-pandemic biomaterial research. With the convergence of disciplines such as material science, biotechnology, and nanotechnology, KIST researchers are forging partnerships with academia, industry, and healthcare providers to create holistic solutions that encompass design, synthesis, testing, and clinical implementation.

ACKNOWLEDGEMENTS: This work was supported by the National Research Foundation of Korea (NRF) grant funded by the Korea government (MSIT) (No.2022M3H4A1A04085301) and (No. 2021K1A3A1A74095)

Development of reactive oxygen species (ROS) scavenging material for ischemia-reperfusion injury (IRI) therapy

Hee-Young Kwon[1,2], Hee Jae Hwang[1], Hyeok Kim[1], Hojeong Jeon[1,2], Hyung-Seop Han[1*]

[1]*Biomaterials Research Center, Biomedical Research Division, Korea Institute of Science and Technology (KIST), Seoul, Republic of Korea*

[2]*KU-KIST Graduate School of Converging Science and Technology, Korea University, Seoul, Republic of Korea*

INTRODUCTION: The scavenging of reactive oxygen species (ROS) is the most crucial therapeutic strategy for preventing damage in ischemia reperfusion injury (IRI). Among many ROS scavenging materials, Prussian blue (PB) have not only high scavenging effect, but also possesses high utility as a biomaterial due to its certificated biocompatibility. In conjugation with ROS scavenging of PB, magnesium can contribute to a synergistic effect in IRI treatment by preserving vascular and biological activity on cellular metabolism. Herein, we propose a development of Prussian blue-Magnesium composite, capable of scavenging ROS and preserving blood vessel integrity for IRI treatment.

METHODS: The Prussian blue nanoparticles were synthesized through a precipitation method. To inhibit the reaction between PB and Magnesium hydroxide($Mg(OH)_2$) and improve dispersity, a polydopamine(PDA) coating was applied to $Mg(OH)_2$ in sonication assisted condition. Finally, a desired amounts of PB and PDA coated $Mg(OH)_2$ were bonded together to fabricate final product. Assessment of ROS scavenging activity and magnesium ion release was evaluated with a commercial assay kit. Cell viability was assessed with a CCK-8 kit and ROS level was evaluated using a DCF-DA probe. Animal IRI model was established with mouse and cardiovascular function was examined with the M-mode echocardiography.

RESULTS: The synthesized Prussian blue formed small particles with a diameter of 5-10 nm. PDA coating $Mg(OH)_2$ was successfully accomplished and coating layer have a thickness within 10 nm. Then we performed morphology analysis of the PB-Mg composite with varying ratio. Size change was observed based on PB content and as the PB content increase, the Fe/Mg atomic ratio also increased. Magnesium release decrease with the increase of PB content and slightly higher in acidic condition than neutral pH. The PB-Mg composite showed negligible cytotoxicity, and both the intrinsic ROS scavenging property of the composite and in vitro ROS assay exhibited a higher efficiency of the composite compared to PB alone.

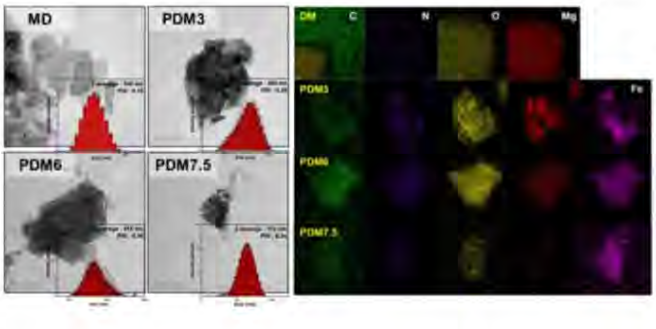

Fig. 1: Morphology, size and composition analysis of PB-Mg composite.

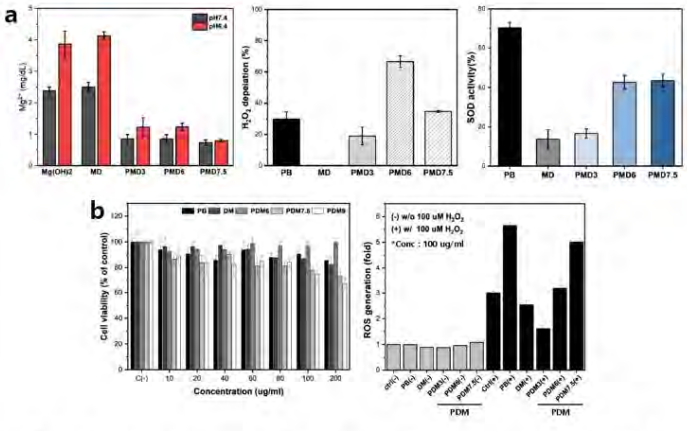

Fig. 2: (a) Magnesium release evaluation and ROS scavenging assessment, (b) Cell viability and in-vitro ROS assay of PB-Mg composite..

DISCUSSION & CONCLUSIONS: We developed PB-Mg composite for effective ROS scavenging and vascular protection for the treatment of ischemia-reperfusion injury. In terms of ROS scavenging efficiency, at certain ration of PB-Mg composite exhibited a higher efficacy than PB alone. Therefore, along with the biological activity of magnesium, we expect a greater therapeutic effect of PB-Mg composite in IRI treatment.

REFERENCES: [1]T. Uemura and S. Kitagawa (2003) JACS, **125**, 7814-7815. [2] W. Zhang et al (2016), JACS, **138**, 5860-5865, [3]H-S Han et al (2020), Adv. Sci, **7**, 2000800

ACKNOWLEDGEMENTS:

R&D and Commercialization of INNOSYS for Orthopaedic Medical Device

HC Jung[1], DK Koo[1], HJ Roh[1], HJ Jeon[2], YC Kim[2]

[1] *R&D Division, INNOSYS Co., Ltd., Korea.* [2] *Center for Biomaterials, Biomedical Research Division, Korea Institute of Science and Technology, Korea*

INTRODUCTION: U&i Corporation of Korea, a leading biodegradable magnesium alloy-based implant manufacturer, has changed the name to Innosys Co., Ltd. in 2022. Currently, although it had been delayed a lot due to Covid-19, Innosys Co., Ltd.is conducting clinical trials about resomet^{TM}, including the biodegradable magnesium bone screw and k-wire, in China. This presentation will introduce various research and commercialization of Innosys Co., Ltd. in the field of orthopedic medical devices, including the development and commercialization of next-generation biodegradable magnesium alloys and the R&D and commercialization for spin cage of new concepts coated HA.

Nano-Gel-Nano vaccines for immune modulation to treat cancers

Sung-Hoon Kim[1,2], Young-Min Kim[1,2*]

[1] *Center for Biomaterials, Korea Institute of Science and Technology, Seoul, Republic of Korea.* [2] *Division of Bio-Medical Science and Technology, University of Science and Technology, Seoul, Republic of Korea*

INTRODUCTION: Cancer immunotherapies have low response rates due to immunosuppressive tumor microenvironments (TMEs). To alter unfavorable TMEs, supplementing tumor-associated antigens and stimulating the immune cells in the target sites are indispensable in eliciting antitumoral immune responses. Herein, we propose a localized and multi-target nano-gel-nano system that 1) can load both chemicals and adjuvants by simple mixing, 2) transform from solution to gel after injection for local and long-term existence, 3) release the nanocomplexes from the hydrogel which deliver drugs to cancer and immune cells via active and passive targeting, respectively, over a long term.

METHODS: The polymer for the nano-gel-nano system was synthesized. Isoleucine ethyl ester, amino ethyl methacrylate, and amino polyethylene glycol (AMPEG) were added slowly to poly(dichlorophosphazene) in dry tetrahydrofuran including trimethylamine. And RC peptides were conjugated in dimethylformamide.

RESULTS: The polymer formed nano-sized complexes with drugs via ionic interaction at low temperatures (Fig. 1a,b). The polymer/drug solution showed temperature-dependent sol-gel transition and released nano complexes from the hydrogel was also confirmed by TEM (Fig. 1c,d). Besides, the maintenance of hydrogel after injection was observed for 3 weeks with drugs (Fig. 1e).

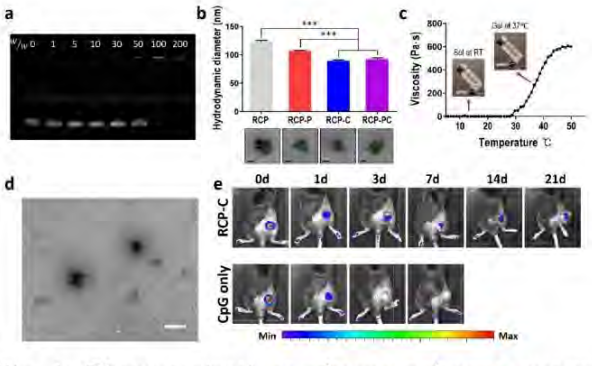

*Fig. 1: Characterizations of nano-gel-nano system. a) Gel retardation assay of polymer/drug complexes as a function of w/w ratios. b) Sizes and morphologies of nanocomplexes. c) Temperature-dependent sol-gel transition of 10 wt % aqueous polymer solutions. d) Transmission electron microscope (TEM) image of dissociated nanocomplexes from hydrogel at day 7 e) Images showing drug retention within the gel hydrogel of 10% and drug alone using FITC-tagged drug in a tumor-bearing mouse. ***p < 0.001.*

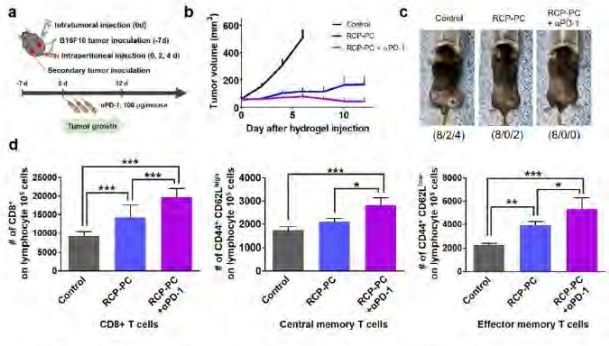

Fig. 2: Generation of a systemic antitumor immune response and inhibition of recurrence by the combination of the polymer/drug and αPD-1.

After administration of the nano-gel-nano system to tumor-bearing mice, whether local immunogenic responses in primary tumors could elicit systemic therapeutic effects on distant tumors was checked. Regressed secondary tumor formation was observed in the experimental group and it was related to increased memory T cells (Fig. 2). It suggested therapeutic efficacy of the system induces long-lasting immune responses by maintaining the activity of memory T cells against tumors

DISCUSSION & CONCLUSIONS: We developed the nano-gel-nano system for effective *in situ* cancer vaccines for extended periods with a single intratumoral administration and it could be applied to various cancers as a patient-specific therapy.

ZnP-coated Zn alloy membrane with excellent mechanical, antibacterial, biocompatible, and osteogenesis properties for biomedical applications

Cuie Wen[1]*, Jixing Lin[2], Xian Tong[2], Yue Han[2], Li Zhu[2], Runqi Zhou[2], Zhiqiang Lin[2], Hongning Wang[2], Shengbin Huang[2], Jianfeng Ma[2], and Yuncang Li[1]

[1] *School of Engineering, RMIT University, Melbourne, Victoria 3001, Australia.*

[2] *School and Hospital of Stomatology, Wenzhou Medical University, Wenzhou 325027, China.*

INTRODUCTION: Guided bone regeneration (GBR) technology typically involves placing a membrane for bone regeneration between the hard and soft tissues of the oral cavity, preventing fibroblasts from growing into the bone defect area, avoiding the interference of fibroblasts in the osteogenesis process, and achieving bone tissue repair and bone expansion in the operation area and successful aesthetic implant restoration. In this study, a Zn–Cu–Ti alloy (denoted as ZCT hereafter) membrane with a zinc-phosphate (ZnP) coating is developed for oral GBR membrane applications.

METHODS: As-cast (AC) ZCT alloy ingot was prepared by casting. Subsequently, 10 mm thick ZCT plates were cut from the AC ingots using electrical discharge machining (EDM) to prepare 0.2 mm thickness membranes by hot rolling in two steps: the plates were hot-rolled (HR) to a thickness of 1 mm at a 1 mm reduction per pass using a two-high cogging mill and then hot-rolled to a final thickness of 0.2 mm at a 0.2 mm reduction per pass by a six-high cluster mill after being pre-heated at 250 °C for 5 min.

The ZCT membrane samples were ground with SiC papers up to 2000-grit and washed with ethanol and deionized water for surface coating. ZnP coating on the ZCT membrane samples was performed by immersing the membranes into a phosphating solution for 5 min at room temperature. The ZnP-coated membrane (denoted as ZnP-coated ZCT hereafter) samples were then rinsing using deionized water and drying in air.

Disc samples with 8 mm diameter and 0.2 mm thickness were cut from the membranes using EDM and tested using electrochemical, immersion, surface contact angle testing, nano-scratch testing, alkaline phosphatase (ALP) analysis, and assessments of cytotoxicity and expression of osteogenic and mitochondrial dynamics genes.

RESULTS: The ZnP-coated ZCT membrane is promising for biodegradable GBR membrane applications for oral bone defect repair due to its unique combination of material properties including high strength-ductility, mechanical stability, suitable degradation rate, good antibacterial ability, cytocompatibility, and osteogenesis and contour shaping ability, good cytocompatibility, osteogenetic effect, and osteoinductivity (see Fig. 1).

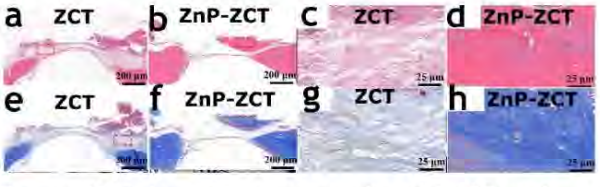

Fig. 1: Histological micrographs with HE and Masson staining of rat skull regeneration in calvarial defects of ZCT and ZnP-coated ZCT after 3 months of surgery.

DISCUSSION & CONCLUSIONS: The microstructure of the ZCT membrane mainly consisted of an α-Zn matrix phase and the second phases of $CuZn_5$ and Cu_2TiZn_{22} that are uniformly streamlined parallel to the rolling direction. Surface conversion phosphating produced a homogeneous and dense ZnP coating with a thickness of ~3.3 μm, and the ZnP-coated ZCT membrane showed significantly increased hydrophilicity with the water contact angle decreased from ~78.7° to ~21.9°. The ZnP-coated ZCT sample exhibited the highest σ_{ys} of 264 MPa, σ_{uts} of 312 MPa, and ε (elongation) of 36.0%. The ZnP coating possessed a good bond strength, deformation resistance, and healing effect, meeting the contour shaping requirements of the GBR membrane. The rat skull defect repair model confirmed the complete biosafety and considerable osteogenesis performance of the ZnP-coated ZCT in vivo, better than those of the ZCT. The ZnP-coated ZCT showed significantly promoting effect on bone defect repairing.

ACKNOWLEDGEMENTS: This work was supported by the Zhejiang Public Welfare Technology Application Research Project of China (No. LGF22H140008). CW and YL also acknowledge the financial support for this research by the Australian Research Council (ARC) through the Discovery Project DP210101862.

Current status of R&D and regulatory science on biodegradable metal medical devices in China

Yufeng Zheng[1] Deyuan Zhang[2] Xiaonong Zhang[3] Lei Tian[4]

[1] *School of Materials Science and Engineering, Peking University, Beijing 100871, China*
[2] R&D Center, *Biotyx Medical (Shenzhen) Co. Ltd., Shenzhen 518109, China*
[3] *Suzhou Origin Medical Technology Co. Ltd., Jiangsu 215513, China*
4 School of Stomatology, The Fourth Military Medical University, Xi'an 710032, China

In this paper, we would like to take three examples to illustrate the R&D situation on the medical devices using biodegradable metals.

For Mg-based biodegradable metals, Suzhou Origin Medical Technology Co. Ltd. successfully develops a biodegradable high-purity (99.98%) magnesium (HP-Mg) ligation clip for general surgery. The HP-Mg ligation clips possess excellent clamping functions, effectively avoiding haemorrhage, tissue fluid leakage, clip loosening and slipping. The complete degradation period was about 1 year in vivo, preventing permanent foreign body retention. Single-blind clinical trials involve 156 patient cases of laparoscopic cholecystectomy. The follow-up validates that the HP-Mg ligation clip does not cause Mg^{2+} or H_2 accumulation in major organs, pH value deviation of local tissues, severe local and systemic inflammation reactions, and artefacts in an imaging test. The NMPA (China) registration submission was received on Sep 2022 and will be approved for registration as predicted at the end of 2023.

For Fe-based biodegradable metals, IBS employs Fe-0.05%N as its backbone, with PDLLA coatings to control not only drug release, but also to create a local low pH environment, in which iron may corrode fast into soluble ions, and zinc layer between backbone and PDLLA coatings to delay the onset of iron corrosion as sacrificed anode. FIH trials of coronary and pediatric pulmonary stenoses enrolled first patient in 2018 in China and Malaysia, while first enrollment of peripheral artery was in 2020 in China. More than 1100 implantations of iron bioresorbable scaffolds were completed in China, Europe and USA (via compassionate use approval from FDA) with 100% success rate. TLF was comparable with its control Xience so far. Full endothelialization was achieved in six months after implantation, then scaffolded lumen became larger and larger, which is quite different from other DES or BRS, maybe related to the hemosiderin movement to the adventitia. IBS Angel™ for pediatric use has obtained its CE MDR marking in Feb, 2023, and CE applications of IBS™ for coronary use and IBS Titan™ for peripheral use have been submitted.

For Zn-based biodegradable metals, a multicenter randomized controlled trail was designed to evaluate the efficacy, safety and biodegradability of a novel biodegradable Zn–Mg– Fe alloy maxillofacial osteosynthesis system which is produced by HuaXiang Meditech. There are seven maxillofacial surgical centers attended this clinical trial and 150 patients with mild facial fracture were planned to be enrolled in total. The patient was randomly assigned to experimental group or control group which was treated by traditional titanium internal fixation system (Depuy Synthes, USA). From October 2021 till now, there are 78 patients completed the surgery in total, and all patients gained good bone healing without infections. There were no severe adverse events occurred and the concentration of blood metal ions were stable before and after surgery. The efficacy and safety of Zn alloy maxillofacial osteosynthesis system were approved, while the degradability was still on study.

15th Biometal
AUGUST 21 TO 27, 2023
Grand Hôtel San Michele, Cetraro, CS, Italy

Direct cellular penetration of supramolecular nanomachine via molecular movements

Soyeong Jin[1], Dagyeong Guk[1], Hyemin Park[1], Youngdo Jeong[1, 2,*]

[1] *Center for Advacned Biomolecular Recognition, Korea Institute of Science and Technology, Seoul 02792, Republic of Korea*

[2] *Department of HY-KIST Bio-convergence, Hanyang University, Seoul 04763, Republic of Korea*

INTRODUCTION: Proteins, one type of biological nanomachines, can activate their function through conformational change induced by supramolecular recognition in biological processes. The development of artificial nanomachines that mimic the biological functions for potential application as therapeutics is emerging. However, the development of artificial nanomachines for therapeutic purposes is still limited to the lower hierarchical level of the molecular components.

RESULTS & DISCUSSION: We fabricated an artificial nanomachine in which actuatable molecular machines are integrated into a hierarchical nanomaterial in response to external stimuli to regulate biological functions.[1] As a nanomachine, protein-sized gold nanoparticle nanomachine is coated with ligand layers as machinery components, allowing direct penetration of the nanomachine over the cellular membrane to damage intracellular organelles due to their folding/unfolding motion response to the cellular environment. (Fig. 1) Furthermore, the pH-responsive latch molecules, acting as a switch, can control the conformational changes of the molecular machineries, initiating the selective apoptosis of cancer cells. This approach based on the mechanical motion of molecular components on a hierarchical nanocluster might act as an effective platform for biomimetic nanomachines.

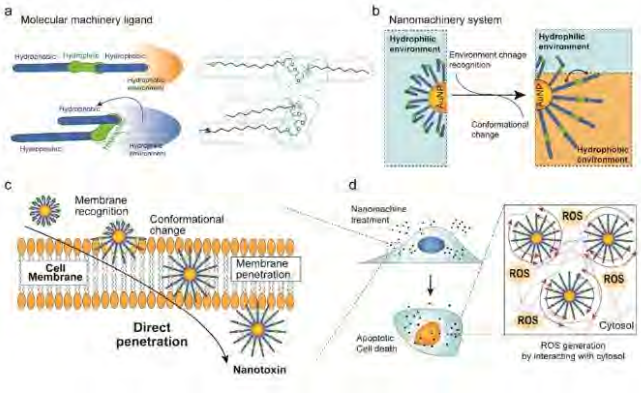

Fig. 1: Schematic description of the developed nanomachine. (a) Chemical structure of the actuatable ligand and its conformational change (b) The nanomachine comprises an inorganic core to anchor the movement of the ligands and the actuatable ligands. (c) The nanomachine can directly penetrate the cell membrane by the conformational change of their ligands. (d) After uptaken by cells, the hydrophobic alkyl end group pulled out to the outer surface can interact with cellular components, disrupting their functions.

CONCLUSIONS: In summary, we have developed a synthetic nanomachine that uses a motionable molecular ligand anchored on a gold nanoparticle. The molecules undergo folding and unfolding, allowing the nanomachine to permeate into the cytosol and disrupt cellular functions, resulting in apoptosis. The toxicity can be switched on and off as a function of pH using pH-responsive latch molecules. This platform has potential for therapeutic applications, as it can protect healthy cells at pH 7.4 and perform nanoscale movements that can be controlled intracellularly. Our system integrates molecular machines for nanoscale motion and nanomaterials as support, providing a new platform for the development of therapeutic nanomachinery and pharmacological treatments based on the mechanical movement of synthetic tools.

REFERENCES: [1] Y. Jeong et al (2022) *J Am Chem Soc* **144**:5503-16.

ACKNOWLEDGEMENTS: This research was supported by the National Research Foundation of Korea (2023R1A2c1004389) and the KIST Institutional program (2E32311, 2Z06985, and 2E3232N).

Metals

Wednesday, August 23rd, 2023

A novel biodegradable high nitrogen iron alloy

Ke Yang, Qingchuan Wang, Sihan Lu, Lili Tan

Institute of Metal Research, Chinese Academy of Sciences, Shenyang, China

INTRODUCTION: Among biodegradable metal materials, iron (Fe) alloys have optimal mechanical properties, and thus exhibit great potential in the applications of biodegradable stents [1]. However, slow degradation rate and local corrosion are the bottleneck problems which limit the development of Fe alloys and have not been solved well [2]. Based on these, a novel FeMnN austenitic alloy has been developed to simultaneously obtain excellent mechanical properties, degradation performance and local corrosion resistance.

METHODS: The experimental materials were Fe-30Mn-xN (x=0.3, 0.6 wt.%) austenitic alloys, and Fe-30Mn was selected as the comparison. Tensile, XRD, SEM, EBSD, TEM, immersion and animal tests were performed to examine microstructure, mechanical properties, degradation rate and biocompatibility of the FeMnN alloy.

RESULTS: The strength and plasticity of FeMnN alloy could be significantly improved with increase of the N content. The degradation rate of FeMnN alloy was enhanced obviously with increase of the N content, while the local corrosion was suppressed. Both blood and pathological results showed good biocompatibility of the high-N Fe alloy [3].

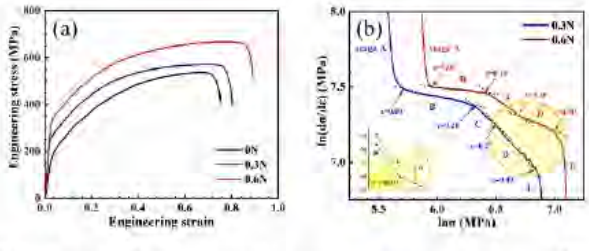

Fig. 1: (a) Engineering stress-strain curves; (b) ln(dσ/dε)-lnσ curves of FeMnN alloys

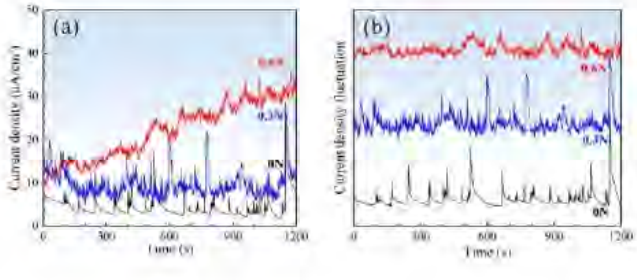

Fig. 2: Current density (a) and relative fluctuations (b) of potentiostatic polarization of FeMnN alloy in Hank's solution

DISCUSSION & CONCLUSIONS: The improvement of strength for FeMnN alloy resulted from the solid solution strengthening effect of N, the increase in twin number and the decrease in twin size, and the enhancement of plasticity mainly originated from the additional work-hardening contributed by ultrafine nano-twins. N alloying could enhance the degradation rate and local corrosion resistance of FeMnN alloy through forming [FeN] clusters. [FeN] clusters are more likely to have non-redox reactions with H_2O to increase the degradation rate. The reaction product NH_3 can consume H ions to form NH_4^+, thus improving the local corrosion resistance. The novel biodegradable high-N Fe alloy has excellent comprehensive performance and great application potential for biodegradable vascular stents and anastomosis nails.

REFERENCES: [1] M. Schinhammer, P. Steiger, F. Moszner, et al. Materials Science and Engineering: C 33(4) (2013) 1882-1893. [2] E. Mouzou, C. Paternoster, R. Tolouei, et al. Materials Science and Engineering: C 61 (2016) 564-573. [3] S. Lu, Q. Wang, Y. Zhang, et al. Journal of Materials Science & Technology 152 (2023) 94-99.

ACKNOWLEDGEMENTS: This work was financially supported by the National Natural Science Foundation of China (Grant No. 51801220).

Iron-molybdenum composite wires for thin vascular devices

Adam J. Griebel, Jeremy E. Schaffer
Fort Wayne Metals, Fort Wayne, IN, USA

INTRODUCTION: Neurovascular devices like flow diverters require very thin materials and are often comprised of wires with diameters of 20-30 microns which are braided together and deployed in a self-expanding manner. Absorbable versions of such devices could improve subsequent imaging and interventional procedures[1]. Selection of a material with the appropriate combination of strength, elasticity, radiopacity, and corrosion rate is challenging. Alloys of magnesium, zinc, iron, and even molybdenum[2-4] have various advantages and weaknesses across these criteria.

This work proposes and investigates a new patented[5,6] composite concept combining an iron-manganese-nitrogen alloy[7] (FeMnN) with one or more inner filaments of molybdenum (Mo). These constructs provide for high strength wires with high bending elasticity suitable for self-expanding stents and a degradation rate that is low and controlled through stages via the galvanic relationship between the FeMnN and Mo. The Mo also provides enhanced radiopacity.

METHODS: Fe-35Mn-0.15N (FeMnN) tubes were fabricated and filled with varying sizes and quantities of Mo and FeMnN/Mo composites. The composite tubes were drawn to fine wire sizes ranging from 25 to 250 µm. Several constructions were drawn to 80 µm and formed into 16-wire braids. Strength, corrosion, and radiopacity characteristics were assessed via tensile testing, immersion in PBS, and x-ray imaging.

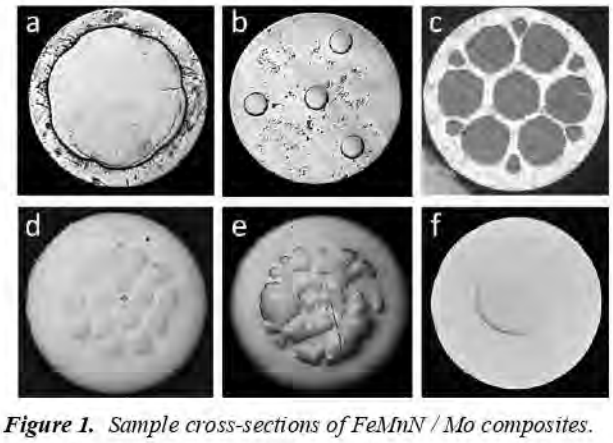

Figure 1. *Sample cross-sections of FeMnN / Mo composites.*

RESULTS: Most intended wire cross-sections were able to be produced through conventional drawing practices (Fig.1), though some proved challenging. Tensile strengths of cold drawn composites ranged from 1.7-2.4 GPa, with elastic strains exceeding 1%. Corrosion testing confirmed the sequential breakdown of the wire (Fig.2). X-ray imaging highlighted the radiopacity advantages of Mo over FeMnN, and that ferrous-shelled wires benefited from molybdenum content (Fig.3).

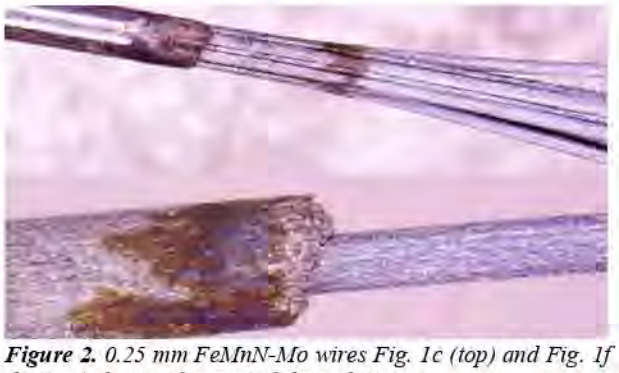

Figure 2. *0.25 mm FeMnN-Mo wires Fig. 1c (top) and Fig. 1f (bottom) shown after partial degradation.*

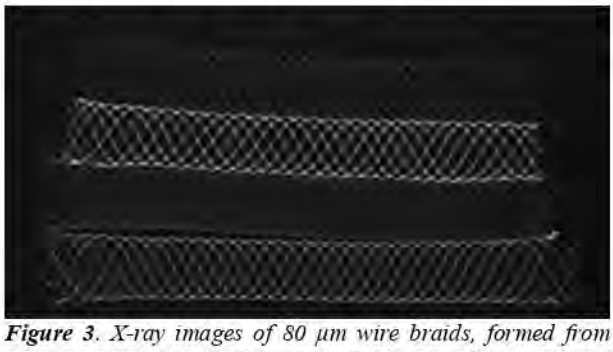

Figure 3. *X-ray images of 80 µm wire braids, formed from wire of, from top, FeMnN, Mo, FeMn-Mo of Fig. 1f, and FeMn-Mo of Fig 1c.*

DISCUSSION & CONCLUSIONS: Wire composites formed from Fe- and Mo-based materials show promise in meeting the requirements of a neurovascular device. *In vitro* and *in vivo* testing of these wires is underway to further characterize their degradation behaviour.

REFERENCES: [1]A. Oliver, C. Bilgin, A. Vercnocke, et al (2022), *J Neurosurgery*. [2]C. Redlich, P. Quadbeck, M. Thieme, B. Kieback (2020), *Acta Bio* **104**:241-251. [3]M. Sikora-Jasinska, L. Morath, M. Kwesiga et al (2022) *Bioactive Mat* **14**:262-271. [4]Schaffer, Jeremy E., et al (2013), Acta Bio **9.10**:8574. [5]J. Schaffer, USA Patent US9561308B2, 2017. [6]M. S. Michael, H.-J. Wachter and R. J. Myers, USA Patent US7745732B2, 2010. [7]J. Schaffer, EU Patent EP2872663B1, 2020.

ACKNOWLEDGEMENTS: The authors are grateful for the assistance of Ken Sorg, Harold Perez, Justin Lothamer, Terry Twitchell, and Aubrey Ehle.

Mechanical properties, in vitro biodegradable behaviour, biocompatibility and osteogenic ability of additively manufactured Zn-0.8Li-0.1Mg alloy scaffolds

A Liu[1,2], Y Lu[3], J Dai[1,2], D Xia[3], P Wen[1,2], Y Zheng[4]

[1]State Key Laboratory of Tribology in Advanced Equipment, CHN. [2]Dept. Mechanical Engineering, Tsinghua University, CHN. [3]Dept. Dental Materials, Peking University School and Hospital of Stomatology, CHN. [4]School of Materials Science and Engineering, Peking University, CHN.

INTRODUCTION: Zn is a life element and has exhibited promising prospects for biodegradable applications. Zn-Li-Mg alloys were developed to improve mechanical strength and biodegradable performance[1]. Porous scaffolds fabricated by laser powder bed fusion (L-PBF) provided an efficient way to further modulate properties[2]. So far, high-strength Zn-Li-Mg alloy has not been fabricated by L-PBF yet. In addition, the influence of porosity on performance of Zn-Li-Mg scaffolds needs further clarification. Herein, Zn-0.8Li-0.1Mg alloy was first fabricated by L-PBF. Scaffolds designed by triply periodic minimal surfaces (TPMS) were produced with different porosities. Mechanical properties, degradation behaviour, osteogenic ability and biocompatibility were investigated.

METHODS: The geometry of scaffolds (IWP unit cells with porosities of 60%, 70% and 80%) was shown in Fig. 1. Zn-0.8Li-0.1Mg scaffolds with varying porosities (P60, P70 and P80) were fabricated. Pure Zn scaffolds with a porosity of 70% (Zn-P70) were utilized for the comparison.

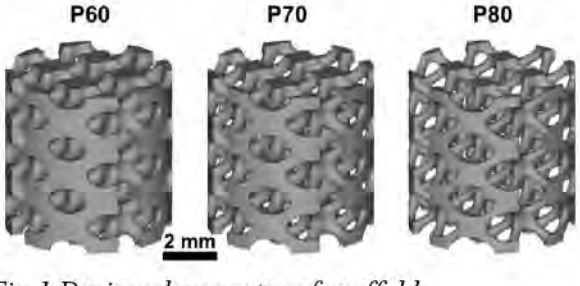

Fig.1 Designed geometry of scaffolds.

RESULTS: Compressive strength (CS) decreased with increasing porosities. P70 had a higher CS compared with Zn-P70, indicating considerable strengthening effect (Fig. 2a). Weight loss of scaffolds increased with increasing porosities, and P70 had a lower degradation rate compared with Zn-P70, due to the formation of Li_2CO_3 during degradation (Fig. 2b). As shown in Fig. 3 and 4, among all scaffolds, P70 showed the best biocompatibility and osteogenic ability, because P70 released the lowest content of Zn^{2+} and a moderate content of Li^+ in extracts.

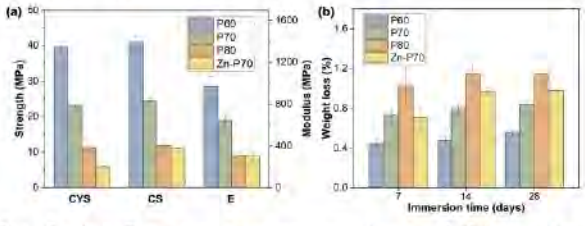

Fig. 2: (a) Compressive properties and (b) in vitro degradation behaviour of scaffolds.

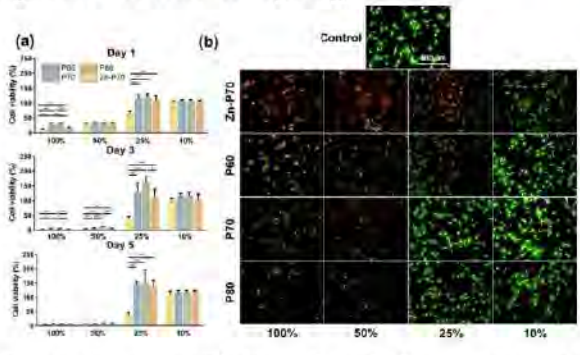

Fig. 3. Biocompatibility of scaffolds in vitro: (a) CCK-8 results, (b) Live/dead staining assay.

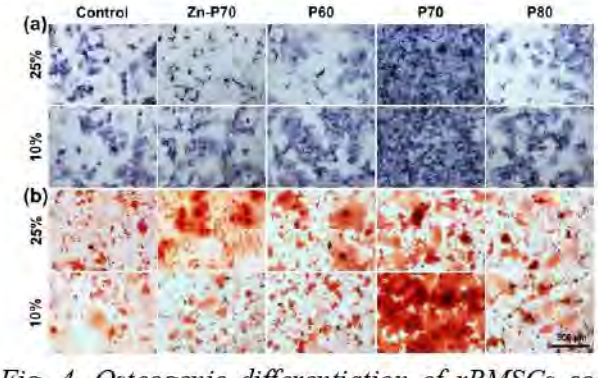

Fig. 4. Osteogenic differentiation of rBMSCs co-cultured with extracts: (a) ALP, (b) ARS.

DISCUSSION & CONCLUSIONS: By alloying and porous design, P70 scaffolds exhibited higher strength than Zn-P70 as well as the best biocompatibility and osteogenic ability among all the used porosities.

REFERENCES: [1] H. Yang, B. Jia, et al (2020) *Nat Commun* **11**: 401. [2] Y. Qin, P. Wen, et al (2019) *Acta bio*, 2019, 98: 3-22.

15th Biometal
AUGUST 21 TO 27, 2023
Grand Hôtel San Michele, Cetraro, CS, Italy

Multicomponent zinc alloys with high mechanical performance – challenges and solutions

M. Bieda[1], A. Jarzębska[1], M. Wróbel[1], Ł. Maj[1], Ł. Rogal[1], W. Gozdur[1], S. Przybysz[2], J. Skiba[2]

[1] *Institute of Metallurgy and Materials Science of Polish Academy of Sciences, Krakow, Poland*
[2] *Institute of High Pressure Physics, Polish Academy of Sciences, Warsaw, Poland*

INTRODUCTION: Zinc based biodegradables materials attracted attention of scientific community thanks to their outstanding biocorrosion property. The application of this kind of alloys is limited by difficulties in optimization of required mechanical, biocorrosion, and biological properties [1-2]. The main goal is to obtained material with good strength and plasticity and to not deteriorate uniformity of corrosion and biocompatibility. Thanks to alloying zinc with magnesium and subjected to hydrostatic extrusion high mechanical properties could be reached [3]. In this work influence of addition of Mg, Ca and Sr on mechanical and biocorrosion performance was investigated.

METHODS: Quaternary, ternary and binary alloys composed of zinc with 0.5 % wt. of magnesium and 0.5 wt. % of calcium and 0.5 wt. % of strontium (ZnMg, ZnMgSr, ZnMgCaSr). were prepared by gravity casting in an argon atmosphere followed by hot extrusion at 250 °C and then by hydrostatic extrusion. Hydrostatic extrusion was performed in one, two and three passes at room and at elevated temperatures. Microstructural characterization using SEM, TEM, and XRD phase analysis was performed. The mechanical properties including microhardness and static tensile tests were examined. Corrosion properties were analysed by using immersion tests carried out in Hanks' solution, under conditions mimicking a human body (temperature = 37 °C, pH = 7.4). Polished samples were immersed in Hanks' solution for 14 days. Samples were subjected to SEM observations to investigate the corrosive products by EDS technique. Sample surfaces without corrosion products were characterized to observe the evidence of uniform degradation (arrangement of pits). The weight loss of the samples was measured after cleaning the surface to remove corrosion products and the corrosion rate was calculated.

RESULTS: The microstructure of investigated zinc alloys after hydrostatic extrusion consists of the α-Zn grains and intermetallic phases Mg_2Zn_{11}, $CaZn_{13}$ and $SrZn_{13}$. Difference in microstructure between different components addition was observed. It could be noticed that the largest grain refinement was observed for quaternary alloy. Due to that the highest pressure during extrusion caused the highest temperature during deformation, higher fraction of dynamically recrystallized grains was observed for quaternary alloys extruded in one pass. The four components alloys after one pass of hydrostatic extrusion received also good thermal stability up to 150°C. The highest strength was noticed for quaternary alloy after 2 passes the highest elongation for ternary alloy after one pass. Quaternary alloy has the best corrosion properties in terms of uniformity and acceptable corrosion rate.

DISCUSSION & CONCLUSIONS: Synergy effect of alloying and plastic deformations was observed and analysed for complex quaternary system. Input of each element was described on both mechanical and corrosion study. A wide range of behaviour was obtained with the same composition of the material. The comparison of the properties for different composition and process parameters was performed and compromise solutions were proposed.

REFERENCES: [1] G. Li, H. Yang, Y. Zheng, X.-H. Chen, J.-A. Yang, D. Zhu, L. Ruan, K. Takashima,(2019) *Challenges in the use of zinc and its alloys as biodegradable metals: Perspective from biomechanical compatibility,* Acta Biomaterialia, Vol. 97, 2019, 23-45,
[2] J. Venezuela, M. S. Dargusch, The influence of alloying and fabrication techniques on the mechanical properties, biodegradability and biocompatibility of zinc: A comprehensive review. *Acta Biomater.* 87, 1–40 (2019). [3] W. Pachla, S. Przybysz, A. Jarzębska, M. Bieda, K. Sztwiertnia, M. Kulczyk, J. Skiba (2021) *Structural and mechanical aspects of hypoeutectic Zn–Mg binary alloys for biodegradable vascular stent applications,* Bioactive Materials, Vol. 6, 26-44,

ACKNOWLEDGEMENTS: This work was supported by Norwegian Financial Mechanism and National Centre for Research and Development (NCBR) - grant NOR/SGS/BioAbsMat/0096/2020

Effect of additive manufacturing energy on the evolution of microstructure, mechanical properties, and degradation behavior of porous Fe-Mn-C alloys

Quang Nguyen Cao[1], Abdelhakim Cherqaoui[1], Carlo Paternoster[1], Simon Gélinas[2], Carl Blais[2], Diego Mantovani[1*]

[1]*Laboratory for Biomaterials and Bioengineering*, CRC-I, Department of Min-Met-Materials Eng., & University Hospital Research Center, Regenerative Medicine, Laval University, QC, Canada; [2]*Laboratory for Powder Metallurgy, Department of Min-Met-Materials Engineering, Laval University, QC, Canada*.

INTRODUCTION: Recently, Fe-Mn-C alloys emerged as interesting candidates for biodegradable implants, which can overcome the drawbacks of permanent stents [1]. Fe-Mn-C alloys have several unique advantages including good mechanical properties, acceptable biocompatibility and biodegradability [2]. However, the degradation rate of these alloys when fabricated by casting is too slow for some applications [3]. Therefore, the objective of this study was to design and develop porous Fe-Mn-C alloys susceptible to degrade faster than those produced by casting. Fe-16Mn-0.7C alloys with various pore densities were produced by selective laser melting (SLM) with different energy densities. The effect of energy on porosity, microstructure, mechanical properties, and degradation behavior was investigated.

METHODS: Water atomization was employed to produce Fe-Mn-C powder from three initial bulk materials: 4 kg of Fe-Mn alloy, 16 kg of Fe-C AISI 1018 steel, and 151 grams of carbon. After atomization, powder size in range of 20-53 µm was used. The atomized powder was then reduced in an Ar-H_2 atmosphere by annealing, to reduce the overall amount of oxygen. The atomized powder properties were evaluated by flowability measurement, oxygen content quantification, and morphology and composition analysis. SLM process was carried out with different energy densities ranging from 64.67 to 125.0 J/mm^3. The microstructure and chemical composition of the manufactured alloys were characterized by optical microscopy, scanning electron microscopy (SEM), energy dispersive X-ray spectroscopy (EDX), and x-ray diffraction (XRD). Micro hardness test and tensile test were employed to evaluate the mechanical properties of the processed alloys.

RESULTS: Figures 1a-d shows SEM images of the four porous alloys fabricated by SLM. Pores were formed in all four manufactured alloys. The density and size of pores decreased with the increase of the manufacturing energy density. Specifically, for the sample fabricated with E = 64.67 J/mm^3, pores are very deep with the average size of 300-400 µm. Pores in the sample fabricated with E = 83.33 J/mm^3 are much smaller at about 100-150 µm. There were some powder particles remained and trapped inside the pores of samples fabricated with E = 64.67 and 83.33 J/mm^3. The smallest pore size was obtained for the sample fabricated with E = 104.17 J/mm^3 at approximately 100 µm.

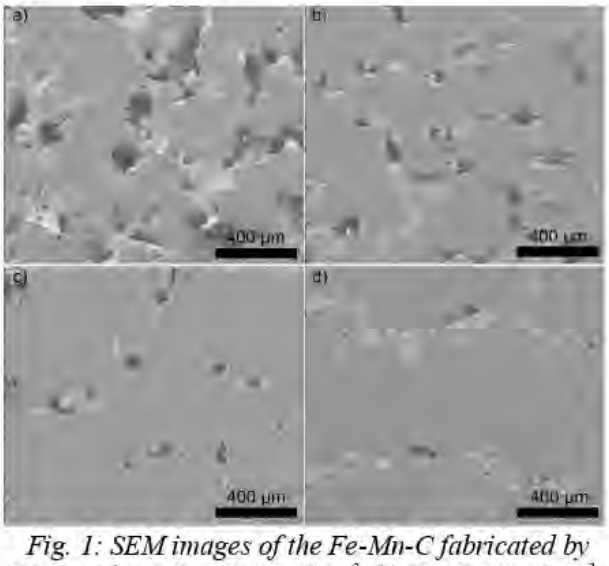

Fig. 1: SEM images of the Fe-Mn-C fabricated by SLM with: a) E = 64.67 J/mm^3, b) E = 83.33 J/mm^3, c) 104.17 J/mm^3, d) 125.0 J/mm^3.

EDX analysis indicated that C accumulated inside the pores, and MnO_2 formed around the pores of all samples. EDX analysis also showed that the distribution of all elements in the bulk region is very uniform. SEM analysis of samples etched with nital solution showed that austenite was formed as main component of bulk region (grain size of 10-50 µm).

DISCUSSION & CONCLUSIONS: This work investigated the effect of energy density on the microstructure, mechanical property, and degradation behavior of porous Fe-Mn-C alloys fabricated by SLM. The preliminary results indicated that increasing the energy density results in decreasing the formation of pores. The optimal microstructure and properties were obtained by the alloy manufactured with E = 104.17 J/mm^3.

REFERENCES: [1] P.K. Bowen, et al (2016) *Adv Health Mater* **5**: 1121–40. [2] M Peuster, et al (2006) *Biomaterials* **27**:4955–62. [3] S. Loffredo, et al (2021) *ACS Biomater Sci* Eng **7**:3669−82.

ACKNOWLEDGEMENTS: This work was supported by NSERC-Canada-Alliance and Prima-Quebec- partnership funds. DM holds a Canada Research Chair Tier I (2012-2026).

Mechanical properties and degradation behavior of sputtered amorphous ZnMgZr thin films for biodegradable devices

C. Poltronieri[1], F. Challali[1], T. Simon-Yarza[3], F. Tetard[1], V. Bockelée[1], F. Chaubet[2], Ph. Djemia[1]

[1]*Université Sorbonne Paris Nord, UPR CNRS 3407- LSPM, France*

[2] *Université Sorbonne Paris Nord, Inserm U 1148 – LVTS, France*

[3]*Université Paris Cité, Université Sorbonne Paris Nord, Inserm U 1148 – LVTS, France*

INTRODUCTION: In biomedicine, the removal of permanent devices from the patient's body might lead to complications and extensive research is carried out to overcome the possible issues. A solution is the development of biodegradable implants able to mechanically support the damaged apparatus for the needed healing period while degrading in time until complete dissolution [1]. Among the most used materials, ZnMg alloys are known in terms of biodegradability, biocompatibility and mechanical properties [2]. Nevertheless, crystalline alloys might be susceptible to localized corrosion and pitting phenomena, making the development of alloys with uniform and controlled corrosion rates still an open challenge. Recent studies [3] showed that amorphous materials (such as ZnMgCa) are promising candidates. For instance, the homogeneous and isotropic atomic structure could lead to generalized corrosion with tunable corrosion rates in function of the alloy composition. This work aims to improve the glass forming ability (GFA) and corrosion resistance of ZnMg alloys by adding Zr, synthetizing ternary amorphous ZnMgZr thin films metallic glasses (TFMGs) by magnetron co-sputtering and correlating their structure with their mechanical properties and degradation behavior.

METHODS: ZnMgZr TFMGs were deposited on Si and Kapton® substrates by RF magnetron co-sputtering from pure metallic targets. The structural and chemical properties were investigated by SEM, XRD and EDS techniques. Elastic properties were assessed by nanoindentation and non-destructive opto-acoustic techniques. Moreover degradability test were performed up to 8 weeks in simulated body fluid (SBF) at 37°C under static conditions. Cytotoxicity was evaluated by standard colorimetric test (lactate dehydrogenase).

RESULTS: The amorphous phase is confirmed by XRD diffractograms of ZnMgZr TFMGs. *Fig. 1* shows that Young's modulus (*E*) covers a wide range of values (from 45 to 100GPa) as function of the composition. Similarly to the hardness (*H*), its maximum has been found for ZnZr TFMGs and it decreases by Mg addition. *H* is proportional to the yield strength of the material which provides indirect information about the elastic limit. The results are coherent with the elastic strain measured by tensile test of TFMGs on Kapton®. Static immersion tests showed a minimum content of Zr (~20% at.) is necessary for the sample to resist in SBF for 8 weeks without delamination. Preliminary cytotoxicity test revealed a cell mortality ratio smaller than 10%, validating the non-toxic behavior of ZnMgZr TFMGs.

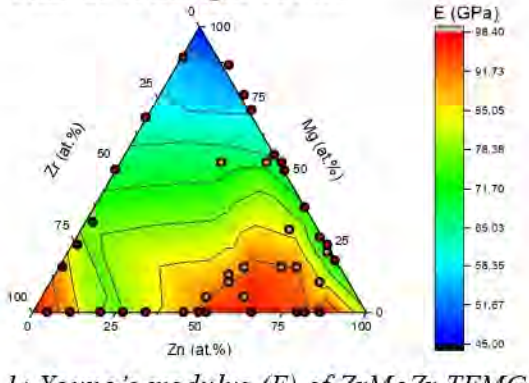

Fig. 1: Young's modulus (E) of ZrMgZr TFMGs. The points on the diagram represent the investigated compositions.

DISCUSSION & CONCLUSIONS: ZnMgZr TFMGs were deposited by magnetron co-sputtering. ZnMgZr TFMGs cover a large range of mechanical properties maintaining their biocompatibility, making these materials interesting for different biomedical applications. Overall, these results may potentially orientate the research on the development of amorphous coating of already existing metallic or polymeric biomedical implants.

REFERENCES: [1]C. Li et al (2020) Nat. Rev. Mater. **5**(1):61-81. [2]E. Mostaed et al (2018) Acta Biomater. **71**:1-23. [3]C. Jin et al (2022) Mater. **15**:2172.

Microstructural evaluation and mechanical properties of bioabsorbable as-cast hypoperitectic Zn-based alloys.

AL Ramírez[1], P Roncagliolo[1], JS Flores[1], LA Domínguez[1], JA Juárez[2], C Paternoster[3], D Mantovani[3]

[1] *Facultad de Química*, [2] *Instituto de Investigaciones en Materiales*, *Universidad Nacional Autónoma de México, Ciudad de México, México.* [3] *Lab. for Biomaterials & Bioengineering (CRC – I) Laval University, Quebec City, Canada*

INTRODUCTION: Peritectic alloys have been few studied and less understood despite several important binary bioabsorbable systems being the basis of potential biomedical devices such as the Zn-Ag alloy system [1]. In the present work, novel hypoperitectic ternary Zn-based bioabsorbable alloys intended for cardiovascular applications are investigated.

METHODS: For the fabrication of the Zn-based ternary alloys (Table 1), the starting materials (Zn, Ag, Mg, and Cu with 99.99% purity) were melted in a vacuum induction furnace in alumina crucibles under the protection of Ar atmosphere. For the solidification experiments, the alloys were casted into sand molds to obtain cylinders with the following dimensions: 5 cm in diameter and 10 cm in length. Scanning electron microscopy (JEOL 7600f) was used to observe the microstructure, and all microanalyses were carried out with an EDS coupled system. XRD technique was used for phase identification. Tensile tests were carried out according to the ASTM E8 standard.

Table 1. Chemical compositions (weight %) of the investigated alloys (ICP – OES).

Material	Composition (wt%)			
	Zn	Ag	Mg	Cu
Pure Zn	100.00	---	---	---
Zn-Ag-Mg	96.76	2.93	0.31	---
Zn-Ag-Cu	96.21	3.47	---	0.32

RESULTS: The microstructures corresponding to the hypoperitectic ternary systems Zn-Ag-Mg and Zn-Ag-Cu are shown in Fig. 1a and 1b, respectively.

DISCUSSION & CONCLUSIONS: As shown in Fig. 1, when the third element is changed (Mg or Cu) in the Zn-Ag hypoperitectic alloy system, the microstructure and all the material's performance can be modified. In the present work, two novel hypoperitectic ternary Zn-based alloys are presented. Their microstructures, mechanical properties, and corrosion behavior were investigated with the main purpose of being applicated as cardiovascular devices.

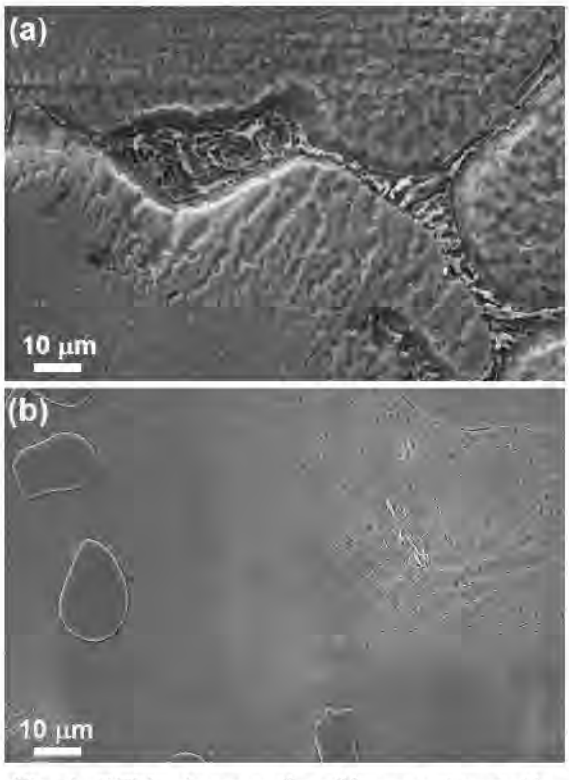

Fig. 1: SEM micrographs of hypoperitectic Zn-based ternary alloys (a) Zn-Ag-Mg, and (b) Zn-Ag-Cu in the as-cast condition.

REFERENCES: [1] H.W. Kerr and W. Kurz (1996) *Int Mater Rev* **41**:129-164. [2] A.L. Ramírez-Ledesma, P. Roncagliolo-Barrera, M.A.Álvarez-Pérez, J.A. Juárez-Islas, C. Paternoster, F. Copes, and D. Mantovani (2023) Mater. Today Commun. **35**: 105544.

ACKNOWLEDGEMENTS:

This work was supported by Programa de Apoyo a Proyectos de Investigación e Innovación Tecnológica (PAPIIT – TA100222) and the Natural Science and Engineering Research Council of Canada. Beca para las Mujeres en la Ciencia L'Or´eal-UNESCO-CONALMEX-AMC. The authors gratefully acknowledge the technical support from Adriana Tejeda–Cruz, Agustín Ruíz–Tamayo, Ciro Márquez–Herrera, and Eliezer Hernandez–Mecinas.

Graphene nanoplatelet–reinforced zinc matrix composites for implant applications

Y Li, H Kabir, K Munir, C Wen

School of Engineering, RMIT University, Melbourne, Victoria 3001, Australia

INTRODUCTION: Zinc-based alloys and composites are gaining increasing interest as promising new biodegradable implant materials due to their appropriate biodegradation rates and biological functionalities. However, the inadequate mechanical strength and ductility of pure zinc have restricted its application [1-2]. Metal matrix composites containing suitable alloying elements and reinforcing particulates can show the required mechanical properties for metallic biomaterials [3]. Graphene-based materials are considered promising reinforcement materials to improve the mechanical properties, corrosion performance, and wear resistance of metal matrix composites [4]. This study investigated zinc matrix composites (ZMCs) reinforced with 0.1-0.4 wt.% graphene nanoplatelet (GNP) fabricated via powder metallurgy as potential biodegradable implant materials.

METHODS: High-energy ball milling was used for preparing the GNP-Zn powder mixtures and the GNP-reinforced ZMC samples were fabricated by sintering at 420 °C for 6 h under a high-purity Ar atmosphere. The microstructures, mechanical properties, and corrosion behaviours of the GNP-reinforced ZMCs were characterized using optical microscopy, scanning electron microscopy combined with energy-dispersive X-ray spectroscopy, Raman spectroscopy, compression testing, and electrochemical and immersion testing in Hanks' balanced salt solution. The cytotoxicity of the GNP-reinforced ZMCs was evaluated by indirect contact method using the human osteoblast-like SaOS2 cells.

RESULTS: The microstructural study revealed that the GNP was uniformly dispersed in the ZMCs after ball milling and sintering at 420 °C for 6 h. The microhardness, compressive yield strength, ultimate compressive strength, and compressive strain of the ZMC-0.2GNP were 68.7 HV, 123 MPa, 247 MPa, and 22.9 %, respectively, with improvements of ~ 18 %, 50 %, ~ 28 %, and ~ 15 % compared to pure Zn. The corrosion rate of the ZMCs was lower than that of the pure Zn, and the ZMC-0.2GNP composite exhibited the lowest corrosion rate of 0.09 mm/y as measured by electrochemical testing. The extract of pure Zn and GNP-reinforced ZMCs at a concentration ≤ 12.5% showed no cytotoxicity in relation to SaOS2 cells.

DISCUSSION & CONCLUSIONS: Zn matrix composites reinforced with different contents of GNP were fabricated using a powder metallurgical process. High-energy ball milling was found to be an effective technique for uniformly dispersing GNP in Zn matrices. Microstructural studies showed that strong interfacial bonding between the GNP and Zn matrix was achieved without the formation of any intermetallic carbide phases. The GNP-reinforced Zn matrix composites showed significantly enhanced strength via synergetic strengthening mechanisms including load-transfer and grain-refinement strengthening. The optimum GNP content in the GNP-reinforced ZMCs was found to be 0.2 wt.% in terms of mechanical strength and corrosion resistance. Higher GNP content (0.4 wt.%) in the Zn matrices caused agglomeration of GNP. ZMC-0.2GNP showed good vitro biocompatibility. Overall, ZMC-0.2GNP composite exhibited promising mechanical properties, satisfying corrosion rate and biocompatibility for biodegradable load-bearing implant applications.

REFERENCES: [1]H. Kabir, et al. (2021) *Recent research and progress of biodegradable zinc alloys and composites for biomedical applications: Biomechanical and biocorrosion perspectives*. Bioact Mater 6(3):836-879. [2]S. Agarwal, et al. (2016) *Biodegradable magnesium alloys for orthopaedic applications: A review on corrosion, biocompatibility, and surface modifications*, Mater. Sci. Eng. C 68:948-963. [3]M. Shahin, et al. (2019) *Magnesium matrix nanocomposites for orthopedic applications: A review from mechanical, corrosion, and biological perspectives* Acta Biomater. 96:1-19. [4]K. Munir, et al. (2020) *Graphene nanoplatelets-reinforced magnesium metal matrix nanocomposites with superior mechanical and corrosion performance for biomedical applications* J. Magnes. Alloy 8(1):269-290.

ACKNOWLEDGEMENTS: The support from the Australian Research Council through the Future Fellowship (FT160100252) and the Discovery Project (DP210101862).

Investigation of the ultra-structure around Mg implant alloys utilising three-dimensional imaging methods

D.C.F. Wieland[1], K. Ishkakova[1,2], B. Zeller-Plumhoff[1], R. Willumeit-Römer[1]

[1] *Institute of Metallic Biomaterials, Helmholtz-Zentrum Hereon, Geesthacht, DE*

[2] *Institute of Catalysis Research and Technology, Karlsruhe Institute of Technology, Karlsruhe, DE*

INTRODUCTION: Biodegradable magnesium implants are becoming a promising material for bone fracture treatment due to their high bio-compatibility and good mechanical properties, similar to the bone itself. Today, only a few studies on the bone ultrastructure reaction exist despite the increased importance of understanding the regeneration process and the bone tissue reaction.[1,2] While the degradation of an implant is in progress, the degradation products start to form, which might impact the hydroxyl apatite crystal lattice parameters by atomic substitutions or crystallite size.[3,4]

Within this study, we collected and analysed both micro-computed tomography (µCT) and X-ray diffraction computed tomography (XRD-CT) with a focus on the HAp crystal parameters in rat explants. We examined this parameter concerning the implant material and healing time.

METHODS: We used rat bone explants of femurs having a screw with a diameter of 2 mm and a length of 2.3 mm of Ti, Mg or WE43 Mg-alloy. After 3 and 28 days rats were sacrificed, and the explants containing the degraded screw and bone tissue were embedded into resin.

We imaged the embedded samples at the beamline P07 at PETRA III, Hamburg. We used a combined approach to measure high-resolution µCT with a spatial resolution of 2.8 µm and XRD-CT with a resolution of 80 µm. The photon energy used was 60 keV. Data reconstruction and analysis were performed by MATLAB.

RESULTS: Figure 1 shows a reconstructed slice from the XRD-CT data showing the phase distribution of the metallic implant and the bone. This data was further used to extract the distance depended properties of the ultrastructure from the implant interface and can be directly correlated to the 3D known from µCT as both data sets overlap.

DISCUSSION & CONCLUSIONS: Figure 2 shows the crystallite size of WE43 and Ti samples after 28 weeks of healing. The data indicate a difference between the crystallite size near the implant, with Ti having larger crystals. For the Magnesium containing implant, such a difference can not be seen (data not shown). One explanation might be a different maturation stage of the bone as it still keeps remodelling around the degradable implant interface. Similar differences can be seen for the lattice spacing, indicating an impact on the HAp crystal structure.

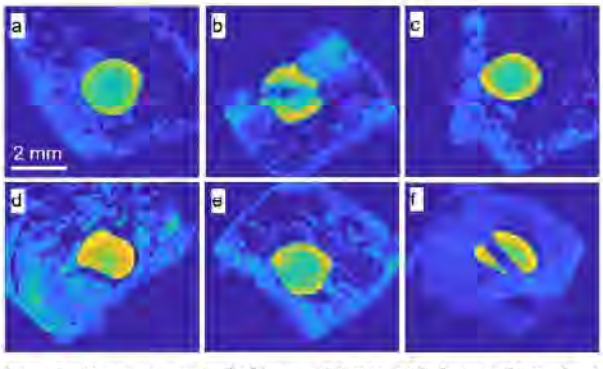

Fig. 1: Reconstructed slices of XRD-CT data of Mg (a & d), WE43 (b & e) and Ti (c & f) showing the phase distribution of metal parts (yellow) and the bone (blue)

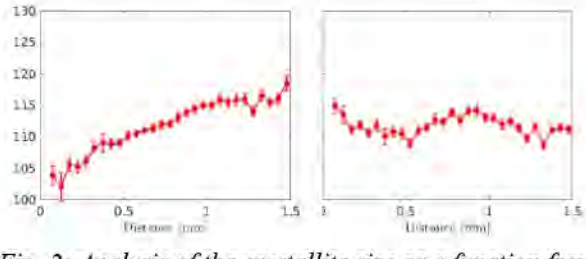

Fig. 2: Analysis of the crystallite size as a function from the implant interface extracted from the XRD-CT. left) WE43, right) Ti (reference)

REFERENCES: [1] T.A. Grünewald, et al. Acta biomaterialia 31, 448-457 (2016), [2] T.A. Grünewald, et al. Biomaterials 76, 250-60 (2016) [3] B. Zeller-Plumhoff, et al. Acta Biomaterialia 101, 637-645 (2020) [4] T.A. Grünewald, et al., Biomaterials 76, 250-260 (2016)

ACKNOWLEDGEMENTS:. We acknowledge the P07 of Perta III operated by Hereon (Geesthacht, Germany). We would like to thank Felix Beckmann for help at the P07.

Effect of high temperature oxidation on WE43 magnesium alloy fabricated by laser powder bed fusion

P Wen[1,2], F Song[3], J Liu[1,2], Y Tian[4], Y Zheng[5]

[1]State Key Laboratory of Tribology in Advanced Equipment, CHN. [2]Dept. Mechanical Engineering, Tsinghua University, CHN. [3]Beijing Tsinghua Changgung Hospital, CHN. [4]Peking University Third Hospital, CHN. [5]School of Materials Science and Engineering, Peking University, CHN.

INTRODUCTION: WE43 (4% Y, 3% (Nd+Gd), 0.5% Zr, remaining Mg, in mass) has been one of the limited types of biodegradable metals that have achieved clinical application so far. WE43 porous scaffolds fabricated by laser powder bed fusion (L-PBF) exhibited superior fusion quality, mechanical strength and osteogenic capability, but the degradation was excessively fast due to massive precipitates[1]. High temperature oxidation (HTO) formed a passivated barrier of rare earth oxides on the surface, which inhibited the degradation of extruded WE43 samples[2]. However, there has been no report on how HTO influences WE43 samples fabricated by L-PBF. In this work, the effects of HTO on WE43 L-PBF samples were investigated regarding mechanical properties, degradation rate, hemocompatibility and osteogenesis.

METHODS: WE43 powder was atomized from cast bars and was selectively melted by a commercial L-PBF machine[1]. The L-PBF samples were heated to 525 °C in a muffle furnace with circulating fresh air for 8 hours and then quenched in water, so called HTO. Tensile, compressive, in vitro immersion, hemocompatibility and ALP activity tests were performed.

RESULTS: The ultimate compressive and tensile strength of the HTO samples decreased by 26% and 9% respectively compared with the L-PBF samples, however, the Young's modulus barely changed and the elongation significantly increased by 51% (Fig. 1). Compared with L-PBF and cast samples, the degradation of HTO samples was substantially inhibited. After 28 days, the weight loss of HTO samples was 6.88%, approximately one eighth of cast samples, while L-PBF samples collapsed after 7 days as shown in Fig.2.

For L-PBF samples, no adherent platelets but cracks were observed; the BMSCs shrank and separated at the surface. At the surface of HTO samples by contrast, no crack was found and a few of platelets were confirmed; the BMSCs spread out and connected each other (Fig.3). HTO group exhibited a considerably higher ALP activity of 6.10 U/mg, more than 3 times that of the control group and 2 times that of the L-PBF group.

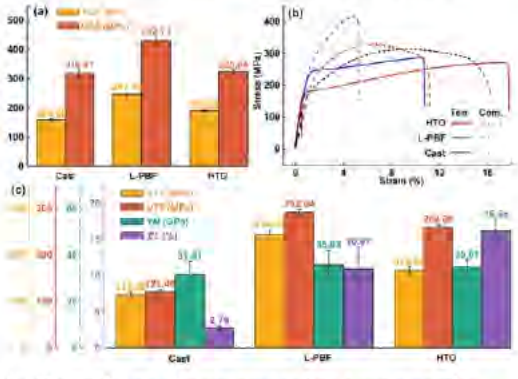

Fig. 1: Tensile and compressive test results.

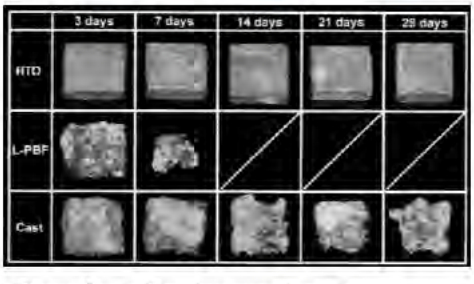

Fig. 2: Samples after immersion tests.

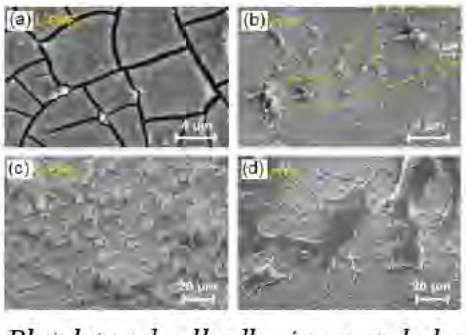

Fig. 3: Platelet and cell adhesion morphology.

DISCUSSION & CONCLUSIONS: The HTO significantly inhibited degradation and improved ductility, hemocompatibility and osteogenesis of WE43 fabricated by L-PBF. It is biocompatible, convenient and efficient, thus has promising prospects for future clinical applications.

REFERENCES: [1]J. Liu, B. Liu, et al (2022) *Bioact Mater* 16: 301-319. [2]A. Haenzi, P. Gunde, et al (2009) *Acta Bio* 5: 162-171.

Additively manufactured biodegradable ZnMg alloy

Yuzhe Zheng[1], Yageng Li[1], Luning Wang[1]

[1] *Beijing Advanced Innovation Center for Materials Genome Engineering, School of Materials Science and Engineering, University of Science and Technology Beijing, Beijing, China*

INTRODUCTION: Additive manufacturing (AM) provides unprecedented opportunities for the development of customized bone implants. Biodegradable zinc is one of the promising biodegradable metals which has moderate degradation rate, good biocompatibility, and high mechanical property. Thus, the development of zinc implants through AM has been attracting increasing attention. However, since AM zinc alloy has just emerged recently, it is necessary to investigate the process-structure-property relationship.

METHODS: Laser powder bed fusion (LPBF) was used to fabricate biodegradable ZnMg alloy. Firstly, the process parameters of LPBF ZnMg were optimized to achieve high densificaiton. Then the microstructure, mechanical properties, *in vitro* degradation behavior, and biocompatibility of LPBF ZnMg alloy were systematically characterized. The effects of process parameters and building orientation on the microstructure and comprehensive properties of LPBF ZnMg alloy were investigated in comparison with those of LPBF pure Zn.

RESULTS: The experimental results showed that the optimized process window of LPBF ZnMg was 40-70 J/cm^3. The grain size of LPBF ZnMg was significantly refined and the second phase of Mg_2Zn_{11} were produced. Different process parameters caused changes in grain size and differences in building orientation led to variation in the grain morphology. Mechanical properties also varied with different printing parameters. The degradation rate of LPBF ZnMg alloy was slower than that of Zn, and the degradation products were mainly $Zn_5(OH)_2(CO)_3$, $Zn(OH)_2$, ZnO, and Ca-P minerals. Meanwhile, we found that different process parameters and building orientations can cause different degradation rates of LPBF ZnMg. Moreover, the biocompatibility of LPBF ZnMg was significantly improved compared to Zn, and LPBF ZnMg with optimal process parameters showed the best cellular activity and osteoinductive properties.

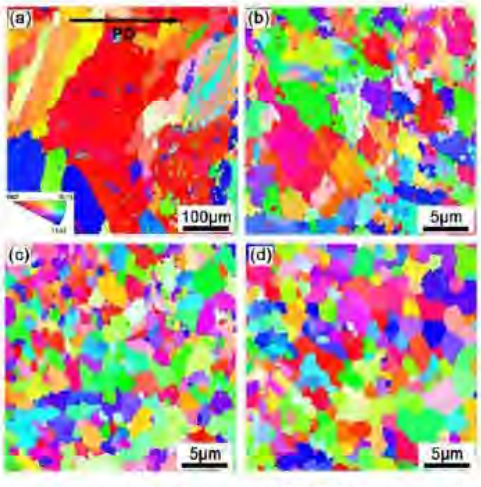

Fig. 1: Inverse pole figure of LPBF zinc and ZnMg alloy: (a) pure zinc, (b-d) ZnMg with different printing parameters.

DISCUSSION & CONCLUSIONS: In this work, we summarize the influence of LPBF process parameters on the microstructure and comprehensive properties of ZnMg alloy. LPBF parameters can be used as an effective tool to tune the mechanical property and biodegradation behaviour of zinc alloy. This work will pave the way for the application of LPBF Zn alloy in the future. It can also serve as a good reference for the study of other LPBF biodegradable metals.

REFERENCES: [1] Y. Li, P. Pavanram, et al (2020) *Acta Biomater* 101:609-623.

ACKNOWLEDGEMENTS: The work was financially supported by the National Natural Science Foundation of China (52201294), China Postdoctoral Science Foundation (2022M710345), Natural Science Foundation of Beijing (L212014), and Fundamental Research Funds for the Central Universities and the Youth Teacher International Exchange & Growth Program (No. QNXM20220022).

Electroforming process of Fe-Mn alloys for biomedical application using choline-chloride/urea deep eutectic solvent

V.F. Sales[1,2], C. Paternoster[1,2], G. Kolliopoulos[2], D. Mantovani[1,2]

[1] *Laboratory for Biomaterials and Bioengineering, CRC-I, Department of Min-Met-Materials Eng., & University Hospital Research Center, Regenerative Medicine, Laval University, QC, Canada..*
[2]*Department of Mining, Metallurgical and Materials Engineering, , Laval University, QC, Canada..*

INTRODUCTION: Recently, Fe-Mn alloys have been proven effective as a promising material for temporary implants (i.e., coronary stents and bone screws).[1,2] Currently, most of these materials are fabricated by casting. This method is generally used as the primary fabrication technique and is usually followed by thermomechanical processes, but this form of manufacturing makes their production time and energy-consuming. The electroforming technique could be a valid alternative to reduce the steps required for producing biomedical implants, especially when specific chemical composition, microstructures, and specific shapes are required.

Electroforming consists of reducing dissolved metallic ions onto a cathodic electrode by electrodeposition.[3, 4] However, the deposition of certain specialty metals and alloys (i.e., Fe-Mn) is not feasible from aqueous solutions. Deep Eutectic Solvents (DESs) have recently been proposed as an effective and promising green alternative for water in metal electrodeposition processes. DESs are eutectic mixtures of inexpensive, biodegradable salts, which usually consist of a quaternary ammonium salt (i.e., Choline chloride – ChCl) and a metal salt or a hydrogen bond donor (HBD) compound (i.e., urea).

METHODS: The DES was prepared by mixing dried ChCl with urea at a 1:2 molar ratio at T= 90 °C until a homogeneous colorless liquid was formed. The electrolyte solution was obtained by adding (1.0M) $FeCl_2.4H_2O$ and (0.5M) $MnCl_2$ to the DESs. The samples were produced by chronopotentiometry analysis in a 100 mL three-electrodes electrochemical cell. The tests were performed at T=80 °C, and several current densities in the range 20 – 80 mA/cm^2. The used characterization techniques were scanning electron microscopy, energy dispersive spectroscopy, x-ray diffraction, atomic force and optical microscopy.

RESULTS: Figure 1 shows the topmost layer of the electroformed Fe-Mn alloys at different current density values. It is possible to observe the formation of pores in the surface of samples produced with high values of current densities (40 and 80 mA/cm^2). The variation of the current deposition determined not only a change in the microstructure of the produced samples, in the amount of deposited Mn, but also in the current efficiency η, which attained a maximum of 83.1% for a deposition current density i = 30 mA/cm^2.

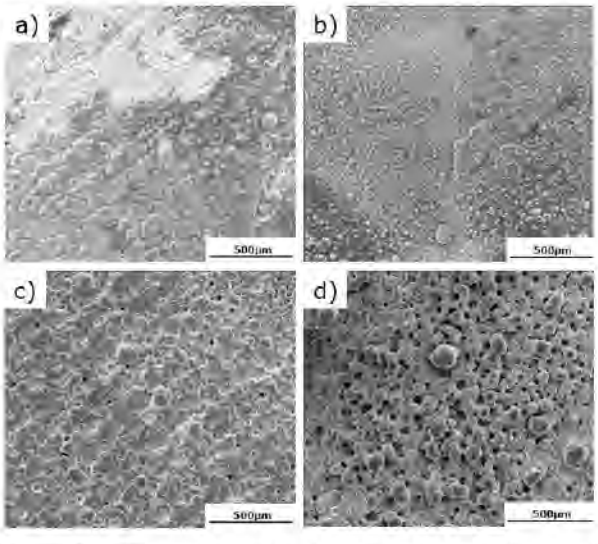

Fig. 1: Scanning electron microscopies of electroformed Fe-Mn samples produced at current densities of a) 20 mA/cm^2; b) 30 mA/cm^2; c) 40 mA/cm^2, and d) 80 mA/cm^2 at 80 °C.

DISCUSSION & CONCLUSIONS: The change in current density affected the metal nucleation process and the final morphology of the electroformed Fe-Mn alloys. The sample produced at 30 mA/cm^2 showed a higher current efficiency (83.1 ± 2 %). After that, it was observed a decrease in η. This behaviour can be related to forming of pores and more irregular surfaces. Based on the results obtained by chronopotentiometry, the mechanism of nucleation for Fe-Mn alloys from ChCl/urea occurred through the progressive nucleation mechanism.

REFERENCES: (1) H. Hermawan, et al., J Biomed Mater Res A, 93 (2010) 1; (2) D. Hong, et al., Acta Biomater, 45 (2016) 375; (3) T. H. and A. Watson, The Ni Dev. Inst., (2000) 372; (4) J. M. Yang et al., Int J Mach Tools Manuf, 48 (2008) 329.

ACKNOWLEDGEMENTS: This work was supported by NSERC-Canada-Alliance and Prima-Quebec- partnership funds. DM holds a Canada Research Chair Tier I (2012-2026).

Investigation of the microstructure, mechanical properties, and corrosion behavior of a highly oxidized biodegradable FeMnC sintered steel for biomedical applications

Abdelhakim Cherqaoui[1], Quang Nguyen Cao[1], Carlo Paternoster[1], Simon Gélinas[2], Carl Blais[2], Diego Mantovani[1]

[1] *Laboratory for Biomaterials and Bioengineering, CRC-I, Department of Min-Met-Materials Eng., & University Hospital Research Center, Regenerative Medicine, Laval University, QC, Canada;*
[2]: *Laboratory for Powder Metallurgy, Department of Min-Met-Materials Engineering, Laval University, QC, Canada.*

INTRODUCTION: FeMnC alloys have recently raised interest in temporary biodegradable implants thanks to their outstanding mechanical properties, and good biocompatibility [1]. However, the acceleration of their degradation rate could open the applicability of bioresorbable Fe-based biomaterials to several applications [2]. Therefore, this study aimed to develop by pressing and sintering a FeMnC steel with a network of interconnected pores, and rich in oxide precipitates to enhance its degradation rate. The effect of porosity and oxide precipitates on the microstructure, the degradation rate, and the mechanical performances of FeMnC was investigated.

METHODS: FeMnC pre-alloyed powder was produced by water atomization of a FeMn low-carbon ferroalloy, AISI 1018 steel, and graphite. The powder features such as particle size, chemical composition, and morphology, were investigated using sieving tests, MP-AES/EDS, and SEM, respectively. Particles ranging from 20 µm to 212 µm have been compacted in a uniaxial press (500-700 MPa) to obtain green compacts. These latter were sintered at 1200°C under an Ar-10%H_2 atmosphere for 3h followed by furnace cooling. Microstructural and mechanical characterization of final samples were performed using SEM/XRD and transverse rupture tests, respectively. The degradation behavior was investigated through electrochemical measurements and static degradation immersion tests (up to 14 days) in Hanks' solution (pH 7.4) at 37 °C.

RESULTS: The amount of oxygen was high (1.9 wt.%) even after the reduction of the powder. EDS mapping carried out on a cross-section of sintered samples revealed that Mn and Fe were uniformly distributed in the dense regions. *Fig. 1a-d* shows that a network of interconnected pores was formed in the four samples, and Fe/Mn oxide precipitates were found to be concentrated around the large pores. Porosity decreased when the compaction pressure increased. The highest density was obtained for the sample compacted at 700 MPa (*Fig. 1d*). The latter had a tensile rupture strength of 341 MPa, which is considered very low compared to the same grade of alloys fabricated via casting [3].

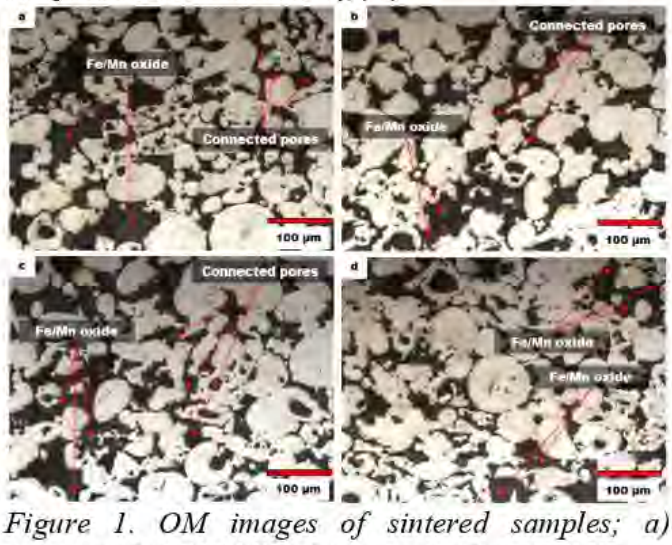

Figure 1. OM images of sintered samples; a) compacted at 500 MPa; b) compacted at 600 MPa; c) compacted at 650 MPa; d) compacted at 700 MPa.

DISCUSSION & CONCLUSION: Preliminary results showed that the compressibility of the powder is low due to its high amount of carbon and oxygen. In addition, Fe/Mn oxides were formed around large pores, making the alloy more fragile. All these factors lead to a considerable decrease in the mechanical strength of the material. Then, an increase in the alloy's relative density is necessary to tune its mechanical performance. Also, the corrosion behavior is to be investigated.

REFERENCES: [1] Gambaro, S. *et al.* (2021). Mechanical and degradation behavior of three Fe-Mn-C alloys for potential biomedical applications; [2] Schinhammer, M. *et al* (2010). Design strategy for biodegradable Fe-based alloys for medical applications; [3] Loffredo, S. *et al.* (2021). Metallurgical development of high-performance biodegradable twinning-induced plasticity steels.

ACKNOWLEDGEMENTS: This work was supported by NSERC-Canada-Alliance and Prima-Quebec- partnership funds. DM holds a Canada Research Chair Tier I (2012-2026).

15th Biometal
AUGUST 21 TO 27, 2023
Grand Hôtel San Michele, Cetraro, CS, Italy

How accurate does accuracy have to be?

N. Hort[1,2], P. Maier[3,4], Carla Vogt[5]

[1] *Helmholtz-Zentrum Hereon, Geesthacht, Germany;* [2] *Leuphana University Lüneburg, Lüneburg, Germany*
[3] *University of Applied Sciences Stralsund, Stralsund, Germany;* [4] *Lund University, Lund, Sweden*
[5] *TU Bergakademie Freiberg, Freiberg, Germany*

INTRODUCTION: Numerical data are collected in a variety of experiments, and mean values and standard deviations (SD) are calculated. The data can often be measured with considerable accuracy and can therefore be very meaningful. However, experimenters should also be aware of the accuracy that can be achieved by the chosen methods. This requires knowledge of how these methods work and what their limitations are. The same care should also be taken when evaluating the data, which are often input variables in calculations. Here, too, it is necessary to consider the limitations of methods and statistics.

EXAMPLES: Let's take the corrosion rate (CR) based on weight loss as an example. You need measure height and diameter, mostly by using callipers like in Figure 1, and the weight before and after the experiment of the clean specimen and a precision analytical balance (accuracy for weight in the range of mg). Numerous specimens will be measured. However, the measured values also depend on the correct handling of the instrument and of course environmental parameters like the position of the specimen on the balance pan. We know that air flow should be avoided.

However, there are already uncertainties due to the calculation and of course due to the accuracy of the instrument and in the way the calculated values are presented: If a measurement was made in mg, then it should also be given in mg with the number of decimal places agreeing with the accuracy and not in µg. The indication in µg is possible and correct in theory. However, the impression of accuracy by a factor of 1000 times better is now created which is not covered by the method. The measured data are then often evaluated with a spreadsheet to calculate mean values and SD of the entire population or the sampling, see equation 1. A huge amount of digitals is easily calculated due to the used equations and again you have to decide if the results with e.g. a few decimal places reflect real accuracy or leaves only the impression of an accurate result.

$$a)\ SD = \sqrt{\frac{1}{n}\sum_{i=1}^{n}(x_i - \bar{x})^2} \quad b)\ SD = \sqrt{\frac{1}{n-1}\sum_{i=1}^{n}(x_i - \bar{x})^2}$$

Equation 1: Standard deviation of the a) population, b) sampling

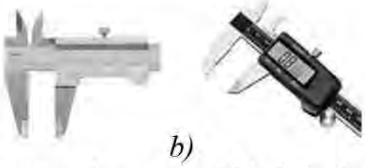

a) *b)*

Figure 1: a) analogous and b) digital calliper

By calculating CR, the mean values, mass loss and specimen geometry are considered and, again errors may occur. Depending on an analogous or a digital calliper the results are more or less accurate and rounding effects again will influence the final result, see Figure 2. However, the accuracy of the analogous calliper is in the range of 0.1 mm while the digital calliper can be in the range of 0.01 mm.

Basically, the error propagation and the major error source/consideration for each should always be discussed, and mathematical methods are available [1]. In this case it means that the errors of weight loss, geometry as well as rounding errors during calculation of mean values and SD will have impact on the final result. Rounding to 5 and less decimal places shows different values to using all decimals.

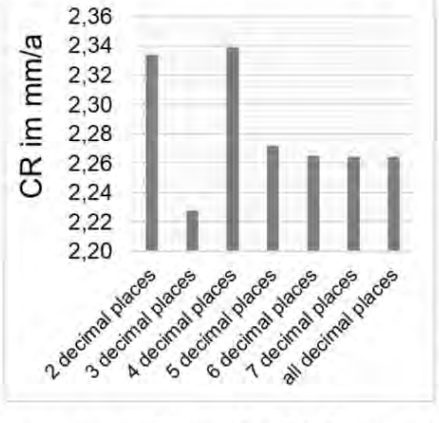

Figure 2: calculated CR influenced by number of decimal places for mean value of weight and surface

SUMMARY: You should know about the basic principles of the methods you are applying and in any case their accuracy and almost any limitations. It is also important to know the intrinsic errors of all steps involved. Some of these errors might be large enough to have a severe impact. This could lead to a wrong interpretation especially when results fit your expectations [2].

REFERENCES: [1]H. Pham (2023) *Handbook of Engineering Statistics*, Springer London Ltd. [2]D. Kahnemann (2012), *Thinking fast and slow*, Penguin

Powder bed fusion – laser beam of biomedical Mg alloys: Challenges and possibilities

Hanna Nilsson Åhman[1,2], Francesco D'Elia[1], Cecilia Persson[1]
[1]Divsion of Biomedical Engineering, Uppsala University, Sweden [2]Swerim AB, Kista, Sweden

INTRODUCTION: Additive Manufacturing (AM) such as Powder Bed Fusion – Laser Beam (PBF-LB) has made it possible to produce tailored bone implants with complex structures, designed for increased bone ingrowth. As Mg alloys are already used in bone screws, PBF-LB of the same could make personalized, biodegradable implants for the improved healing of large bone defects possible[1].

PBF-LB of Mg alloys was first proven feasible in 2010[2], but the number of studies has remained limited (Fig 1). An increase has been observed in the last 4-5 years, showing prints of both fully dense material and complex geometries. Nevertheless, for a successful commercialization, a number of challenges remain. Herein these are discussed, along with the current status, and the next step for PBF-LB of Mg alloys.

Figure 1: Articles published on PBF-LB of Mg alloys.

REACTIVITY OF MG: In PBF-LB, metal powder is melted in layers according to a digital 3D file. Due to the reactivity of Mg, the handling of such powder and the highly reactive condensates formed during PBF-LB, have been major hurdles for the process development. Another challenge consists in the unstable process unless the O_2 content is controlled. Increased knowledge in powder handling along with the development of new PBF-LB systems for reactive powders, will be key enablers for printing Mg alloys.

PBF-LB PROCESSING OF MG: Another challenge is the small difference between the melting (650 °C) and boiling point (1090 °C) of Mg, resulting in evaporation during processing. The high melting point of the MgO surface (2852 °C) further hinders process stability. Energy inputs must be sufficient to penetrate the oxide surface, while minimizing Mg evaporation to maintain alloy content specification and avoid interaction of fumes with the laser. Alloy design is one solution, aiming for the formation of a less stable oxide surface, and to compensate for Mg evaporation. Moreover, proper gas flow during processing is key to

A crucial factor affecting microstructure, and thus final part properties, is the influence of the PBF-LB process parameters on melt pool dynamics, which is very poorly understood today. Solving aforesaid problems would allow researchers to focus on melt pool dynamics and therefore work towards tailoring of microstructure and improved part properties.

MG ALLOYS FOR PBF-LB: High densities (>99%) are continuously being obtained for rare earth- (RE=Y, Gd, Nd) containing and Mg-Al-Zn (AZ) Mg alloys processed by PBF-LB[3,4], while for other Mg alloys lower densities are mostly reported[5]. In addition, PBF-LB-processed Mg-RE reach tensile strengths similar to those of conventionally produced alloys, but they remain brittle[3,4]. Ductility should be improved as a means to also improve fatigue properties. Moreover, the corrosion properties of the as-built material are generally poor, and heat treatments have so far failed in improving them. While surface treatments have shown to impede the early onset of corrosion, for larger implants, the corrosion properties of the bulk also need to be improved[1]. The influence of texture on material properties also needs more research.

Additionally, the obtained microstructures vary among studies of the same alloy. As the primary focus for PBF-LB of Mg alloys has aimed to achieve fully dense material, further exploring the relationship among processing, microstructure, and resulting material properties is important. So is developing new alloys optimized for the PBF-LB process. Due to the good printability of Mg-RE alloys, there are several recent publications investigating new quaternary Mg-RE alloys. Mg-Ca-Zn alloys are also explored but have shown limited printability[5]. Nevertheless, the first in vivo studies on PBF-LB Mg alloys were published in 2022 and show the great promise of the process[6].

A very big hurdle in alloy development for PBF-LB is powder availability. Nevertheless, as the field grows, accessibility to powder will increase, particularly as universities and research institutes install smaller powder producing systems.

CONCLUSION: Despite the varying stability of the PBF-LB process, and limited knowledge of process-structure-property relations, current results show great promise for Mg. As knowledge in safety increases, along with powder availability and new PBF-LB systems, PBF-LB of Mg alloys will be a much more accessible field, and thus result in a leap forward in alloy development and material properties. These are crucial steps towards commercial implementation of a PBF-LB processed Mg based implant.

REFERENCES:[1]Qin et al. (2019) doi:10.1016/j.actbio .2019.04.046; [2]Ng et al. (2010) doi:10.1080/1745275100 3718629; [3]Zumdick et al. (2019) doi: 10.1016/j.matchar. 2018.11.011; [4]Li et al. (2022) doi:10.1016/j.jma.2022. 06.004; [5]Hendea et al. (2022) doi: 10.3390/ma15072561; Xie et al. (2022) doi: 10.1016/j.bioactmat.2021.06.032

ACKNOWLEDGMENTS: Financed by SSF (FID17-0028); Vinnova (2019-05259; 2019-00029).

15th Biometal
AUGUST 21 TO 27, 2023
Grand Hôtel San Michele, Cetraro, CS, Italy

Binder based MIM vs. 3D-printing (FGF) approach of Mg-6Gd for biomedical application

M. Wolff[1], A. Khajeh Sharafabadi[2], H. Helmholz[1], M. Luczak[1], T. Ebel[1], R. Willumeit-Römer[1]

[1] *Helmholtz-Zentrum hereon GmbH, Germany.*

[2] *Chemnitz University of Technology, Germany.*

INTRODUCTION: Rare earth containing Mg-alloys are under development for high strength biodegradable implants since several years [1]. This study introduces the binary Mg-6.3Gd-alloy into FGF (Fused Granular Fabrication), a binder based 3D-printing technology which enable the production of scaffold like strut structures (Figure 1) or even hollow structures with a closed dense shell.

Fig. 1: 3D-printed (FGF) scaffold like demonstrator parts made of Mg-6.3Gd alloy feedstock.

MIM (Metal Injection Moulding), a near net shape mass production technique for complex shape parts was used as reference route to produce comparable test specimen using the identical granular feedstock.

METHODS: The manufacturing of Mg-alloy feedstock is described in detail in [2]. The feedstock batch was used for both, FGF and MIM. Sintered tensile test specimens were investigated using a tensile test machine (Zwick Z050). Degradation test specimens were studied by immersion in DMEM GlutaMAX™ + 10% FBS under physiological conditions for 7 days. Microstructure was deter-mined using SEM (Tescan, Vega3) operating at 15 kV in the BSE mode. X-ray imaging was performed using tomography (Xylon, Cougar SMT).

RESULTS: Both, FGF- and MIM-produced tensile test specimen could achieve sufficient material properties as shown in the following Figure 2.

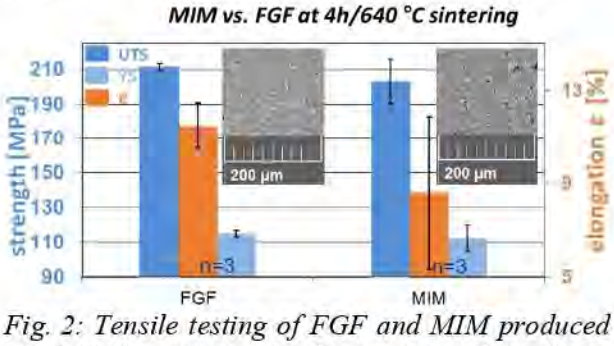

Fig. 2: Tensile testing of FGF and MIM produced Mg-6.3Gd specimens in the as sintered condition with corresponding SEM-image of microstructure.

Surprisingly, the FGF properties slightly exceed those of MIM. Furthermore, the MIM microstructure reveals slightly higher porosity than the FGF material. In contrast, the corrosion rate (CR) of the as sintered FGF material was high as 2.27 ± 0.1 mm/a (no. of specimen n=10) as exemplary shown in Fig. 3 (right side). It can be seen that the degradation test specimens contain roundish shaped pitting scars, corresponding to the printing pattern. For comparison, the identical Mg-6.3Gd material, processed by MIM could achieve a sound CR of 0.31 ± 0.05 mm/a.

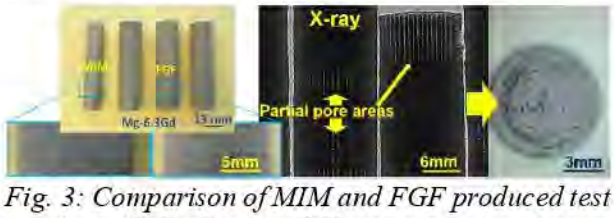

Fig. 3: Comparison of MIM and FGF produced test specimen (left) showing different surface structure. X-ray image pointed out inhomogeneous inner structure (middle) with dense and porous areas. Degradation test specimen discloses roundish pitting scars according to printing direction (right).

DISCUSSION & CONCLUSIONS: Despite of sufficient material properties of the FGF material, even better than the MIM reference route, the degradation performance of the FGF material fails due to instabilities in the FGF processing, visible in sections with insufficient infill the x-ray image in Fig. 3 (middle). On the other hand, the MIM-route demonstrated that the material generally pass the degradation test. Hence, more effort on optimisation of FGF processing has to be performed further on.

REFERENCES: [1] N. Hort et al: Magnesium alloys as implant materials – Principles of property design for Mg–RE alloys. Acta Biomaterialia, DOI: 10.1016/j.actbio .2009.09.010. [2] M. Wolff et al: Mg Powder Injection Moulding (MIM) of Orthopedic Implants for Biomedical Applications, JOM, 2016, DOI: 10.1007/s11837-016-1837-x.

ACKNOWLEDGEMENT: Many thanks to our colleagues Henrik Lüneburg, Kai Steinberg and Vasyl Haramus for printing, injection molding and x-ray imaging of test specimen and demonstrator parts.

Limited input metal balance optimization (LIMBO): how low can you go?

Adam J. Griebel, Jeremy E. Schaffer
Fort Wayne Metals, Fort Wayne, IN, USA

INTRODUCTION: Magnesium-calcium binary alloys have been well-known for decades[1], and numerous studies within the past 15 years have indicated promising performance with Ca contents less than 1 wt%[2-4]. Recent work by researchers at ETH Zurich demonstrated impressive mechanical properties of XHP Mg-Ca alloys with Ca as low as 0.2 wt% through thermomechanical process tailoring[5]. Interestingly, that work showed limited impact of Ca content from 0.2-0.6 wt% on attainable strength. That finding motivated the present work, seeking to find a lower limit of Ca content which still allows substantial strengthening in Mg-Ca binary alloys.

METHODS: Mg-Ca alloys were prepared by vacuum induction melting pure Mg and a Mg-Ca master alloy and casting into 50 mm diameter molds. Compositions are shown in Table 1. A pure Mg ingot was prepared as a control. Ingots were homogenized at 450°C for 16 hours and directly extruded to 12 mm. To refine the microstructure and increase strength, extruded bars were then subjected to a continuous ECAP process[6] regime consisting of 4 B_c passes with shear angle of 120° at 300°C followed by 4 B_c passes at 250°C. Optical microstructures for each alloy were obtained at various stages, as were microhardness measurements. A single dogbone tensile specimen was machined from each alloy after 8 passes and tensile tested.

Table 1. Alloys investigated in this study.

Alloy Name	Target Ca (wt %)	Measured Ca (wt %)
Mg	0	< 0.01
Mg0.075Ca	0.075	0.081
Mg0.15Ca	0.15	0.17
Mg0.3Ca	0.3	0.37

RESULTS: All alloys were successfully processed through the 8-pass ECAP schedule. Hardness values for the 4 alloys at 0, 4, 6, and 8 ECAP passes can be seen in Figure 1. Grain sizes were difficult to resolve optically but were on the order of 2-5 µm for pure Mg and 1 µm for the MgCa alloys. Tensile testing gave UTS values of 180, 317, 314, and 341 MPa for Mg, Mg0.075Ca, Mg0.15Ca, and Mg0.3Ca, respectively.

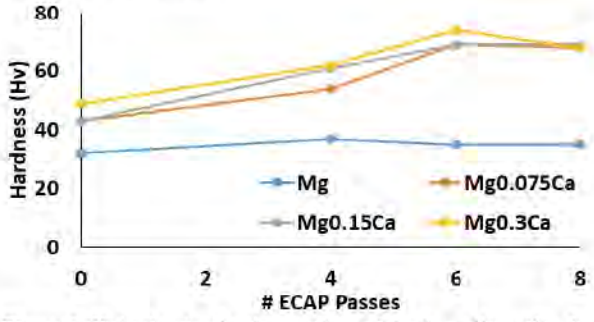

Figure 1. *Vicker's microhardness values of the four alloys after 0, 4, 6, and 8 ECAP passes*

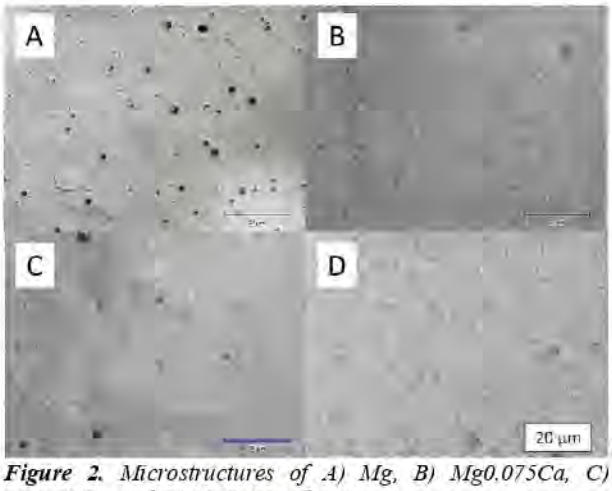

Figure 2. *Microstructures of A) Mg, B) Mg0.075Ca, C) Mg0.15Ca, and D) Mg0.3Ca after 8 passes.*

DISCUSSION & CONCLUSIONS: Additions of as little as 0.075 wt% Ca can provide substantial strengthening to Mg. Ongoing work is exploring even lesser amounts (0.04, 0.02 wt%). Assessment of the impact of alloying content and microstructure on corrosion behaviour is also underway.

REFERENCES: [1]J. Hanawalt (1941) US 2380838 A. [2]N Kirkland, N Birbilis, J Walker, et al (2010) *J Biomed Mat Res B* **95** 91-100. [3]Y Wan, G Xiong, H Luo, et al (2008) *Materials & Design* **29** 2034-2037. [4]M Salahshoor and Y. Guo (2012) *Materials* **5** 135-155. [5]T. Akhmetshina, L. Berger, S. Montibeller et al (2022) *Biometal14, **O8***. [6]C.F. Davis, A.J. Griebel, T.C. Lowe (2020), *JOM* **72**, 2603-2611.

ACKNOWLEDGEMENTS: The assistance of Dale Herndon, Lane Bailey, Caleb Richardson, and Harold Perez is gratefully acknowledged.

Additive manufacturing as a means to tailor the texture and mechanical behaviour of a biodegradable magnesium WE43 alloy

L Larsson[1], F D'Elia[1], T Maimaitiyili[2], M Sahlberg[3], C Persson[2]

[1] *Department of Materials Science and Engineering, Uppsala University, Uppsala, SE*

[2] *Swerim AB, Stockholm, SE*

[3] *Department of Chemistry – Ångström Laboratory; Uppsala University, Uppsala, SE*

INTRODUCTION: Additive manufacturing (AM) has great potential for fabricating biomedical implants as it allows for creating patient-specific solutions and complex geometries in a way that conventional manufacturing techniques cannot. For AM of biodegradable metals such as magnesium, many challenges remain, particularly when it comes to understanding the connection between the printing process and the final part microstructure and properties. The aim of this work was to use different printing strategies during laser powder bed fusion (LPBF) to tailor the texture and mechanical properties of a biodegradable magnesium alloy.

METHODS: LPBF was carried out using an EOS M100 with gas-atomized spherical powder (particle size 23-60 µm) of biodegradable rare-earth magnesium alloy WE43 (Mg-4wt%Y-3wt%Nd-0.5wt%Zr). The influence of laser scan strategies (67 vs. 90° rotation between each scanned layer) and build (horizontal vs. vertical) on the final microstructure and mechanical properties was investigated. In addition, the bulk texture of the printed parts was measured by neutron diffraction (MEREDIT, Nuclear Physics Institute, Czech Republic).

RESULTS: Build direction had a pronounced effect on the mechanical properties, where printing in the horizontal direction resulted in an average yield strength of 221 MPa (51% higher than the vertically printed samples) and an average ultimate tensile strength of 267 MPa (19 % higher than the vertically printed samples). On the other hand, there was no statistically significant effect of the laser scan strategy on the mechanical properties. The neutron diffraction results (Figure 1) showed strong orientation of basal planes perpendicular to the build direction and the possibility to tune out-of-plane texture through build orientation. The use of the 67° scan rotation showed no in-plane texture, while using a 90° scan rotation resulted in a cross-like pattern in-plane.

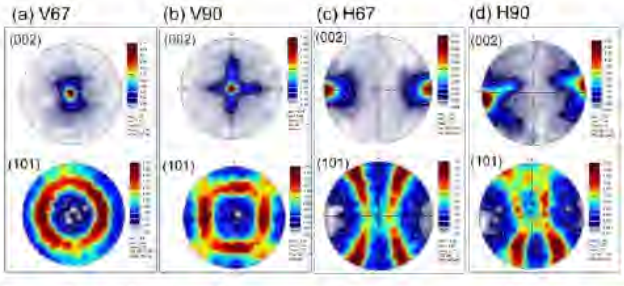

Fig. 1. Calculated neutron diffraction pole figures showing preferential crystallographic grain orientations perpendicular to the direction of loading during tensile testing. Sample (a)-(b) are printed vertically (i.e. build direction in direction of loading) and (c)-(d) horizontally (i.e. build direction perpendicular to direction of loading).

DISCUSSION & CONCLUSIONS: The findings in this work suggest that altering build orientation during AM can tailor the out-of-plane texture of Mg alloy WE43. The strong orientation of basal planes perpendicular to the build direction allows for an improved ability to tailor mechanical properties, and thus, increased freedom of design during LPBF of WE43. In regards to laser scan strategy, other metals typically show a large effect on the texture and resulting mechanical properties[1-2]. Here, we showed that it is possible to tune the in-plane texture using different laser scan strategies, which in this case had no major influence on mechanical behaviour. Future work will investigate the possibility of tailoring the out-of-plane texture and thus mechanical properties using scan strategies related to the hexagonal crystal structure.

REFERENCES: [1]J. J. Marattukalam et al., 2020, Materials & design, vol. 193. [2]S.H. Sun, et al., 2018, Mater. Des., vol. 140.

ACKNOWLEDGEMENTS: Funding from SSF (SwedNess, GSn15-0008), and VINNOVA (AM4Life Competence Centre, 2019-00029) is gratefully acknowledged. We are also grateful to AM@Å (UU) and CANAM (NPI VAS Rez) for providing experimental facilities.

15th Biometal
AUGUST 21 TO 27, 2023
Grand Hôtel San Michele, Cetraro, CS, Italy

Nanosized biodegradable powder fabrication by nanosecond pulsed laser ablation for biodegradable metal applications

Seung-Hoon Um[1], Carlo Paternoster[1], Francesco Copes[1], Pascale Chevallier[1], Hyung-Seop Han*[2] Diego Mantovani*[1]

[1] *Lab Biomaterials and Bioengineering, CRC-I, Department of Mining, Metallurgical and Materials Engineering & CHU de Quebec Research Centre, Regenerative Medicine, Laval University, Quebec City, QC, Canada*

[2] *Biomaterials Research Center, Biomedical Research Division, Korea Institute of Science and Technology (KIST), 02792 Seoul, Republic of Korea*

INTRODUCTION: The use of biodegradable metals in the medical field is gradually expanding [1]. Among these ones, Fe-Mn-C alloys raised the interest of the scientific community for their high mechanical strength and interesting corrosion rate. In addition, there is an extreme lack of research on the fabrication of sub-nano-sized biodegradable metal powders, which are for example essential for maximizing skin or cell penetration ability [2]. and improving the resolution of bio 3D printers [3]. In this study, we will discuss about the fabrication and properties of nanoscale biodegradable metal powders based on pulsed laser process.

METHODS: A pulsed nanosecond laser (Wave length: 1064 nm, power: 20 W, frequency: 30 kHz, scan speed: 1000 mm/s, pulse width: 100 ns) was used in different media (ethanol, methanol, acetone, silicone oil, distilled water) for the production of powders, from a biodegradable metal alloy (Fe-12Mn-1.2C, 20 mm x 10 mm x 2 mm), The microstructure analysis was performed with a JEM-1230 TEM (JEOL), while the powder size distribution analysis was studied through a Nano-S, DLC, (Malvern). Powder morphology and chemical composition were assessed by SEM and EDS.

RESULTS: Biodegradable metal powders were prepared using a pulsed laser process. The size of the powder was adjusted from 0.5 nm to 10 µm depending on the medium used in the laser process, and the microscopic shape of the powder was also modified to be either spherical or irregular. The powder showed a range of crystalline microstructure, depending on the production conditions.

The powder size distribution was related to the different used medium; in particular, several size ranges were found even for a single medium, for example for production in de-ionized (D.I.) water powders showed a size of 0.5-5 nm, 1-5 µm and ~7 µm.

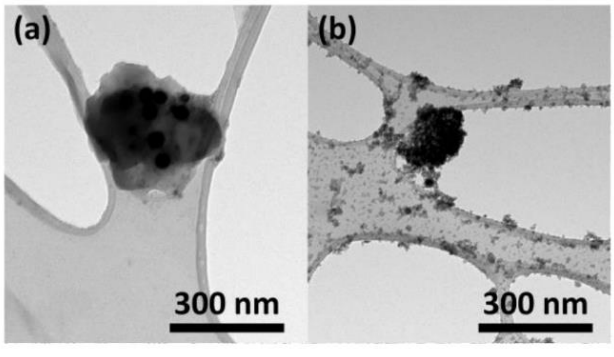

Fig. 1 TEM images of powder size and shape according to solution type acetone (a), D.W (b) during powder fabrication process.

DISCUSSION & CONCLUSIONS: The size and shape of the powder were adjusted according to the type of solvent used in the process, which is based on laser ablation parameters and relies on the effect of the thermal energy source. It is assumed that the differences in thermal conductivity between solvents may account for the observed control over the powder's size and shape. This study will be advantageous for high-resolution 3D printing of bio implants based on biodegradable metals, as well as for drug research that requires the penetration of tissues.

REFERENCES: [1] Han, H. S., D Mantovani , et al. (2019). *Current status and outlook on the clinical translation of biodegradable metals.* Mater. Today, 23, 57-71. [2] Ghasemiyeh, P., et al. (2019). *Cyproterone acetate-loaded nanostructured lipid carriers: effect of particle size on skin penetration and follicular targeting.* Pharm. Dev. Technol, 24(7), 812-823. [3] Zhang, J., et al. (2021). *3D printing of silk powder by Binder Jetting technique.* Addit. Manuf., 38, 101820.

ACKNOWLEDGEMENTS: This work was supported by NSERC-Canada-Alliance and Prima-Quebec- partnership funds. DM holds a Canada Research Chair Tier I (2012-2026).

Rotary barrel finishing for magnesium sample preparation

N. Dühring[1], N. Petersen[2,3], H. Helmholz[3], B. Wiese[3], N. Hort[1,3]

[1] *Leuphana University Lüneburg, Lüneburg, Germany*
[2] *Hamburg University of Technology, Germany*
[3] *Helmholtz-Zentrum Hereon, Geesthacht, Germany*

INTRODUCTION: Alloy development also means that necessary tests must be carried out. In addition to mechanical properties, the degradation behaviour this also includes investigations regarding the biological behaviour. However, it is precisely here that statistics also play an essential role. Therefore, the number of samples examined is also important. In order to be able to make reliable statements, it is essential that all samples have undergone the same process. Also of greatest importance is the condition of the surface. Rotary barrel finishing and related processes (fig. 1) are already established itself in many fields of industry as a processes that makes exactly this achievable: reproducible surface quality on a large number of samples.

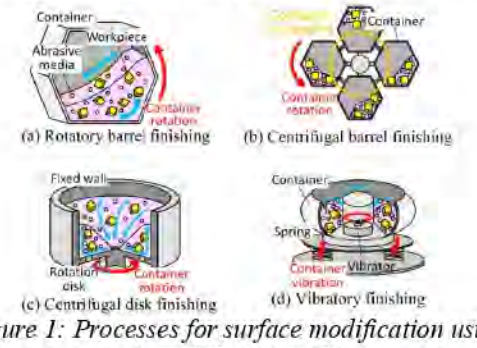

Figure 1: Processes for surface modification using barrel finishing [1]

Figure 2: specimens for biological testing (9 mm Ø)

Disk like specimens were produced by casting, extrusion, and machining. However, machining influences the surfaces and it is necessary to ensure that the surface quality is more or less identical to assure proper comparison between different materials regardless composition and processing history.

EXPERIMENTAL: For the rotary barrel finishing discs (pure Mg, Mg2Gd, Mg5Gd, Mg1Zn0.04Zr) were treated at different time (0.5-24h) together with in total 6 different abrasives (plastic, ceramic, Makrolon, ZrO_2, nut and corn granules). Additionally the Rösler P35 agent was used for cleaning and degreasing. Abrasives and P35 were supplied by effer-handel, Aalen, Germany, without additionnal informations. The rotary speed was varied as well. Surface roughness was determined using a Keyence VK-X1050 Laser Scanning Microscope (LSM, resolution 0.2 µm) and a Bruker DektakXT profilometer (resolution 10 nm).

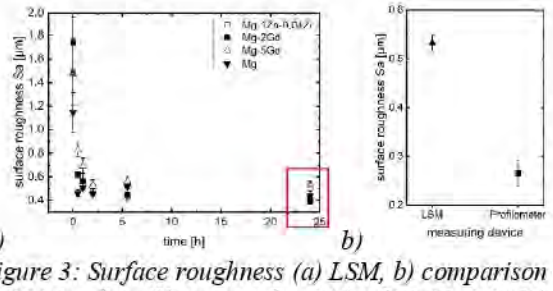

Figure 3: Surface roughness (a) LSM, b) comparison of LSM and profilometer after 24 h of Mg1Zn0.04Zr)

RESULTS & CONCLUSION: A decrease in surface roughness with time can be observed in all alloys under investigation. After 24h similar values are reached for all combinations of the chosen parameters. Fig. 3 shows this exemplarily for Mg1Zn0.4Zr and the surface roughness determined by LSM. However, using the profilometer also shows that this method is much more sensitive compared to the LSM. It therefore needs to be clarified if the resolution of the LSM is acceptable and if the inherent systematic error is having impact on results in further biological tests.

Rotary barrel finishing is a suitable method to achieve reproducible surfaces for extremely large amounts of Mg components regardless the alloy composition. But of course, the method has to be qualified with respect to the alloys composition and processing history.

OUTLOOK: The aim is to use these results to develop a standard operation procedure for processing specimens prior to biological testing: Mg – discs will be immersed in complete cell culture medium with 10% fetal calf serum (FCS) and kept under physiological conditions at 37°C, 5% CO_2 and humidified atmosphere. The degradation rate will be calculated based on mass loss after removal of the degradation layer utilizing chromic acid. These conditions are comparable to cell culture conditions for adjacent biocompatibility and effect related *in vitro* studies.

REFERENCES: [1] Y. Hashimoto (2021), Precision Engineering, 10.1016/j.precisioneng.2020.09.009

15th Biometal
AUGUST 21 TO 27, 2023
Grand Hôtel San Michele, Cetraro, CS, Italy

Magnesium-Based Nanocomposites for Bone Implant Applications

C. Hash[1], M. S. Jia[2], M. Elsaadany[2] and H. Ibrahim[1]

[1]*College of Engineering and computer science, University of Tennessee at Chattanooga, USA*
[2]*Department of Biomedical Engineering, University of Arkansas, USA*

INTRODUCTION: Magnesium (Mg) has been the focus of several studies as a candidate biodegradable alternative to the currently in-use inert metallic alloys for orthopedic applications due to its biodegradable nature inside the body and its biocompatibility [1]. However, the low mechanical strength and fast degradation of Mg in physiological environments are some of the main challenges to the use of Mg in several orthopedic applications [2]. A possible solution to these limitations is the incorporation of a small content of nanoparticles into the Mg matrix to increase strength and possibly slow down the degradation rates of the resulting nanocomposites [3]. In this work, we assessed the mechanical properties, corrosion behavior, and biocompatibility of Mg-based nanocomposites.

METHODS: Different types of nanoparticles (*e.g.*, boron nitride, and samarium oxide) at various contents (up to 1.5 Vol%) were fabricated and studied. A combination of powder metallurgy, hybrid sintering, and hot extrusion manufacturing processes was used to produce the nanocomposites. Microhardness was the main test used to assess the enhancement in the mechanical properties and the potentiodynamic polarization test (PDP) was the main test used to investigate the relative change in the *in vitro* corrosion behavior due to the incorporation of the nanoparticles. Also, the cytotoxic properties of the samples were determined using an effluent-based testing method following the ISO 10993-5 cytotoxicity testing standard.

RESULTS: The microhardness of the prepared nanocomposites increased compared to pure magnesium (without the addition of any nanoparticles), see **Figure 1**. That increase varied depending on the type and the content of the nanoparticles. The most improvement was found to be around 1.3 times increase in the microhardness after the addition of 1.5 Vol% of the samarium oxide nanoparticles. The increase in the microhardness can be attributed to the presence of the hard nanoparticles along the interfaces of the magnesium matrix grains which limits the deformation of the matrix grains that can be caused by dislocation movement and twining. In terms of corrosion characteristics, the incorporation of 0.5 Vol% resulted in the lowest corrosion currents, hence the slowest corrosion rates, see **Figure 1**.

The *in vivo* assessments of the prepared nanocomposite samples showed high levels of biocompatibility in terms of cytotoxicity. This was represented in cell viability levels similar to that of ultra-pure magnesium coupons *in vitro*.

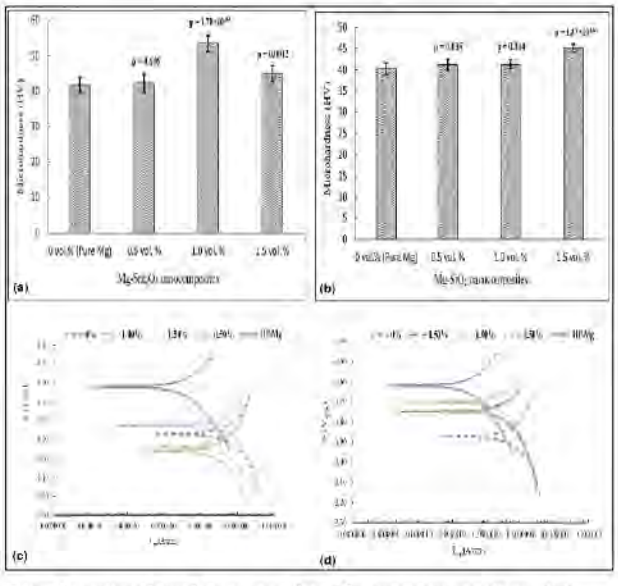

Fig. 1: microhardness results of nanocomposites: (a) samarium oxide, (b)silicone dioxide, and PDP curves: (c) samarium oxide, and (d) silicone dioxide.

DISCUSSION & CONCLUSIONS: This work confirms that the addition of nanoparticles to the Mg matrix can be a promising approach to increase strength and corrosion resistance without being cytotoxic. Further *in vitro* and *in vivo* studies are needed to determine the potential impact of corrosive byproducts on biocompatibility. Also, coatings that can be used to increase corrosion resistance and the viability of these materials *in vivo* are also needed.

REFERENCES: [1] Y. Chen, et al (2014) *Acta biomaterialia* **10**:4561-4573. [2] H. Ibrahim, et al (2017) *Materials Science and Engineering: C* **70**:870-888. [3] M. Haghshenas, et al (2020) *Nanocomposites* ***6***:22-30.

ACKNOWLEDGEMENTS: This work was supported by Center of Excellence for Applied Computational Science competition at the University of Tennessee, Chattanooga.

Application of two new Mg-Li-Y alloy wires in a novel bioresorbable vascular scaffold

K MacLeod[1], D Nash[1], R Guillory II[2], D Bow[3], C MacLeod[3], E Knox[3] and M Steckel[3]

[1] University of Strathclyde, Glasgow, UK, [2] Michigan Technological University, [3] Houghton, MI, USA, MedAlliance Ltd., Glasgow, UK,

INTRODUCTION: Bioresorbable vascular scaffolds (BVS) offer the potential to improve clinical outcomes when treating arterial disease relative to current drug eluting stents (DES) due to elimination of the foreign body implant. However, clinical adoption of BVS has been limited by the mechanical properties of available bioresorbable materials, resulting in lower expansion capacity, susceptibility to fracture and reduced radial strength compared to DES, and increased rates of thrombosis and device failure.[1] This work investigates a novel wire-form BVS device manufactured from 2 variants of a novel Mg-Li-Y alloy. The processing parameters applied during manufacture of the device are optimised to maximise its over-expansion range (beyond nominal diameter) whilst maintaining a radial force of >1N/mm.

METHODS: Mg-4Li-0.5Y (0.5Y) and Mg-4Li-2Y (2Y) alloy wires with a diameter of 125µm were applied in the manufacture of a new wire form BVS device (Figure 1a and b). The thermal processing and surface treatments applied during manufacture of the device were optimised. Their effect on the mechanical performance of the devices were investigated through benchtop expansion and radial force testing. The microstructural features of the devices were analysed with SEM and EBSD analysis.

RESULTS: Optimisation of the thermal processing and surface treatment procedures applied during manufacture allowed the 0.5Y and 2Y devices to survive over-expansion of 1.5mm and 1.0mm respectively. Minor adjustments to the processing conditions resulted in strut fracture during over-expansion. When treated for optimal over-expansion capabilities, the devices had a radial force of >1N/mm. Following annealing, the devices manufactured from both alloys had a grain size of approximately 1-2µm throughout the bulk of the device with a distinct split in texture dependent on tension/compression during forming history, Figure 1c.

DISCUSSION & CONCLUSIONS: During benchtop testing, devices manufactured from both alloys were shown to meet the mechanical performance criteria set. The new device was shown to exhibit, relatively, high over-expansion range and

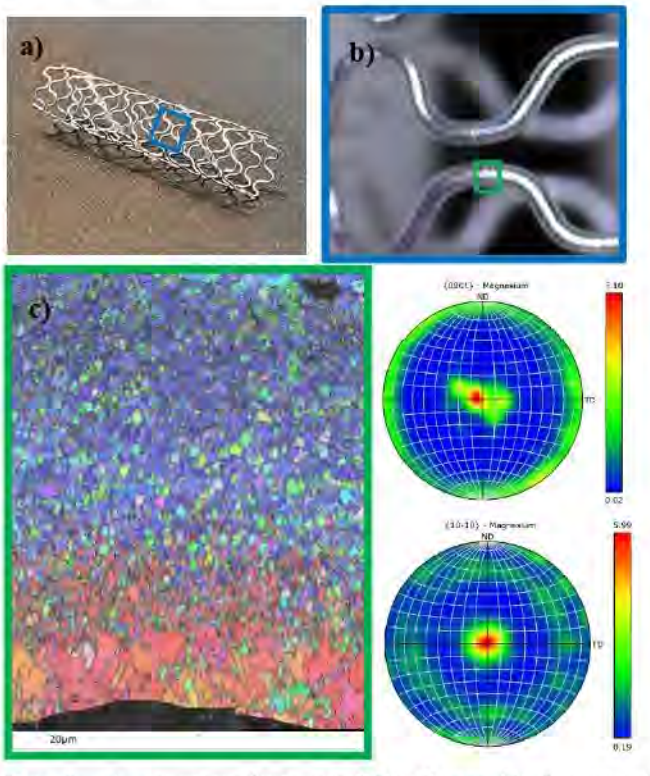

Fig. 1: a) As manufactured BVS device b) Image of struts of BVS c) Inverse pole figure map of the device and accompanying pole figures

radial force comparable to similar devices. Microstructural analysis revealed a split in texture through the device which is attributed to different deformation mechanisms being activated through the wire during device manufacture. This results in the dominate nucleation sites varying through the device during a final annealing stage. The split in texture is not expected to be beneficial to device performance. However, despite this texture, devices manufactured from both alloys exhibited a ≥1.0mm over-expansion range and >1N/mm radial force. Future work will investigate reduced strut size and the behaviour of these devices in *vivo*.

REFERENCES:

1. Peng X, Qu W, Jia Y, Wang Y, Yu B and Tian J. Bioresorbable Scaffolds: Contemporary Status and Future Directions. *Front Cardiovasc Med*. 2020; 7: 589571.

ACKNOWLEDGEMENTS: This research was partially funded by the Henry Royce Institute

15th Biometal
AUGUST 21 TO 27, 2023
Grand Hôtel San Michele, Cetraro, CS, Italy

Effect of storage and reuse on powder and bulk specimen properties for powder bed fusion – laser beam of a WE43 magnesium alloy

Giulio Pietro Cavaliere[1*], Pelle Mellin[2], Francesco D'Elia[1], Cecilia Persson[1]
[1] *Department of Materials Science and Engineering, Uppsala University, Uppsala, Sweden* [2]*Swerim AB, Kista, Sweden*

INTRODUCTION: WE43 alloys (e.g. Mg-$Y_{3.9wt\%}$-$Nd_{3wt\%}$-$Zr_{0.5wt\%}$) have been largely considered among the best alloys for biodegradable bone implants thanks to their slower degradation rate compared to many other Mg-based alloys. Processing this alloy by Powder Bed Fusion–Laser Beam (PBF–LB) has the potential of realizing patient-specific implants for healing of large bone defects. However, while additive manufacturing (AM) is largely considered a sustainable manufacturing technology, many improvements are still to be made. E.g., the powder production for PBF-LB accounts for more than 30% of the total built cost and 24% of the energy consumption. Moreover, in PBF-LB a high amount of powder feedstock used for the build, (40-80% by volume) remains unused during processing. Depending on the application requirements, unused powder is either scrapped if, or (re)used until its chemical composition (e.g. O content) is no longer within determined material quality limits. Hence, it is essential to understand the reusability for Mg-based powders to reduce costs and material waste, as well as minimize the carbon footprint. Previous studies on other alloy systems[1] have shown a degradation of powder properties (e.g., flowability, sphericity) with reuse, but to date, no such studies have been carried out on Mg alloys.

METHODS: The properties of PBF-LB WE43 powders were studied in stored virgin and reused conditions. We measured spreadability using a modified TQC Sheen automatic film applicator as developed by Hulme C.N. et al.[2]. Flowability and apparent density were also measured using a Hall flowmeter. The particle size distribution and shape of the powder were examined using SEM. Finally, the different powder conditions were used as feedstock for PBF-LB of bulk specimens using an EOS M100 and the resulting density measurements were compared.

RESULTS: Results of spreadability measurements showed a higher variability for reused powder compared to stored virgin powder (Fig. 1). The hall flow was lower for the reused powder. The SEM analysis showed the formation of bigger agglomerates and more irregular particles. The density of samples printed with reused powder was on average 5% lower than samples printed with stored powder.

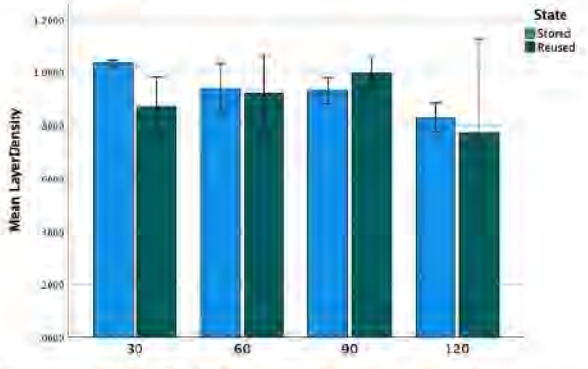

Fig. 1: Spreadability results expressed as mean layer density for different layer thicknesses (30 to 90 µm) for stored and reused powders.

DISCUSSION & CONCLUSIONS: The formation of larger particles and agglomerates resulted in a higher variability in the powder spreadability and a lower flowability. This can greatly influence the quality of the final printed product as indicated by the density analysis. A lower quality of the final build could also be attributed to the increase in surface coverage of the powder by thermodynamically stable oxides due to the high temperatures reached during the PBF-LB process[3]. This first study indicates that powder reuse has a substantial impact on powder properties and therefore on the final printed product. A precise threshold for the number of reuse cycles for WE43 powder used for critical printing applications should be determined.

REFERENCES: [1]X. He (2022), Addit. Manuf., vol. 55. [2]C.N. Hulme (2022), Prog. Addit. Manuf. [3]E. Hryha (2018), Addit. Manuf., no. 3.

ACKNOWLEDGEMENTS: This Project has received funding from the European Union's Horizon 2020 research and innovation program under the Marie Skłodowska-Curie grant agreement No. 956004.

15th Biometal
AUGUST 21 TO 27, 2023
Grand Hôtel San Michele, Cetraro, CS, Italy

Mechanical assessment of engineered porous WE43 alloy coupons produced by Laser Powder Bed Fusion, a control for bone reconstruction device applications.

LH Olivas-Alanis[1,2], S Niezgoda[1], A Chmielewska[1], D Cho[1], T Avey[1], C Rodriguez[1,2], A Luo[1], D Dean[1]

[1]*Department of Materials Science and Engineering, The Ohio State University, Columbus, OH.*

[2] *Escuela de Ingeniería y Ciencias, Tecnologico de Monterrey, Monterrey, Nuevo Leon, Mexico*

INTRODUCTION: Magnesium (Mg) alloys are being studied for medical device applications due to their elastic modulus, which is significantly lower than the standard of care alloys (e.g., Ti6Al4V). Thus, Mg alloys are promising materials for reducing the stress-shielding effect. In specific, the WE43 Mg alloy has an elastic modulus of E= 44 GPa and a typical yield strength of 172 MPa [1]. Furthermore, the application of debulking strategies and cellular materials produced by metallic powder-based Additive Manufacturing (AM) techniques (e.g., Laser Powder Bed Fusion, Binder Jetting), allow stiffness-matched of these devices [2].

METHODS: Mechanical testing coupons were 3D printed via Laser Powder Bed Fusion in an inert environment using Mg WE43 metallic powder. Tensile dog bone and cylinder compression samples were designed according to ASTM E606 and ISO 13314, respectively. These studies will determine bulk material properties and device mode of failure.

Ongoing work employs the experimental mechanical properties of the AM samples for use in a Finite Element Analysis (FEA) model. The computational validation will test the structural stiffness of different engineered porosities under static loading conditions, with varying levels of apparent density and strut thickness. The stiffness reduction and stress concentration of different pore geometries, such as orthogonal struts and Triply Periodic Minimally Surface (TPMS) Gyroid, shown in Figure 1, are being studied.

Porous samples are being printed to validate the computational model under the same experimental loading conditions.

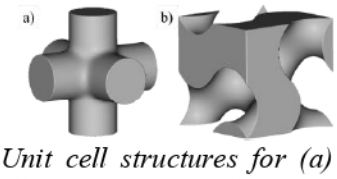

Figure 1. Unit cell structures for (a) orthogonal strut (a) and (b) TPMS gyroid, employed for FEA static analysis.

RESULTS: LPBF produced samples showed an elastic modulus (E) of 12.59±1.48 GPa, a yield strength (σ_y) of 167.20±9.02 MPa and an Ultimate Tensile Strength (UTS) of 194±10.89 MPa.

Computational FEA preliminary results, show the benefits of tailoring the normalized elastic modulus ⟨E⟩/E by altering the apparent density ⟨ρ⟩ (i.e. interconnected porosity) in TPMS gyroid structures, as seen in Figure 2. The FEA model will be validated with experimental data from 3D-printed WE43 Mg samples.

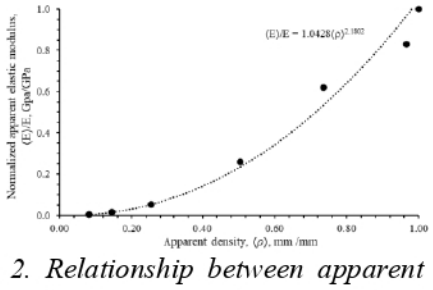

Figure 2. Relationship between apparent density and normalized apparent elastic modulus in TPMS gyroid structure.

DISCUSSION & CONCLUSIONS: Tailoring the mechanical properties of LPBF-produced WE43 Mg components via engineered porous structures, it is beneficial for the design of stiffness-matched smart structures, such as orthopaedic and graft fixation implants. We also plan to compare these results to 3D-printed Mg1.2Zn0.5Ca0.5Mn porous coupons. Furthermore, having information about the initial mechanical properties of biodegradable metallic structures, such as Mg-based, enables the development of smart structures with time dependant properties.

REFERENCES: [1] H. Hyer et al., "High strength WE43 microlattice structures additively manufactured by laser powder bed fusion," Materialia (Oxf), vol. 16, p. 101067, 2021, [2] M. Marvi-Mashhadi, W. Ali, M. Li, C. González, and J. Llorca, "Simulation of corrosion and mechanical degradation of additively manufactured Mg scaffolds in simulated body fluid," J Mech Behav Biomed Mater, vol. 126, p. 104881, 2022.

ACKNOWLEDGEMENTS: This research was supported by the State of Ohio's Third Frontier Accelerator program and The Ohio State University James Comprehensive Cancer Center Cancer Engineering Center and Biomedical Device Initiative.

Research on grain boundary segregation and partial nanograins in the biodegradable Mg alloy

Wenhui Wang [1, 2], Han, Yu [1], Xiyue Zhang [1], Xinbao Kang [1], Jiahua Ni [2], Xuanyong Liu [2], Xiaonong Zhang[1, 3*]

[1]State Key Laboratory of Metal Matrix Composites, School of Materials Science and Engineering, Shanghai Jiao Tong University, Shanghai 200240, China. [2]College of biological science and medical engineering, Donghua University, Shanghai 200240, China. [3]Suzhou Origin Medical Technology Co. Ltd., Suzhou 215513, China;

INTRODUCTION: Magnesium (Mg), a biodegradable metal, is a promising material for degradable implant devices due to its excellent mechanical compatibility with bone, superior biocompatibility, and special bio-functions, which have been researched and developed for more than ten years. Applying biodegradable Mg requires high strength, low corrosion rate, and proper biosafety. Lean alloy (low alloyed) benefits the long-term sustainable development of metal materials. Creating refined grains is a desirable approach to improve the biodegradability and mechanical properties of lean biomedical Mg alloy, but it is nearly impossible to realize. The present study characterizes the microstructures of Z2 alloy and discusses the grain refinement mechanism during the rolling process. This work provides a practical approach to realize a new lean biodegradable Mg alloy and contributes to the development of nanocrystalline Mg alloys.

METHODS: The as-cast ingots of Z2 alloy were provided by Suzhou Origin Medical Technology Co. Ltd., China. The specimen for determination of the microstructure was characterized by Electron Backscatter Diffraction (EBSD) measurements performed with a scanning electron microscope (Mira3 (SEM) & Aztec Nordlys Max3). TEM images were obtained using an FEI Talos-F200X (200kV) equipped with a field-emission gun. Corrosion morphology was characterized through an SEM with energy dispersive spectroscopy (TESCAN-RISE).

RESULTS: Figure 1 shows the partial nanograins with Zn segregation at grain boundaries (Fig.1a) and the mechanism for grain refinement of Z2 alloy during hot working processes (Fig.1b). Through control grain boundaries precipitates and segregation, the degradation property can be improved. Finally, the degradation rate in vivo within two weeks of implantation for Z2 alloy is slower than high-purity Mg (Fig. 1c).

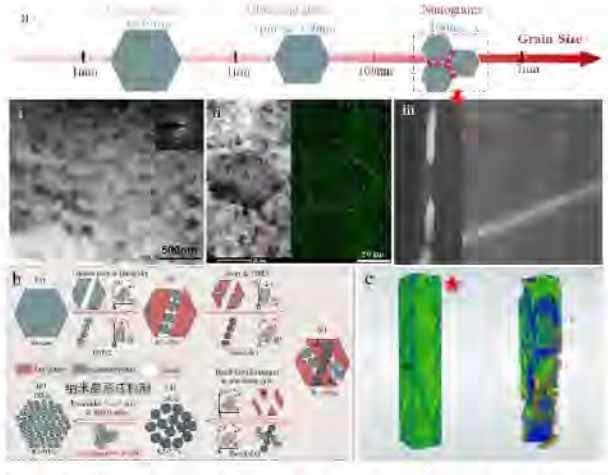

Fig. 1: The formation of nanocrystals and grain boundary segregation in Z2 alloy during dynamic recrystallization.

DISCUSSION & CONCLUSIONS: Nanograins with Zn segregation at their GBs were successfully produced in a lean biodegradable Z2 alloy via hot rolling. The nanocrystalline Z2 alloy demonstrates high strength and good corrosion resistance. During the hot working processes, the created sample microstructure and rolling parameters meet the condition for the activation of pyramidal <c+a> slip, and multi-slips dominated the deformation mechanism and DRX to form the nanocrystals rounded by Zn atom final microstructure.

REFERENCES: [1] Wenhui Wang, Carsten Blawert, Rui Zan, Yu Sun, Hongzhou Peng, Jiahua Ni*, Pei Han, Tao, Suo, Yang Song, Shaoxiang Zhang*, Mikhail L Zheludkevich*, Xiaonong Zhang*, A novel lean alloy of biodegradable Mg-2Zn with nanograins, Bioactive Materials, 6, (2021), 4333-4341.

ACKNOWLEDGEMENTS: This work was supported by grants from the National Natural Science Foundation of China (No. 52201300) and the China Postdoctoral Science Foundation (No. 2021M702090).

15th Biometal
AUGUST 21 TO 27, 2023
Grand Hôtel San Michele, Cetraro, CS, Italy

Metal-calcium phosphate biodegradable composites for load-bearing orthopaedic applications

EB Montufar[1], M Casas-Luna[1], S Tkachenko[1], K Slámečka[1], S Diaz-de-la-Torre[2], N Hort[3], L Čelko[1]

[1] CEITEC, Brno University of Technology, Brno, CZ. [2] CIITEC, National Polytechnic Institute, CDMX, MX, [3] Helmholtz-Zentrum Hereon GmbH, Geesthacht, DE

INTRODUCTION: Biodegradable metals allow the fabrication of temporal osteosynthesis devices, which provide functional and safe reduction of bone fractures without the need for a second surgery. However, the larger the implant the major is the generation of degradation products and the greater the challenge for their elimination. One approach to reducing the production of corrosion products is the development of metal matrix composites [1,2], in which a resorbable calcium phosphate (CaP) replaces an important fraction of metal, while ideally producing a mechanically stronger and more bioactive material. This work shows the processing (two different approaches), performance and cytocompatibility of magnesium and iron composites reinforced with CaPs.

METHODS: Iron/tricalcium phosphate (Fe/TCP) particle-reinforced composites were produced by spark plasma sintering (SPS). Homogeneous powder mixtures (0 to 100 % Fe) were sintered at 1000 °C for 10 min (heating rate of 100 °C/min) and 35 MPa compaction load. In contrast, magnesium/hydroxyapatite (Mg/HA) interpenetrating phase composites were produced by liquid Mg infiltration into HA scaffolds. The scaffolds were produced by extrusion-based additive manufacturing (robocasting) to control the geometry, distribution and fraction of the constituents. The infiltration of Mg was conducted by current-assisted metal infiltration (CAMI), in the SPS device at 670 °C for 2 min. Materials' characterization included XRD, SEM, EDX, µCT, degradation kinetics, changes in composition and mechanical performance with degradation, and evaluation of cytotoxicity.

RESULTS: SPS produced high strength, low modulus and biodegradable Fe/TCP composites (Fig. 1a). The addition of 25% TCP generated the highest compressive strength and toughness, whereas, at 75% TCP, a lightweight composite with stiffness and specific strength fulfilling the requirements for bone fracture fixation was obtained. The composites had a degradation rate of around 200 µm/year and were cytocompatible.

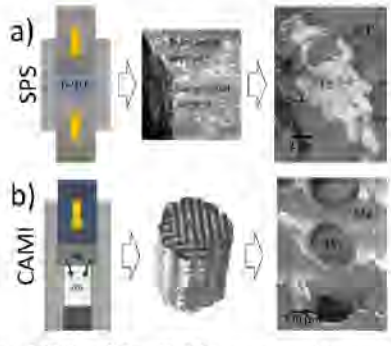

Fig. 1: a) SPS of Fe/TCP composites and b) CAMI of Mg/HA composites.

CAMI produced dense (99%) Mg/HA composites with an interpenetrating biphasic structure (Fig. 1b), where each phase (about 50%) was self-connected, run continuously through the material and provide mechanical stability, resulting in a yield strength similar to that of pure Mg. The high reactivity of liquid Mg produced a MgO layer at the Mg-HA interface and Mg_2Ca precipitates on the Mg grain boundaries. The composites had a degradation rate of around 5 mm/year and generated cell viability of 70% after 24 h of culture.

DISCUSSION & CONCLUSIONS: SPS and CAMI minimize the formation of secondary phases improving the interfacial contact and efficient stress redistribution, which increase the mechanical strength. Strong Fe/TCP composites have a low degradation rate suitable for the fabrication of load-bearing implants that resorb in the long term, whereas Mg/HA composites need further optimization to reduce the degradation rate before exploiting their advantages.

REFERENCES: [1] E.B. Montufar, et al (2018) *Acta Biomat* **70**:293-303. [2] M. Casas-Luna, et al (2022) *J Mg Alloys* **10**: 3641-56.

ACKNOWLEDGEMENTS: This work was supported by Czech Science Foundation (GACR 23-07879S).

Laser-Induced Single-Step Coating Of Hydroxyapatite On SPS-Consolidated Fe And Fe-Mg Alloys

R Estrada[1,2], Kwon Dae-Hyeok[3], M Multigner[2], B Torres[2], J Rams[2], M Lieblich[1], Han Hyung-Seop[3]

[1] CENIM-CSIC, Madrid 28040, ES, [2] URJC, Madrid 28933, ES, [3] KIST, Seoul 02792, KR

INTRODUCTION: Fe and Fe-Mg alloys have been suggested as viable materials for temporary bone scaffold implants because of their ability to achieve appropriate degradation rates, mechanical properties and cell attachment to promote bone tissue regeneration [1-3]. In this study, Fe and Fe-Mg scaffolds were fabricated through spark plasma sintering. To control the degradation behavior and enhance cell attachment, hydroxyapatite coatings were applied to the sample surfaces using laser-induced single-step coating (LISSC) with Hanks' and DMEM solutions.

METHODS: Fe, Fe5Mg and Fe10Mg powder (Fe: 99.7% purity, dia. ≤74 µm; Mg: 99.8% purity, dia. ≤100 µm) were obtained by attrition ball milling under nitrogen atmosphere at 1400 rpm. SPS was carried out at 600 ºC and 80 MPa during 5 minutes. The resulted SPS samples were also covered by LISSC technique in modified Hanks´ and DMEM solutions by the addition of $CaCl_2$ (1 M, C5670, Sigma-Aldrich, USA) and H_3PO_4 (1 M, P5811, Sigma-Aldrich, USA) until increasing x100 the original Ca and P content in the solutions. For the surface treatment a nanosecond ytterbium fiber laser (Biolino MOPA, Laservall, Hong Kong) with a wavelength of 1064 nm and focal length of 160 mm was used. Power, scan speed and loop count were modified in order to produce a heterogeneous hydroxyapatite coating.

RESULTS: SPS samples made of non-milled Fe showed very low porosity (*Figure 1a*) when compared with milled Fe and Fe-Mg SPS samples (*Figure 1b*).

Different conditions were tested for the production of hydroxyapatite coatings on the SPS samples using Hanks´ and DMEM solutions as precursors. For the hydroxyapatite production higher power was employed when using Hanks´ solution, as a result the laser pattern is more noticeable (*Figure 2a*) compared with the DMEM treatment (*Figure 2b*). Higher magnification revealed that the covering obtained with Hanks´ solution (*Figure 2c*) consisted on a very thin surface on top of the laser pattern, whereas hydroxyapatite was found on the whole surface of the SPS samples when using DMEM (*Figure 2d*).

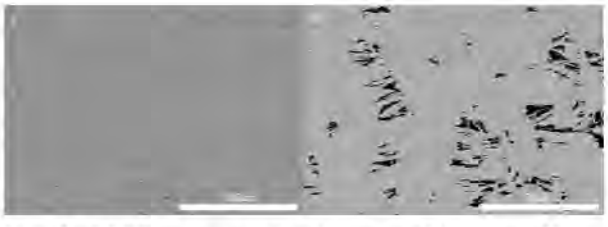

Fig. 1: SEM cross section images of (a) pure Fe and (b) milled Fe sintered SPS samples.

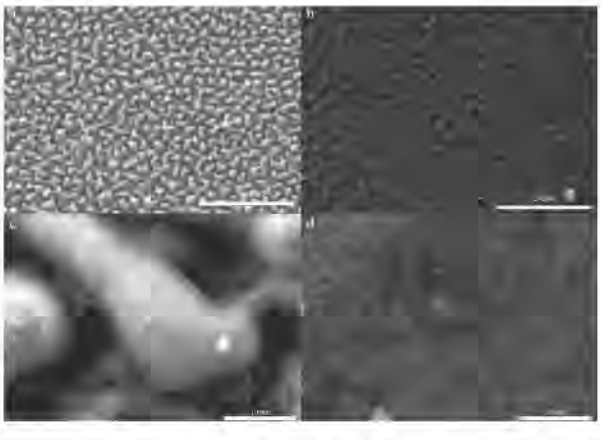

Fig. 2: SEM images of SPS Fe10Mg hydroxyapatite covered samples in (a,c) Hanks´ and (b,d) DMEM solutions by LISSC technique.

DISCUSSION & CONCLUSIONS: Different laser conditions produced different hydroxyapatite coatings, slower scan speed and higher loop counts increase the hydroxyapatite coating production. Also, DMEM appears to be more suitable for a higher covering of the sample surface than Hanks´ solution.

REFERENCES: [1] Y.Guangyin and N.Jialin, Patent CN103028148A (2012). [2] R Oriňáková, A Oriňák, et al. (2013) *Int J Electrochem Sci* 8:12451. [3] M.Multigner, M.Lieblich et al. (2019) *11th Sym. on Biodegradable Metals*, Met-3.

ACKNOWLEDGEMENTS: Spanish MICINN: PID2019-104351GB-C21, RTI2018-096391-B-C31, PID2021-123891OB-I00 and thanks to student Sara Suárez Ordóñez.

Biodegradable zinc and zinc-magnesium alloy subjected to thermal shocks – microstructural and mechanical aspect

M.Wróbel[1], A.Jarzębska[1], Ł.Maj[1], M.Kulczyk[2], M.Bieda[1]

[1] *Institute of Metallurgy and Material Science, Polish Academy of Sciences, Kraków, Poland*
[2] *Institute of High Pressure Physics, Polish Academy of Sciences, Warszawa, Poland*

INTRODUCTION: The low recrystallization temperature and low mechanical properties of pure zinc limit the use of this material as a potential candidate for cardiovascular stents[1]. While the mechanical properties can be improved by the use of alloying additives and plastic deformation[2], the problem of recrystallization processes of this material is more complicated, yet interesting in terms of future application. Considering the fact, that recrystallization processes results in microstructural changes it can significantly affect stability of mechanical properties Alloying additives can improve this temperature, however, plastic deformation, by increasing the stored energy of the material, can lead to acceleration of recrystallization processes[3]. Knowing the fact, that zinc-based materials are particularly susceptible to temperature effect it is important to check a behavior of zinc and zinc-based alloys under the critical conditions, bearing in mind stents manufacturing process and transporting the final product.

METHODS: Pure zinc, as a reference material, and zinc-magnesium alloy with 0.6 wt.% of Mg addition were prepared by gravity casting followed by hot extrusion (HE) and hydrostatic extrusion (HSE) at 4 consecutive passes. Subsequently, various annealing to 50°C and cooling to -50°C sequences were applied. The investigations of microstructural stability by SEM/EBSD were performed on both longitudinal and transverse cross-sections to the extrusion direction (ED). Moreover, the mechanical stability by the use of static compression tests at room temperature was examined.

RESULTS: Depending on the material, microstructures consisting of α-Zn fine grains or α-Zn fine grains with Mg_2Zn_{11} intermetallic phase, which formed bands parallel to ED were achieved. The performed annealing, cooling and thermal shocks revealed the positive effect of the magnesium addition on the stability of materials. Moreover, an improvement in yield strength obtained for materials subjected to temperature treatment was achieved. The highest value, i.e. 365 MPa was observed for Zn-0.6Mg after annealing at 50°C Furthermore, based on stress-strain curves slight differences in mechanical behaviour of zinc-based materials depending on the type of used treatment were observed.

DISCUSSION & CONCLUSIONS: The zinc-magnesium alloy is characterized by better thermal stability during heat treatment due to the presence of an Mg_2Zn_{11} phase that inhibits the static recrystallization process. Orientation maps from both cross-sections did not reveal significant differences in the microstructure. Performed compression tests revealed that comparing the initial state and annealed at 50 degrees, the latter led to improvement in yield strength as a result of recovery processes. Both, the cooling and the combination of annealing and cooling resulted in a decrease in strength compared to the material after hydrostatic extrusion. However, mechanical properties even after two cycles of extreme temperatures are higher than minimum requirements for cardiovascular stents.

REFERENCES: [1]E.Mostaed et.al (2018) *Zinc-based alloys for degradable vascular stent applications* Acta Biomaterialia, **71**:1-23. [2]A. Jarzębska et.al (2018) *A new approach to plastic deformation of biodegradable zinc alloy with magnesium and its effect on microstructure and mechanical properties* Mat. Letters **211**:58-61. [3]G. Li et.al (2019) *Challenges in the use of zinc and its alloys as biodegradable metals: Perspective from biomechanical compatibility* Acta Biomaterialia **97**:23-45.

ACKNOWLEDGEMENTS: This research was partially co-financed by National Science Centre Poland, project number UMO 2020/39/O/ST5/02692.

Titanium Surface Coated by polypyrrole /Gelatin-methyl acrylic Electroconductive Hydrogel for Bon Formation

GX TAN[1], Y Liu[1], L Zhou[2]

1 School of Chemical Engineering and Light Industry Guangdong University of Technology Guangzhou, 510006, China

2 Guangzhou Key Laboratory of Spine Disease Prevention and Treatment, Department of Spine Surgery The Third Affiliated Hospital, Guangzhou Medical University Guangzhou, 510150, China

INTRODUCTION: Titanium due to elastic modulus which close to the bone and the advantages of strong corrosion resistance and biocompatibility has been widely used as hard tissue replacement materials. However, because of a shortage of bone induction ability, lack of strong chemical combination with the surrounding tissue, titanium materials increased the risk of implants and limited its clinical application in many areas. In this work, titanium surface was modified by grafting different functional hydrogel coatings to enhance the substrate binding force.

METHODS: Chondroitin sulfate reacted with methyl acrylic acid anhydride (MA) after introducing crosslinking agent methyl acrylamide, oxidation of CS-MA solution in the presence of ultraviolet light and light initiator type UV polymerization for oxidation CS-MA hydrogel. ^{1}H-NMR, Infrared Spectrum (IR), Scanning Electron Microscope (SEM) characterization were used to characterize the composition and morphology of aldehyde CS-MA. The polymer monomer pyrrole solution was deposited through electrochemical method for preparing the conductive hydrogel coatings on titanium surface. Covalent bonding of electroconductive hydrogel layers to gold-sputtered titanium surfaces via photoinitiated thiol-ene click reaction.

RESULTS:

Table1 Electrochemical parameters obtained by fitting the impedance diagram of chemically modified electrode

Eleetrodes	n	R_s (Ω)	R_{ct}(Ω)	$10^3 Z_w(\Omega_s^{\frac{1}{2}})$
Ti-SH	0.8	87.34	23.16	13.46
Ti-SH-GelMA	0.8	45.45	992.3	5.353
Ti-SH-	0.8	37.08	190.0	5.692

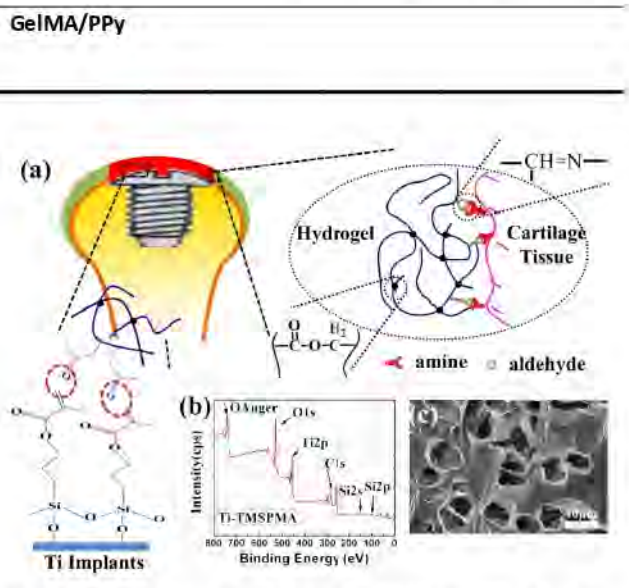

Fig.1 Schematic illustration of mechanism for CS-MA aldehyde hydrogel construction on titanium and simultaneous tissue integration; (b) XPS overview spectra of Ti-TMSPMA; (c) Low-magnification and high magnification scanning electron microscope (SEM) images of the CS-MA aldehyde hydrogel on Ti-TMSPMA

DISCUSSION & CONCLUSIONS: The research results showed that titanium surface after dealing with the thiol self-assembly. The bonded strength with the conductive hydrogel/hydrogel increased greatly. The conductivity of materials was higher than through silane coupling agent processing. Conductive hydrogel coatings on titanium surface can be used for glucose biosensor detection. In vitro cell experiment results showed that the conductive hydrogel coatings had good biological compatibility.

REFERENCES: [1] Zhou L, Tan G X,etal(2014). Modification of biomaterials surface by mimetic Frontiers of Materials Science, 8(4): 325-331. [2] Topkaya S N., et al (2015) Biosensors and Bioelectronics, 64: 456-461

ACKNOWLEDGEMENTS: This work was supported by the National Natural Science Foundation of China (Nos. 51932002)

Designing high performance Fe-Mn-Si biodegradable alloys by quaternary element additions

A. Coda[1], C. A. Biffi[2], J. Fiocchi[2], J. N. Lemke[1], A. Tuissi[2]

[1] SAES Getters S.p.A., Lainate (MI), Italy. [2] 2National Research Council - Institute of Condensed Matter Chemistry and Technologies for Energy, CNR ICMATE Lecco, Italy.

INTRODUCTION: Fe-Mn remains one of the most attractive systems for the development of bioabsorbable temporary orthopaedic and vascular implants in applications where high load-bearing capacity are required[1]. However, currently, these materials do not degrade within an appropriate amount of time in the physiological environment. On the other hand, the versatility of tailoring this metallic system by alloying can provide many opportunities to customize bioresorbable devices and represent a promising approach to accelerate degradation by further improving the mechanical properties, allowing for thinner implant structures, and enabling miniaturization. In addition, inducing secondary noble phases in the microstructure could provoke local micro-galvanic corrosion effects that lead to faster absorption rates[2]. By tailoring Fe-Mn content, steels that exhibit a great combination of high strength and ductility due to twinning induced plasticity (TWIP) and transformation induced plasticity (TRIP) effects during mechanical deformation can be designed[3]. Moreover, the addition of Si has already been demonstrated as being an effective strategy to improve the mechanical properties while maintaining a similar corrosion susceptibility and biocompatibility[4].

METHODS: In this study, small additions of noble and biocompatible elements (Au and Pt) were assessed as approach to design Fe-Mn-Si-X quaternary alloys with improved degradation rates and elevated mechanical properties. The alloys were prepared by arc-melting and processed by thermo-mechanical rolling and annealing techniques. Chemical and microstructural analyses were carried out to study the tensile test performance and degradation behaviour of the alloys. Short and long-time corrosion behaviour under simulated body conditions were characterized by pseudo-potentiostatic, potentiodynamic, electrochemical impedance spectroscopy and evaluation of degradation products.

RESULTS: The addition of Au and Pt changed the tensile properties of the Fe-Mn-Si-X alloys. In details, Young modulus and the Ultimate tensile stress values were reduced in the doped alloys than the ternary one (see Figure 1a). The decrease of the alloy's strength was balanced by an increase of the ductility (elongation to failure). The degradation rates were also increased by the addition of the Au and Pt elements, as depicted by Figure 1b.

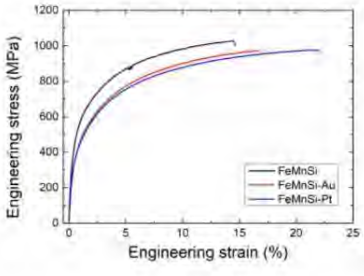

(a)

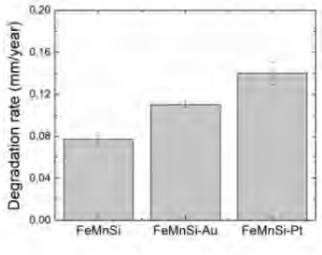

(b)

Fig. 1: Tensile properties (a) and degradation behaviour (b) of the investigated alloys.

DISCUSSION & CONCLUSIONS: This work sheds light on the possibilities to engineer Fe-Mn-Si biodegradable alloys by inducing uniformly distributed particles of quaternary noble element within the alloy matrix so as to tailor them for medical implants, optimizing both mechanical and corrosion performance.

REFERENCES: [1]A. Francis, Y. Yang, S. Virtanen, A.R. Boccaccini - *Journal of Materials Science: Materials in Medicine* (2015), [2]M. Schinhammer, P. Steiger, F. Moszner, J.F. Löf, P.J. Uggowitzer, *Mater. Sci. Eng. C.* (2013), [3]R. Gorejová, L. Haverová, R. Oriňaková, A. Oriňak, M. Oriňak, *J. Mater. Sci.* (2019), [4]J. Fiocchi, J.N. Lemke, S. Zilio, C.A. Biffi, A. Coda, A. Tuissi, *Mat. Today Comm.* (2021).

Degradative response of Fe-Mn-C alloys in albumin-supplemented SBF

Quang Nguyen Cao[1], Abdelhakim Cherqaoui[1], Carlo Paternoster[1], Maria Laura Gatto[1,2], Marcello Cabibbo[2], Paolo Mengucci[3], Diego Mantovani[1]

[1] Laboratory for Biomaterials and Bioengineering, Dept. of Min-Met-Materials Engineering, Research Center of CHU de Quebec, Division of Regenerative Medicine, Laval University, Quebec City, QC, G1V 0A6, Canada; [2] Dept. DIISM, Università Politecnica Delle Marche, Via Brecce Bianche 12, 60131, Ancona, Italy; [3] Dept. SIMAU & UdR INSTM, Università Politecnica Delle Marche, Via Brecce Bianche 12, 60131, Ancona, Italy

INTRODUCTION: Fe-based alloys show long-term degradation, as well as excellent mechanical properties, close to those of standard alloys for reparative surgery (L605 and AISI 316L). In particular, Fe-Mn alloys can be considered as the most promising candidates for absorbable implants, such as cardiovascular stents and orthopedic prostheses. Improved mechanical properties and corrosion rates can be obtained designing the chemical composition of Fe-Mn alloys [1]. Specifically, Fe-Mn-C alloys are of great interest due to the combination of high strength and ductility, and degradability with limited cytotoxic effects in the human body. However, the release of ions has to be controlled, since their local accumulation could lead to the occurrence of adverse biological effects [2]. Degradative behavior of different Fe–Mn alloys has already been investigated by several authors in a variety of pseudo-physiological solutions. However, few studies in literature focused on the degradative response of Fe-Mn-C alloys to artificial biological fluids containing albumin, present in human plasma [3]. Aim of this experimental work is to extend the know-how on degradative response of newly developed Fe-Mn-C alloys to albumin-enriched SBF.

METHODS: Three different Fe-based alloys including Fe-C (AISI 1018), Fe-5Mn-0.4C and Fe-20Mn-1.2C were investigated in as-received condition and after 14 days of static immersion degradative tests in albumin-supplemented Hank's solution (AS-MH), phosphate-buffered saline (AS-PBS), and sodium chloride (AS-NaCl), according to the ASTM G31-03. Morphology, chemical composition and microstructure of samples in as-received condition and after immersion test were analysed my scanning electron microscope (SEM), energy dispersive microanalysis (EDS) and X-ray diffraction (XRD). Corrosion rate (CR) of alloys after immersion tests was compared.

RESULTS: Fe-C and Fe-5Mn-0.4C show α-Fe (ferrite) body-centered cubic (bcc) phase (ICDD 6-696), in both as-received condition and after static immersion degradative tests in all albumin-supplemented SBF. On the other hand, Fe-20Mn-1.2C samples show γ-Fe (austenite) face-centered cubic (fcc) phase (ICDD 52-512). Sample AS-MH also exhibits poorly crystallized $Ca_2P_2O_7$ – calcium phosphate (ICDD 23 – 871), as reported in Fig. 1.

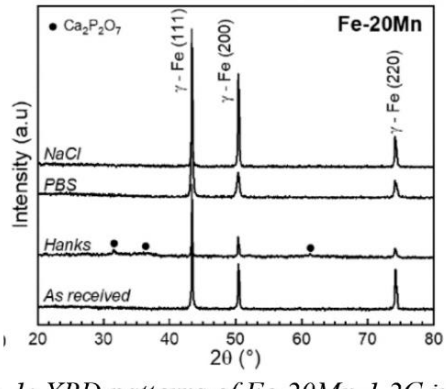

Fig. 1: XRD patterns of Fe-20Mn-1.2C in as-received condition and after 14 days static immersion degradative.

Furthermore, AS-NaCl exhibits the highest CR, regardless to the alloy composition, contrary to AS-PBS, which enables the lowest mm/year rates of degradation. Moreover, Fe-5Mn-0.4C has the highest degradation rates in all three solutions.

DISCUSSION & CONCLUSIONS: Among the different Fe-Mn-C alloys investigated, Fe-5Mn-0.4C shows the highest degradation rate in the albumin-enriched SBF considered in this study. However, static immersion degradative tests should carried out for longer time to detect their effect on microstructure evolution.

REFERENCES: [1] J. Fiocchi et al., *Effect of laser welding on the mechanical and degradation behaviour of Fe-20Mn-0.6 C bioabsorbable alloy*, J. Mater. Res. Technol. (2020). [2] S. Gambaro et al., *Mechanical and degradation behavior of three Fe-Mn-C alloys for potential biomedical applications*, Mater. Today Commun. (2021). [3] E. Mouzou et al., *In vitro degradation behavior of Fe–20Mn–1.2 C alloy in three different pseudo-physiological solutions*, Mater. Sci. Eng. C (2016).

Corrosion

Friday, August 25th, 2023

15th Biometal
AUGUST 21 TO 27, 2023
Grand Hôtel San Michele, Cetraro, CS, Italy

Can We Make Better Use of Magnesium Degradation?

Jia Pei[1*], Guangyin Yuan[1], Wenjiang Ding[1]

[1] *National Engineering Research Center of Light Alloy Net Forming, State Key Laboratory of Metal Matrix Composites and Center of Hydrogen Science, Shanghai Jiao Tong University, Shanghai, 200240, China.*

INTRODUCTION: The biodegradable metallic implants have revolutionized the concept of biomaterials from merely permanent mechanical replacement devices towards biological solutions for considerable efficacy[1,2]. Magnesium (Mg), due to its high reducibility (-2.37 V vs. SHE), is prone to suffer electrochemical and chemical corrosion reactions under aqueous environment in human body, which thus endow it with unique degradability characteristic to dissolve into Mg^{2+} ions and hydrogen gas evolution[3]. On one hand, the overfast, uncontrolled degradation presents as an innate drawback of Mg that arouse concerns on the risk of early structural failure, and moreover, deterioration of biocompatibility and bio-efficacy caused by excessive release of degradation products, e.g., the gas pocket, the local alkalization and elevated level of Mg^{2+} that dramatically disturb the microenvironment and even invoke severe adverse effects[4]. As such, the intrinsic degradation characteristic of Mg poses a critical obstacle for its clinical translation.

Therefore, the question which then arises is can we better leverage the degradation of Mg to exploit its full potential as next-generation revolutionary biomaterials and devices for compelling outcomes? Herein, in light of the potential bio-effects of its degradation products, we would like to show some of our studies in which the degradation behaviours of Mg bulk implants or nanomaterials could be modulated on demand for controlling the release of main degradation products, Mg^{2+} and hydrogen gas, each of which could be employed to elicit appropriate bioactivity, and even additional bio-functions, for a variety of possible applications ranging from supportive implants, tissue regeneration engineering, and nanomedicine to treat chronic diseases.

METHODS: A biocompatible, self-assembly, thin coating system was designed and prepared to control the degradation of Mg matrix. Both the degradation behaviour, particularly the release of degradation products, and biological responses were systematically investigated *in vitro* and *in vivo*, in different animal models regarding the potential applications of vascular stents, bone regeneration implants and nanomedicine.

RESULTS: The controlled, moderate release of Mg^{2+} was shown to be utilized for synergistic effects on accelerated re-endotheliatization and suppressed neointimal hyperplasia for vascular stent application, and on promoting osteochondral regeneration with scaffold implants. On the other hand, sustained, high-amount evolution of H_2 with Mg-based nanomaterials was demonstrated as a efficient treatment to beat cancer, kill bacteria, and ameliorate chronic inflammatory diseases.

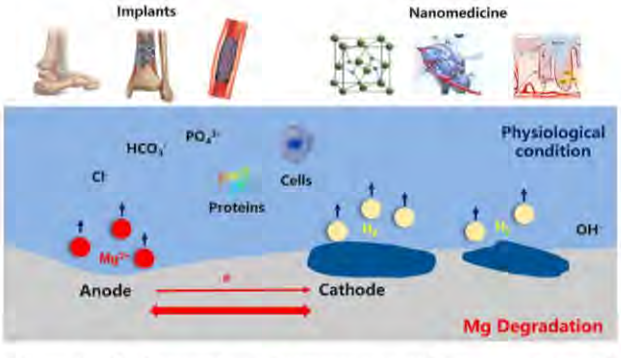

Fig. 1: Schematic illustration of leveraging Mg degradation for various potential applications.

DISCUSSION & CONCLUSIONS: Collectively, our studies provide some hints on harnessing the degradation of Mg, in particular, the degradation products of Mg^{2+} or/and H_2, to promote the development and deployment of Mg for various implants and nanomedicine applications.

REFERENCES: [1]*Nat.Med.* 2016, **22**: 1160. [2] *The Lancet* 2019, **394**:1243. [3]*Adv. Func. Mater.*2019, **29**: 1805402. [4]*Nat. Commun.* 2021, **12**: 2885

ACKNOWLEDGEMENTS: This work was supported by the National Science Fund for Excellent Young Scholars (52222108) and National Key Research and Development Program of China (2021YFE0204900).

Toward a mechanistic understanding of corrosion at the magnesium-biology interface through trace element analysis

M. Hannard[1,2], M. Cihova[1], A. Wichser[3], D. Bleiner[2,3], P. Schmutz[1]

[1] Laboratory for Joining Technologies and Corrosion, Empa - Swiss Federal Laboratories for Materials Science and Technology, Dübendorf CH-8600, Switzerland [2] Graduate School of Chemical and Molecular Sciences Zurich, University of Zürich, Zurich, CH. [3]Laboratory for Advanced Analytical Technologies Empa - Swiss Federal Laboratories for Materials Science and Technology, Dübendorf CH-8600, Switzerland.

INTRODUCTION: Biodegradable magnesium (Mg) implants have emerged as an alternative to permanent metallic implants in various biomedical applications[1]. However, the use of Mg implants is limited by their corrosion behavior in the physiological environment, which is often uncontrolled due to its large dependence on the species present in the peri-implant microenvironment, leading to premature implant failure and potential toxicity. Indeed, the complexity of the physiological environment including inorganic (*e.g.* various ions) and organic components (*e.g.* metabolites and proteins) makes a prediction of the acting corrosion mechanisms challenging. The interface reactivity is critically dependant on elements more noble than Mg, particularly transition metals such as Iron (Fe), which are present as trace elements in the material or biological environment. Indeed, their presence has been identified to create active cathodic sites during Mg biocorrosion, thereby accelerating its dissolution. Key to gain access to underlying mechanistic processes is the chemical nature of the interfacial layer forming on the corroding implant (see Fig. 1). Achieving this requires methods that combine both, high lateral resolution and high elemental sensitivity.

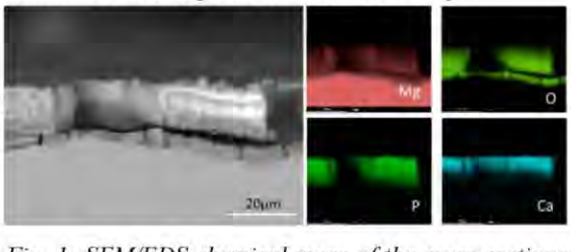

Fig. 1: SEM/EDS chemical maps of the cross-sectioned corrosion products formed on Mg. Adj. from [2].

METHODS: Conventional chemical analysis methods such as SEM/EDS or XPS are insufficient due to lack in elemental sensitivity or spatial resolution, respectively. To overcome this limitation, we here use laser ablation coupled with inductively coupled plasma mass spectrometry (LA-ICP-MS).[3] Optimization of both, lateral probing and trace-element analysis was conducted model systems for which Mg samples of varying trace element purity (*i.e.* 0.4 – 280 mg/kg (ppm) of iron), exposed to Simulated Body Fluids (SBF), were chosen. Additionally, an analysis of the SBF in contact with Mg was conducted using ICP-MS to determine their concentration changes in the liquid phase. Lastly, the electrochemical quartz crystal microbalance (eQCM) technique was employed to study the electrochemical behavior of Fe at low potentials (i.e. those generated by Mg oxidation, -1.5V), as this potential range is known to be impacted by strong hydrogen (H^+) reduction rendering electrochemical assessment of Fe-deposition processes impossible.

RESULTS & DISCUSSION: LA-ICP-MS has demonstrated sufficient sensitivity to detect trace elements of Fe in the corrosion layer and to discriminate the Mg samples with varying purities tested – data that is further correlated to the amount of dissolved Fe obtained by ICP-MS liquid-phase analysis. Current ablation parameters allow for couple-µm probing sizes. Further optimization is required to unlock analysis of early degradation stages (when the layer thickness is low). Finally, the eQCM method has provided complementary Fe-redeposition kinetics as well as trace-element quantification important in a domain of electrochemical potential where electrochemical signal cannot be tracked.

CONCLUSIONS: Combining LA-ICP-MS, ICP-MS and eQCM holds high potential to allow accessing mechanistic insights on Mg biocorrosion at relevant lateral and sensitivity scale, and will be relevant for *in vitro* and explant analysis alike.

REFERENCES: [1]F. Pan, et al. (2016) *J Mater Sci Technol*, 32(12), 1211-1221. [2]E. Bonyadi Rad, et al. (2017) *J Mater Sci: Mater Med*, 28, 1-11. [3]M. Stafe *et al.* (2014) Pulsed Laser Ablation of Solids, Springer Series in Surface science, 53, 241.

ACKNOWLEDGEMENTS: This research is financially supported by the MAGnostic project, funded by the Swiss National Science Foundation (SNSF, grant No: 310030E_205609).

Fatigue and corrosion fatigue behaviors of biodegrable Zn alloys

Huafang Li[1*], Cuie Wen[2], Luning Wang[1]

[1] *School of Materials Science and Engineering, University of Science and Technology Beijing, Beijing 100083, China*

[2] *School of Engineering, RMIT University, Melbourne, Victoria 3001, Australia*

**Corresponding author: Prof. Huafang Li (H.F. Li huafangli@ustb.edu.cn)*

INTRODUCTION: Zn alloys are emerging as a new class of biodegradable metallic materials due to their good biocompatibility, suitable biodegradability, and nontoxicity. However, the dynamic loading in the human body, along with the corrosive physiological environment, brings great challenges for the application of biodegradable Zn alloys. At present, there are few reports on the fatigue and corrosion fatigue properties of Zn alloys in simulated body fluid (SBF). Extruded Zn-0.8Li and Zn-2Cu-0.8Li alloys were selected in order to systematically evaluate their fatigue and corrosion fatigue behaviors.

METHODS: Fatigue testing was carried out using an MTS370.10 fatigue-testing machine produced by MTS Industrial Systems Co. (China) with axial sinusoidal loading. The stress ratio was set at R = −1 (tension–compression fully reversed) and the test frequency was 2 Hz. The fatigue tests were continued until complete failure of the sample or the test was stopped when the sample did not fail after 6.5×10^5 cycles. The maximum stress (stress amplitude) at which the sample did not fail after 6.5×10^5 cycles was defined as the fatigue limit. The corrosion medium used in the corrosion fatigue testing was SBF. A self-designed dynamic circulation system was installed on the fatigue-testing machine to simulate a corrosion fatigue environment. The fatigue and corrosion fatigue fracture morphologies were observed under SEM (Regulus 8100, Japan).

RESULTS:

Fig. 1 shows the fatigue and corrosion fatigue stress–life (S–N) curves of the extruded Zn-0.8Li and Zn-2Cu-0.8Li alloys in ambient temperature air and 37±1 °C SBF solution. It can be clearly observed that all materials had much longer fatigue lives in air than in SBF above the fatigue-endurance limit. In addition, the fatigue life decreased with an increase in stress amplitude.

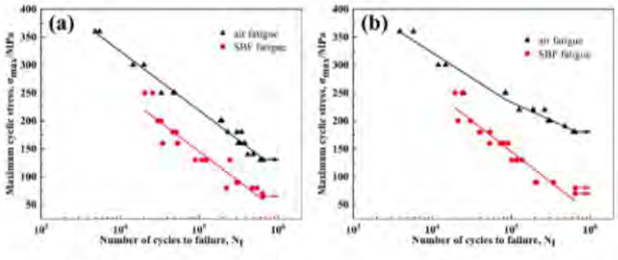

Fig. 1. Stress–life (S–N) curves for: (a) Zn-0.8Li alloy; and (b) Zn-2Cu-0.8Li alloy tested in air and in SBF.

DISCUSSION & CONCLUSIONS: The fatigue limits of the extruded Zn-0.8Li and Zn-2Cu-0.8Li alloys tested in air were about 135 MPa and 180 MPa, respectively, at 6.5×10^5 cycles. However, the corrosion fatigue limits of the Zn-0.8Li and Zn-2Cu-0.8Li alloys decreased by about 52% and 56%, respectively, in SBF, at 65 MPa and 80 MPa, respectively. The fatigue lives of both Zn alloys in SBF were clearly lower than in air and decreased with an increase in stress amplitude. The fracture mode of the Zn-0.8Li and Zn-2Cu-0.8Li alloys was quasi-cleavage fracturing. The corrosion fatigue cracks nucleated at the corrosion pits on the surfaces, which led to corrosion and mechanical deterioration under the actions of the stress cycle and the corrosion solution. Both the extruded Zn-0.8Li and Zn-2Cu-0.8Li alloys exhibited significantly increased corrosion rates in a corrosion fatigue environment and their corrosion rates increased with an increase in cyclic loading.

REFERENCES: [1] G.N. Li, S.M. Zhu, J.F. Nie, Y.F. Zheng, Z.L. Sun. *Bioactive Materials 6(5) (2021)* 1468-1478. [2] Y. Li, W. Li, F.S.L. Bobbert, K. Lietaert, J.H. Dong, M.A. Leeflang, J. Zhou, A.A. Zadpoor. *Acta Biomaterialia 106 (2020)* 439-449.

ACKNOWLEDGEMENTS: This work was financially supported by the Fundamental Research Funds for the Central Universities and the Youth Teacher International Exchange & Growth Program (No. QNXM20220020).

15th Biometal
AUGUST 21 TO 27, 2023
Grand Hôtel San Michele, Cetraro, CS, Italy

Influence of the drying process after electrodeposition of coating on AZ31

P Tamurejo-Alonso[1], ML González-Martín[2,3], MA Pacha-Olivenza[1,3]

[1] Department of Biomedical Sciences, Faculty of Medicine and University Institute of Biosanitary Research of Extremadura (INUBE), [2] Department of Applied Physics, Faculty of Science and University Institute of Biosanitary Research of Extremadura (INUBE). [3] Network Research Center on Bioengineering, Biomaterials and Nanomedicine (CIBER-BBN), Badajoz, Spain. [3]

INTRODUCTION: Magnesium and its alloys biomaterials have a high degradation kinetics in contact with the physiological environment. Electrodeposition of phosphates of calcium, magnesium and zinc oxide (HAMgZn) is an interesting option to this purpose. But the structures generated during electrodeposition are often not in equilibrium, especially in the case of these composite coatings[1]. There is a large amount of research on the different factors that control the electrodeposition. Current density, electrodeposition time and the application modes are extensively studied. However, there is a lack of information on the post-electrolysis processes, as thermal alkaline treatment or drying procedures. Particularly, drying affects the final aspect of the coating. The purpose of this research is to analyse the effect that temperature and pressure during the drying process could have on the electrodeposited coating.

METHODS: $Mg_3(PO_4)_2$ and ZnO were co-deposited with hydroxyapatite on AZ31 discs by electrodeposition. After electrodeposition, the samples were rinsed with distilled water and dried for two hours at 25, 50, 75 or 100 °C under ambient atmosphere or/and vacuum. The morphology and chemical composition of the coatings was analysed by SEM and EDX (Hitachi S-4800, Chiyoda, Tokyo, Japan).

RESULTS: In Figure 1 are shown the images of two of the treatments analysed. At 25 and 100ºC, crackle structures characteristic of the formation of magnesium and calcium phosphates are observed. On these formations, at 25ºC is obtained granular structures (Fig.1A), mainly of zinc according to EDX. These structures appear as opened when vacuum was applied simultaneously as temperature (Fig.1B). When drying temperature was 100ºC, zinc flowers are detected from EDX (Fig.1C-D), which show a great change in morphology when vacuum was applied along the drying process (Fig.1D).

DISCUSSION & CONCLUSIONS: Temperature and negative pressure during the post electroplating treatments affects considerably the final structure of the coverage. Higher temperatures appear as more effective for the appearance of larger structures in the coating, than lower ones. On the other hand, vacuum seems to provoke fractures in the structures of the coverage. On this base, attention has to be paid to the conditions of temperature and pressure during the final steps of material preparation. Different finished will provide surface that could better fit for antibacterial or osteointegration purposes according to the morphology obtained.

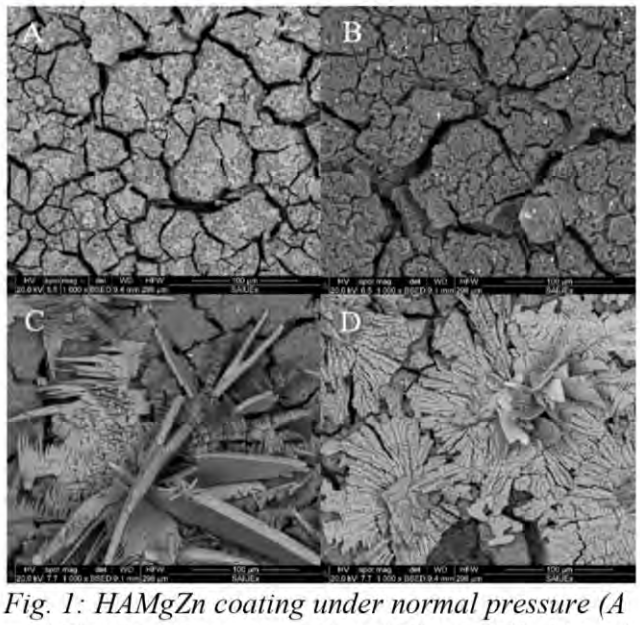

Fig. 1: HAMgZn coating under normal pressure (A and C) dried in vacuum (B and D), at 25ºC (A and B) and 100ºC (C and D).

REFERENCES: [1]Yulily D. Gamrburg, Giovanni Zangari (2011) Estructure and microstructure of electrodeposited metals and alloys, ISBN: 978-1-4419-9668-8

ACKNOWLEDGEMENTS: Authors are grateful to the Junta de Extremadura and FEDER (Fondo Europeo de Desarrollo Regional "Una manera de hacer Europa"), for financial help (RTI2018-096862-B-100 and GR18153). Also, authors acknowledge to NANBIOSIS and SACSS–SAIUEX.

Characterisation of time dependent corrosion by µCT-analysis and calorimetry

P Maier[1,2], R Schwarz[1], B Clausius[1], A Fragkakis[2], L Wadsö[2], D Orlov[2]
[1]*University of Applied Sciences Stralsund, School of Mechanical Engineering, Stralsund, Germany,*
[2]*Lund University, Faculty of Engineering, Lund, Sweden*

INTRODUCTION: Different approaches for determining the corrosion rate (CR) are found in the literature[1,2]. This study focuses on the corrosion rates and morphology of pure-Mg and WE43. Previous research found a CR_{WL} by weight loss measurement when immersed in Ringer's solution (*37 °C, 500 ml, samples 10 mm in diameter and 20/15 mm height*) of 2.7 mm/a for pure-Mg[3] and of 5.0 mm/a for WE43[4]. Critical corrosion pits with a pitting factor of 22.3 were found for pure Mg, and 9.9 for WE43, but with a less critical pit shape.

METHODS: The CR is evaluated by hydrogen gas (pressure evaluation, isothermal calorimetry[5], CR_{cal}) and by immersion in Ringer's solution (at 37±1 °C). Cylindrical samples had a diameter of 5 mm and a height of 10 mm. 17 ml of solution was used during calorimetry (exposure time 24 h) and 330 ml during immersion (exposure time up to 168 h). During immersion, a µCT scan was performed every 24 h. After immersion, the CR was determined from the volume loss using µCT data, CR_{vol}, see Fig. 1 for extraction the of data from the corrosion layer, and the weight loss, CR_{WL}.

Fig. 1: *sample cross-section, left: µCT micrograph, right: extracted from corrosion layer*

RESULTS: Fig. 2 shows the thermal power and CR development by hydrogen gas evolution up to 24 h. In agreement to [5] the CR of Mg decreases (to 3.8 mm/a). The saturation of the pH value lowers reaction kinetics. However, the CR of WE43 rises after reaching a minimum at 7.5 h.

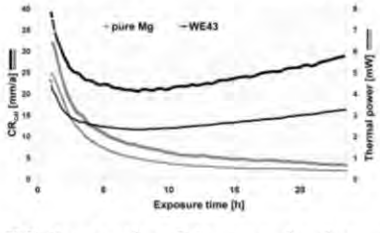

Fig. 2: *Thermal power and CR of WE43 and pure Mg up to 24h, $CR_{calMg-1}$ 3.8 mm/a, $CR_{calWE43-2}$ 27.5 mm/a*

While another Mg sample shows a similar CR_{calMg2} of 4.7 mm/a, WE43 shows a second reading of $CR_{calWE43-2}$ 38.7 mm/a, hinting at a strong influence of second phase appearance.

Fig. 3 shows samples from immersion tests at intervals ranging from 24 h to 168 h. While the corroded surface of WE43 shows overlapping shallow and wide pits, the initial corroded areas of pure Mg do not increase much after 24 h, but deepen[3]. From 96 h the CR_{VOL} of Mg remains at around 2 mm/a, see Fig. 4. The CR of WE43 is with a CR_{VOL} of around 10 mm/a much higher.

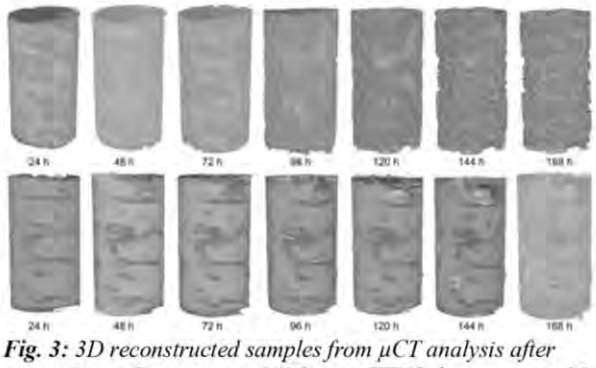

Fig. 3: *3D reconstructed samples from µCT analysis after immersion in Ringer up to 168 h, top: WE43, bottom: pure Mg*

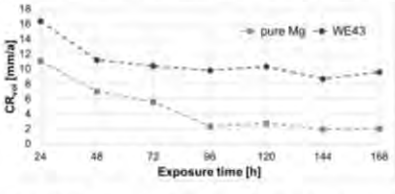

Fig. 4: *CR of WE43 and pure Mg after immersion in Ringer up to 168 h (CR by volume loss)*

According to the CR values in Table 1 (colour markings identify same samples) and Fig. 2 and 4, pure Mg (*italic*) starts off with higher CR and settles around 2-3 mm/a. The CR of WE43 (**bold**) seems very dependent on the corrosion method.

Table 1: *CRs of **WE43** & pure Mg of different methods*

WE43 / *Mg*	calorimetry, 17 ml			immersion, 330 ml		immersion, 500 ml
	CR_{cal}	CR_{vol}	CR_{WL}	CR_{vol}	CR_{WL}	CR_{WL} [3,4]
24 h	**27.5**	**14.9**	**11.9**	**7.9**	**3.8**	
	38.7	**16.7**	**11.4**	**16.4**		
	3.8			*6.2*	*2.6*	
	4.7	*10.4*	*6.9*	*11.1*		
168 h				**9.6**	**6.4**	**5.0**
				2.1	*5.4*	*2.7*

DISCUSSION and CONCLUSIONS: CR_{vol} for WE43 for 168 h is higher than CR_{WL}. This is in agreement with [1, 2] and shows that the corrosion product was not completely taken off by chromic acid. The values of pure Mg agree better, regardless of method, surface area and electrolyte volume, based on the fact that only local corrosion took place. The higher CR of WE43 is observed for all methods and is due to micro-galvanic reactions with second phases and is strongly influenced by the method. While the thermal power of pure Mg decreases after first interface reactions (1 h), WE43 shows an increase that also promotes secondary reactions.

REFERENCES: [1]D. Krüger et al. (2021) *J. Magnes. Alloy* 9, 2207-22. [2]L. Liu et al. (2018) *Appl. Sci.* 8(9). [3]P. Maier et al. (2017) *Magnesium Technology 2017*, 429-37. [4]P. Maier et al. (2018) *TMS Supplemental Proceedings*, 227-37. [5]D. Orlov et al. (2022) *Magnesium Technology 2022*, 253-54.

15th Biometal
AUGUST 21 TO 27, 2023
Grand Hôtel San Michele, Cetraro, CS, Italy

Sol-gel CaP deposition on magnesium alloy skeletal fixation devices for time-certain commencement of bioresorption

M Sanguedolce[1], A Chmielewska[2], L H Olivas-Alanis[2,3], T Avey[2], D H Cho[2], G Krieger[2], A Zhang[2,4], A A Luo[2], R C Advincula[5], D Dean[2,4]

[1]Dept. of Mechanical, Energy and Management Engineering, University of Calabria, Rende, CS, Italy. [2]Dept. of Materials Science and Engineering, The Ohio State University, Columbus, OH, USA. [3]School of Engineering and Sciences, Tecnologico de Monterrey, Monterrey, NL, Mexico. [4]Dept. of Plastic and Reconstructive Surgery, The Ohio State University, Columbus, OH, USA. [5]Dept. of Chemical and Biomolecular Engineering, Joint Institute for Advanced Materials, University of Tennessee, Knoxville, TN, USA.

INTRODUCTION: Resorbable magnesium alloys have been explored for skeletal fixation applications in order to remove the risk of device failure due to stress shielding, a phenomenon associated with the current standard-of-care, inert fixation device material, Ti-6Al-4V (aka Ti64). Ti64 has a bulk stiffness of 116 GPa whereas most biomedical Mg alloys have a stiffness of less than half that value. The stiffness of cortical bone is usually in the range of 18-25 GPa. Once resorbed, Mg alloys that serve in the role of skeletal fixation pose no risk of interrupting the normal loading of the newly healed bone. However, the bone will not heal if the Mg alloy resorbs too quickly or is not strong enough. Different strategies to produce devices with sufficient resistance to corrosion have been investigated with limited success [1]. We have explored the use of surface coatings to delay Mg alloy degradation until surgically repaired bone has healed. Here we present work on the deposition of a CaP ceramic coating via a sol-gel process on a novel magnesium alloy.

METHODS: Cast and heat-treated Mg-1.2Zn-0.5Ca0.5Mn (wt%) cylindrical coupons, polished with grit size up to 2000, were sonicated in absolute ethanol. Next, the coating procedure involves the sequential immersion and air drying of substrates using: 0.1 M titanium(IV) butoxide solution in 1–1(v/v) toluene-ethanol solvent, 1–1(v/v) toluene-ethanol solution, distilled water, a solution of 50 wt% HA and 50 wt% β-TCP nanoparticles dispersed in ethanol (0.9 mg/ml). The procedure, well detailed in [2], was performed for 5, 10, 15, 20 and 25 times to obtain different numbers of layers (i.e., coating thickness). The samples were cross-sectioned and analyzed through SEM to assess the thickness and homogeneity of the coatings and the presence of defects. Immersion tests in Hank's balanced salt solution at 36.5 ± 1 °C were performed based on [1, 3] and according to ASTM G31-72, in triplicates. The coated substrates are weighed before and after immersion tests after removing the corrosion products to estimate the weight loss. Uncoated coupons of the same magnesium alloy are used as a control.

RESULTS: Figure 1 shows an SEM image of a coated coupon and the presence of CaP micro-flakes typical of the deposited coating. As in our prior work, increasing the number of layers in the coating is expected to improve the corrosion resistance of the coupon. Our goal is to delay the commencement of corrosion for 3 months.

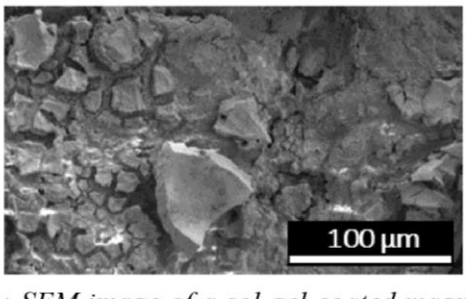

Fig. 1: SEM image of a sol-gel coated magnesium alloy coupon.

DISCUSSION & CONCLUSIONS: The introduction of a surface coating with varying thickness allows modulation of the degradation speed of the studied magnesium alloy, paving the way to proper deployment of stiffness-matched, resorbable skeletal fixation devices. We anticipate titrating coating thickness will allow us to modulate resorption so that the Mg alloy is not exposed to body fluid, and thus degradation does not occur, for 3 months.

REFERENCES: [1] D. Cho, T. Avey, K. H. Nam, D. Dean, and A. A. Luo. (2022) *Acta Biomater.* **150**:442–455. [2] A. Chmielewska, T. MacDonald, H. Ibrahim et al. (2020) *MRS Commun.* **10**:467–474. [3] J. Gonzalez, R. Q. Hou, E. P. S. Nidadavolu, R. Willumeit-Römer and F. Feyerabend, (2018) *Bioact. Mater.* **3**:174–185.

Influence of MnO inclusions in powder-processed FeMn alloys on their long-term corrosion behaviour in HBSS

C Tonna[1], J Buhagiar[1]

[1] *Department of Metallurgy and Materials Engineering, University of Malta, Msida, Malta.*

INTRODUCTION: Powder metallurgical methods for the preparation of materials for biodegradable applications, have gained a lot of interest in the past couple of decades, as have FeMn alloys [1]. However, the high oxygen affinity of Mn means that oftentimes highly stable oxides like MnO, are present in the sintered microstructures. Although it has been hypothesised that MnO inclusions behave cathodically in an austenitic FeMn matrix [2], there has so far been no scientific evidence suggesting that MnO inclusions microgalvanically accelerate the degradation of FeMn alloys.

METHODS: Fe35Mn coupons were prepared through the powder metallurgical route. 10 g of mixed Fe35Mn powder was pressed at 520 MPa using a hydraulic press and sintered for 3 hours at 1120°C under 100 l/hr N_2-5H_2 flow.

Two sets of samples were tested. The first were ground to expose MnO inclusions in the microstructure whereas a second set were ground and subjected to 5 min of ultrosonication in a solution containing 1 M HCl and 3.5 g/L hexamethylenetetramine (HMTA) to dissolve MnO inclusions without largely affecting the metal matrix. The removal of MnO from the microstructure was confirmed through visual inspection using SEM microscopy as well as through X-ray diffraction.

Electrochemical Impedance Spectroscopy (EIS) tests were performed on an exposed area of 1cm^2 of both sets of metals, over the course of 24 h at 37°C in HBSS (ThermoFisher Scientific, 14025). The resultant data was modelled using a nested two-time constant electrical equivalent circuit model to provide more detailed information about the corroding system.

RESULTS: EIS Bode plots generated during testing of both sets of FeMn samples were indistinguishable. On the other hand, fitting results, including fitting of charge transfer resistance (R_{ct}) in *Figure 1,* showed that the behaviour of FeMn without MnO was more repeatable over the first few hours of testing compared to FeMn with MnO inclusions. This is evident considering the presented curves for repeated tests.

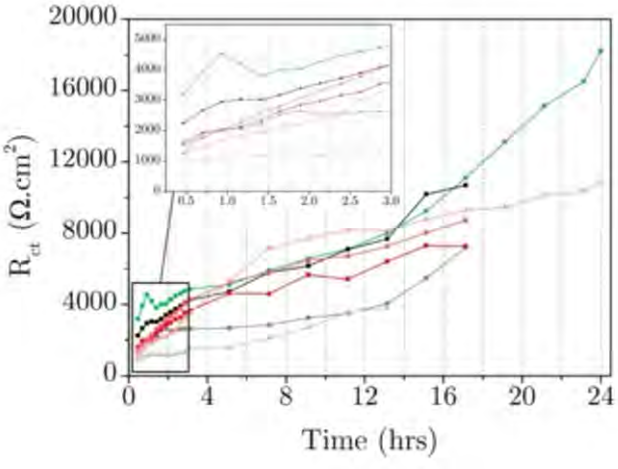

Fig. 1: Charge transfer resistance (R_{ct}) of powder processed Fe (green), FeMn with MnO (grays) and FeMn without MnO (reds) over a 24-h testing period in HBSS.

Post-test SEM analysis of the tested surfaces showed mild localised attack surrounding MnO inclusions whereas the MnO inclusions themselves remained intact, suggesting cathodic protection. Similar corrosion of FeMn matrix for samples from which MnO inclusions were chemically removed, was not observed.

DISCUSSION & CONCLUSIONS: Results indicate that MnO inclusions could have a cathodic influence on the surrounding austenitic matrix, especially during the first few hours from initial contact with the testing electrolyte. However, significant overlap of fitting results for FeMn with and without MnO over the next few hours, indicate that the long-term effects of MnO inclusions from a corrosion point-of-view, are not particularly significant.

REFERENCES: [1] J. Venezuela and M. S. Dargusch (2020) *Curr Opin Solid State Mater Sci* **24**:100822. [2] H. Hermawan, H. Alamdari, D. Mantovani and D. Dube (2008) *Powder Metall.* **51**:38-45.

ACKNOWLEDGEMENTS: The authors would like to thank the Malta Council for Science and Technology, for funding Project BioSA (R&I-2017-037-T) through FUSION: R&I Technology Development Programme.

Characterisation of a MgZnCa wire after corroding in "harsh environment"

P Maier[1], B Clausius[1], F Witte[2], D Mantovani[3], JF Löffler[4], A Griebel[5]

[1]University of Applied Sciences Stralsund, Germany, [2]Charité - Universitätsmedizin Berlin, Germany, [3]Laval University, Lab. for Biomaterials & Bioengineering, Canada, [4]ETH Zurich, Lab. of Metal Physics and Technology, Switzerland, [5]Fort Wayne Metals, USA

INTRODUCTION: *"The heart of man is very much like the sea" – Vincent van Gogh.*

The heart beats, the waves crash, the salt corrodes.

Given the connection between innovation and play[1], the authors seized an opportunity to conduct a unique *in mare* corrosion test at Biometal 14.

METHODS: The MgZnCa wire was cold-drawn to 140 µm with 70% cold work and wound onto an acetal copolymer spool (Fig. 1a). After storage in a plastic bag for several months it was subjected to an impromptu corrosion test in Mediterranean Sea coastal water (Fig. 1b) in August 2022 and fixed on a safety rope near a beach for 5 hours. Water temperature was a pleasant 26 °C with expected salinity of 3.7%[2]. There was a moderate wave action. The corroded wire (Fig. 1c), inspected by eye, changed its metallic glaze to a matte surface.

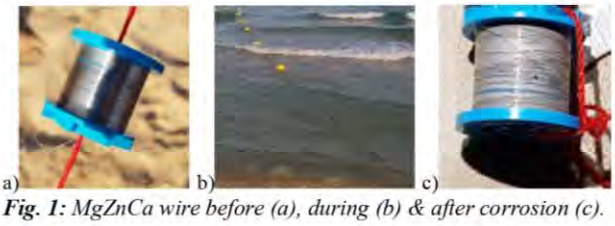

Fig. 1: *MgZnCa wire before (a), during (b) & after corrosion (c).*

µCT analysis was performed using an X-ray nano-tomograph SKYSCAN 2214 with a resolution of less than 500 nm. Knot and bending tests were also done to determine the mechanical properties.

RESULTS: The µCT-images (Fig. 2) show that the corroded MgZnCa wire itself has not changed significantly; a non-uniform growth of corrosion layers of two different densities is seen instead.

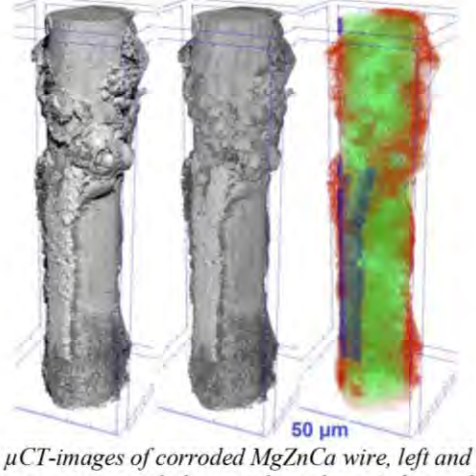

Fig. 2: *µCT-images of corroded MgZnCa wire, left and centre; corrosion morphology, right: colours indicate three densities.*

Figure 3 shows a 3D section of the corroded MgZnCa wire (near the red line) and its transversal and longitudinal cross-sectional µCT micrographs. The layer coloured in blue has a higher density, a constant low thickness and seems to protect the wire from corroding (area 1). The thicker, less dense and porous layer, coloured in red, results from the corroding wire underneath (darkened area near the surface, area 2). The µCT images still reveal a lot of non-corroded wire surface (bottom half at the cross-sections along area 3). A thin layer of higher density can be also seen there.

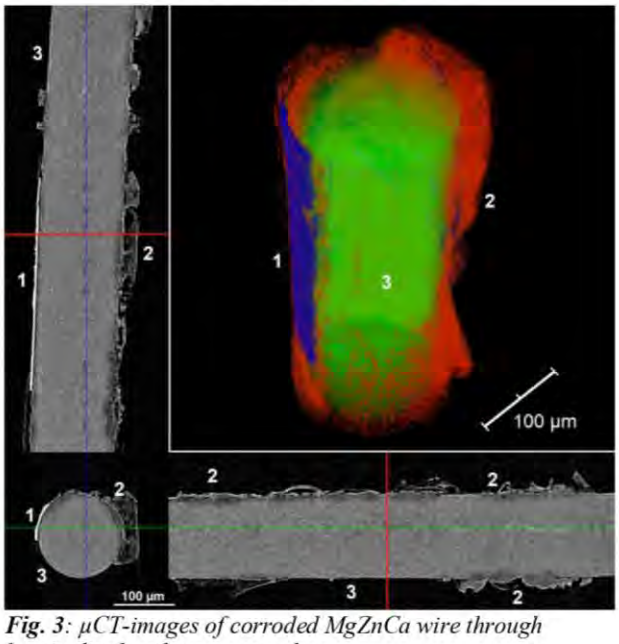

Fig. 3*: µCT-images of corroded MgZnCa wire through longitudinal and transverse planes.*

Manual knot and bending tests on corroded and uncorroded wires indicate some loss of mechanical resilience and formability from the corrosion process.

DISCUSSION & CONCLUSIONS: Corrosion of the MgZnCa wire in the Mediterranean Sea water embrittles the material more than expected from metallographic experiments, where no significant volume loss is observed. Besides the exposure to salty water (and some seaweed), a wave action and sand erosion might have played a role in the corrosion process. Wire corrosion analysis by more traditional methods is ongoing.

REFERENCES: [1]Bateson, P. "Play, Playfulness, Creativity and Innovation", Animal Behavior and Cognition 1(2):1-153, 2011. [2]https://www.esa.int/ESA_Multimedia/Images/2017/05/Mediterranean_Sea_salinity.

In situ investigation of stress-corrosion cracking in biodegradable implant material using SRµCT

B Hindenlang[1], DCF Wieland[1], D Tolnai[1], J Bohlen[2], R Willumeit-Römer[1]

[1] *Institute of Metallic Biomaterials, Helmholtz-Zentrum Hereon, Geesthacht, Germany*
[2] *Institute of Material and Process Design, Helmholtz-Zentrum Hereon, Geesthacht, Germany*

INTRODUCTION: Stress-corrosion cracking (SCC) is a severe problem for a lot of applications. In the case of biodegradable bone implants, its effect is critical since the SCC leads to a loss of mechanical stability and ultimately to a potential early failure of the implant. For future biodegradable bone implant design, understanding the initiation and propagation of SCC in the specific alloy is of high importance. With this knowledge, future implants can be designed to hinder this effect[1-3]. To understand SCC, an *in situ* loading and degradation experiment was performed using the material Mg10Gd. During the experiment, SRµCT images were taken at distinct strains to visualise the material's deformation and degradation process.

METHODS: For the experiment, samples of Mg10Gd, heat treated at 525°C for 8 hours then extruded directly at 400 °C with an extrusion ratio of 1:17, were used in the shape of cylindrical samples. At the region of interest, the samples had a diameter of 1.4 mm. The experiments took place at the P05 imaging beamline at the PETRA III storage ring, Deutsches Elektronen-Synchrotron (DESY). The µCT images were acquired in absorption mode at a photon energy of 33 keV and a binned voxel size of $(2.5\ \mu m)^3$. A custom-made loading frame was used, allowing simultaneous loading and degradation of the samples[4]. As degradation medium simulated body fluid (SBF) and as strain rates 10^{-3}, 5×10^{-4}, 10^{-4}, 5×10^{-5}, and 10^{-5} s^{-1} were used.

RESULTS: The experiments show a distinct difference between being performed in air and in SBF. For samples strained in air, the ultimate tensile strength (UTS) is significantly higher (230 MPa) than for samples in medium (200 MPa). However, comparing the UTS for different strain rates in air or in SBF, the differences are only minor and negligible in the given environmental condition. In SBF, degradation is only visible for slow strain rates lower than 10^{-4} s^{-1}. The degradation is even more pronounced for slower strain rates, indicating SCC. Furthermore, a preferential degradation at regions of highest stress is visible. Fig.1 shows the differences between two samples degraded in SBF and strained using 5×10^{-4} s^{-1} (a) and 10^{-4} s^{-1} (b) close to failure. A significant difference between both samples is visible.

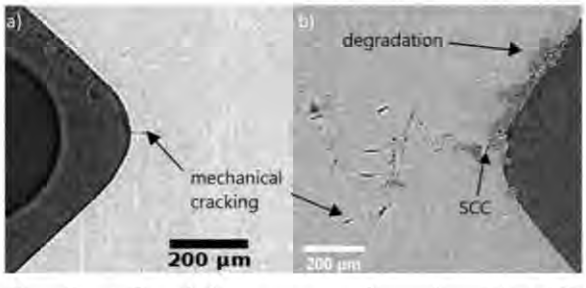

Fig. 1: a) Crack formation in degrading Mg10Gd at 200 MPa and a strain rate of 5×10^{-4} s^{-1}. b) Cross-section of degrading Mg10Gd at 230 MPa and a strain rate of 10^{-4} s^{-1} showing degradation, mechanical cracking, and SCC.

DISCUSSION & CONCLUSIONS: It was shown that for the used Mg10Gd alloy SCC is occurring. The tomograms show that in SBF a transition from a purely mechanical failure at high strain rates (10^{-3} s^{-1}) to SCC (10^{-5} s^{-1}) occurs. Furthermore, the preferential degradation at regions of highest stress enhances the SCC probability. At high strain rates, the time for degradation to influence the cracking and the initiation of SCC is too short, resulting in purely mechanical failure. Due to the lower strain rates, the deformation is slower, enabling more degradation and the occurrence of SCC. This shows that the initiation of SCC in Mg10Gd strongly depends on the applied strain and by that the time available for the material to degrade.

REFERENCES: [1]Winzer, N, (2005), A Critical Review of the Stress Corrosion Cracking (SCC) of Magnesium Alloys, Adv. Eng. Mater., 7: 659-693. [2]Jafari, S, (2015) A Review of Stress-Corrosion Cracking and Corrosion Fatigue of Magnesium Alloys for Biodegradable Implant Applications. *JOM* **67**, 1143–1153. [3]Maier, P, (2020), Characterization of an Extruded Mg-Dy-Nd Alloy during Stress Corrosion with C-Ring Tests. Metals, 10, 584. [4]Moosmann, J, (2019), A load frame for in situ tomography at PETRA III, Proc. SPIE 11113, 41

15th Biometal
AUGUST 21 TO 27, 2023
Grand Hôtel San Michele, Cetraro, CS, Italy

Plasma Treatment of Mg alloys for Biomedical Applications Improved the Degradation Rate of Magnesium Alloys

M Shekargoftar[1], S Ravanbakhsh[1], VS Oliveira[1], C Paternoster[1], A Sarkissian[1], F Witte[2] and D Mantovani1[1]

[1] Laboratory for Biomaterials and Bioengineering, *CRC-I, Department of Min-Met-Materials Eng., & University Hospital Research Center, Regenerative Medicine, Laval University, QC, Canada.*

[2] *Department of Prosthodontics, Geriatric Dentistry and Craniomandibular Disorders, Charité Universitätsmedizin, Berlin, Germany.*

[3] *Plasmionique Inc, QC, Canada.*

INTRODUCTION: Mg alloys are considered as promising biodegradable and oste-compatible materials. However, their rapid corrosion in physiological environments, associated with unpredictable hydrogen production has limited their clinical applications[1]. Surface modification of Mg alloys can be an effective method to improve their electrochemical behavior. In particular, the surface modification can be performed through plasma techniques, which have been widely used in various fields of materials science and engineering [2]. In this study, two plasma-based approaches were used for the treatment of Mg alloys: (1) plasma immersion ion implantation (PIII); and (2) magnetron sputtering for treatment of Mg alloys. The results show that the use of plasma processing resulted in enhanced corrosion properties of the selected Mg alloy (Novamag(R), nominal composition).

METHODS: Plasma treatments were performed on cylinders with a diameter of 3.4 mm and a height h = 2.4 mm. PIII treatments were carried out on PLASMIONIQUE's PBII-300, using O_2, N_2 and H_2 gases at a constant power P = 300 W for 60 min. The MgF_2 film was deposited using SPT320 magnetron sputtering system with a MgF_2 target and treated at constant power of P=200 W for 60 min. The surface properties of the samples were characterized using scanning electron microscope (SEM), and X-ray photoelectron spectroscopy (XPS). The corrosion resistance was evaluated using electrochemical impedance spectroscopy (EIS), and potentiodynamic polarization.

RESULTS: PIII treatment led to the formation of a thin, dense layer on the surface of the Mg alloys. The layer was composed mainly of MgO and $Mg(OH)_2$, confirmed by XPS, with thickness varied from 70 to 250 nm. PIII-treated samples, from SEM images, showed different surface morphologies compared to the untreated ones, and depending on the chosen implantation conditions. In addition, this treatment significantly decreased the corrosion rate (CR): untreated-Mg was 0.2 mm/y and decreased to 0.04 mm/y after PIII treatment. For what concerns the production of MgF_2, F/Mg atomic ratio was 1.8, close to the stoichiometric one in MgF_2. The SEM images showed that the film had a smooth and uniform surface morphology. CR for this family of coatings was around CR ~ 0.02 mm/y.

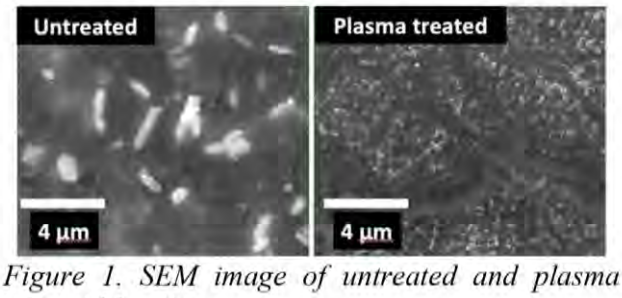

Figure 1. SEM image of untreated and plasma treated Mg alloy.

DISCUSSION & CONCLUSIONS:
The surface modification of Mg alloys using PIII, and magnetron sputtering resulted in differences in the thickness and composition of modified layer that impacted the corrosion properties. The PIII-treated samples had a thinner layer (70-250 nm) composed of stable oxide that increased corrosion resistance. Coatings deposited by magnetron sputtering are thicker (1-2 µm) that act as a physical barrier against corrosion medium. MgO is more stable than MgF_2 due to the stronger bond between the magnesium and oxide ions.

REFERENCES:
1. Rout PK et al. *Biomed Phys Eng Express*. 2022;8(4).
2. Baranov O et al. *Mater Horizons*. 2018;5:765-798.

ACKNOWLEDGEMENTS: This work was supported by NSERC-Canada-Alliance and Prima-Quebec- partnership funds. DM holds a Canada Research Chair Tier I (2012-2026).

15th Biometal
AUGUST 21 TO 27, 2023
Grand Hôtel San Michele, Cetraro, CS, Italy

Microstructure, mechanical properties and corrosion behaviours of Mg and Zn alloys manufactured by LPBF for biomedical applications

Muzi Li[1], Blanca Limones Ahijón[1], Guillermo Domínguez[1], Pedro J. Díaz-Payno[1], Simon Pöstges[2], Alexander Kopp[2], Jennifer Patterson[1] and Jon Molina-Aldareguía[1,3]

[1]*IMDEA Materials Institute, Getafe, Madrid 28906, Spain.* [2]*Meotec GmbH, 52068 Aachen, Germany.* [3]*Department of Materials Science, Polytechnic University of Madrid, 28040 Madrid, Spain*

INTRODUCTION: Biodegradable metals offer unique properties as musculoskeletal implants as they can be fully re-absorbed by the human body, which can spare the trauma-patients from a secondary surgery as compared to their non-biodegradable counter parts. Three classes of biodegradable alloys have been developed over the years, namely Mg-, Fe- and Zn-based alloys. Among the three, several Mg-based alloys exhibit excellent biocompatibility, non-toxicity and appropriate mechanical properties. The fast degradation rate issue of Mg alloys can be alleviated by applying plasma electrolytic oxidation (PEO) which also results in improved biocompatibility. Zn-based alloys, although being the least studied materials, exhibit promising potential due to their intermediate degradation rate and sufficient mechanical properties.

METHODS: A Mg-RE (rare earth) alloy (WE43) and ZnMg1 alloy were manufactured by a Laser Powder Bed Fusion (LPBF) process. The as-printed alloys were sand-blasted and chemically etched to smoothen the surface and WE43 was protected against corrosion by PEO. The alloys were immersed in simulated body fluid (SBF) for different periods of time to study the corrosion behaviours. The microstructure and corrosion properties were carefully analysed using X-ray microcomputed tomography, scanning electron microscopy and electron-backscatter diffraction as well as transmission electron microscopy. In addition, the mechanical properties and fracture mechanisms were determined by tensile testing of intact specimens as well as samples at intermediate times of degradation. Further, *in-vitro* and future *in-vivo* tests will be performed on these alloys with and without PEO modification to examine the biocompatibility, cytotoxicity and cell proliferation behaviour. These results will highlight the mechanical properties, corrosion resistance and biocompatibility of both Mg and Zn-based alloy-derived printed structures manufactured by LPBF.

ACKNOWLEDGEMENTS: This project has received funding from the European Union's Horizon Europe research and innovation programme under grant agreement No 101047008

Effect of coating time on the *in vitro* degradation behavior and mechanical integrity of HA coated biodegradable ZK60 alloy

Le Van Hai[1], Cao Thi Tam[2], **Le Van Tuan**[3], Vu Nhat Dinh[1], Nguyen Viet Nam[4,*]

[1] 103 Military Hospital, Military Medical University, Hanoi, Vietnam
[2] Military Medical University, Hanoi, Vietnam
[3] School of Mechanical Engineering, Hanoi University of Science and Technology, Hanoi, Vietnam
[4] Institute of Traumatology and Orthopaedics, 108 Military Central Hospital, Hanoi, Vietnam

INTRODUCTION: Mg alloys demonstrated their great advantages for applications in biomedical devices including good mechanical properties, biodegradability, and biocompatibility [1]. Although these advantages of Mg alloys make their become potential candidates for use as bioabsorbable and biodegradable materials, their clinical application has been hindered due to their fast biodegradation and low mechanical integrity in the physiological environment [2,3]. Hydroxyapatite coating has been demonstrated as effective method to improve the corrosion resistance and mechanical integrity of Mg alloys. In this research, biodegradable ZK60 alloy was coated by HA with different times. The effect of time on the formation of HA coating layer, degradation behavior, and mechanical properties of the coated alloys was studied systematically.

METHODS: HA coatings was prepared from ethylenediaminetetraacetic acid calcium disodium salt hydrate ($C_{10}H_{12}CaN_2Na_2O_8$, Ca-EDTA) solution with the concentration of 0.5 mol/L and potassium dihydrogen phosphate (KH_2PO_4) solution with the concentration of 0.5 mol/L. The pH of the treatment solution was adjusted to 7.5 by NaOH. The ZK60 alloy discs were immersed in the treatment solution at 90 °C for 0.5, 1, 2, and 4 h for HA coating. The *in vitro* corrosion test was carried out in Hanks' solution at 37 ± 0.5 °C under a 5% CO_2 atmosphere for 14 days. The amount of Mg^{2+} ions dissolved in the sampled medium was quantified by a colorimetric method using Xylidyl blue-I. Mechanical property of the alloy before and after immersion was evaluated by compression test. The microstructure of the samples before and after immersion was characterized by x-ray diffraction (XRD), scanning electron microscope (SEM) equipped with energy dispersive X-ray spectroscopy (EDX).

RESULTS: *Fig. 1* shows the amount of Mg^{2+} ions release into the solution during immersion test. As could be seen that, sample coated for 2h showed its lowest degradation rate. This is because the uniform and dense HA coating layer was formed on the surface of this sample. Sample coated at 0.5 and 4 h showed slight improvement in corrosion resistance compared to uncoated sample. As for the sample coated for 0.5h, only thin HA coating layer formed resulting in least effect in substrate protection from corrosion solution. For the sample coating for 4 h, many cracks appeared inside the HA coating layer, therefore, fast degradation occurred by corrosion solution penetration through these cracks.

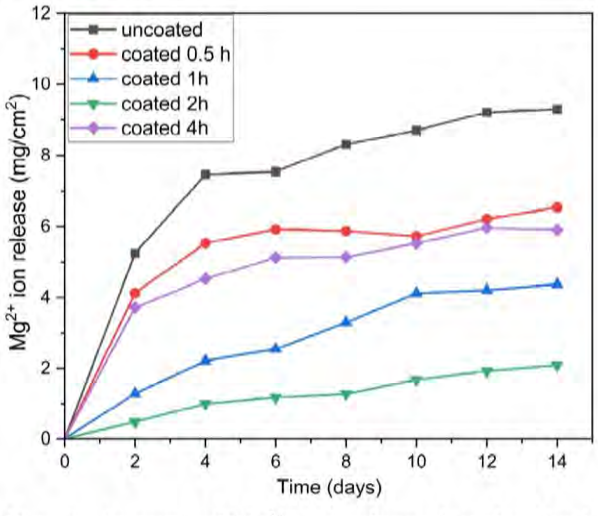

Fig. 1: Amount of Mg^{2+} ion released in the Hanks' solution during immersion test.

DISCUSSION & CONCLUSIONS: This research investigated corrosion behavior and mechanical integrity of HA coated ZK60 alloys. Coating time has strong impact on the structure and properties of HA coating layer. The coating layer formed in 0.5h was thin and not able to significantly improve the corrosion resistance of the substrate, while coating for 4 h resulted in formation of cracks inside the coating layer. The coating layer formed in 2 h demonstrated the strongest impact in improving corrosion resistance and mechanical integrity for the alloys.

REFERENCES: [1] N. Li, et al (2013) *J Mater Sci Technol* **29**;489-502. [2] F. Witte, et al (2005) *Biomaterials* **26**;3557–63. [3] N.T. Kirkland, et al (2010) *Corros Sci* **52**;287–91.

ACKNOWLEDGEMENTS: The authors would like to thanks to Department of Pathophysiology, Military Medical University for their support in *in vitro* immersion test.

15th Biometal
AUGUST 21 TO 27, 2023
Grand Hôtel San Michele, Cetraro, CS, Italy

Tuning of phosphate-based Plasma Electrolytic Oxidation bioactive coatings on AZ31 magnesium for bone applications

M Pavarini[1], G Uboldi[1], M Moscatelli[1], R Chiesa[1]

[1] *BioSurf lab, Department of Chemistry, Materials and Chemical Engineering "G. Natta", Politecnico di Milano, Milan, Italy*

INTRODUCTION: Magnesium and its alloys represent promising bone substitute candidates due to their biodegradability and bone-matching mechanical properties[1]. However, their typically low corrosion resistance can impair their load-bearing abilities and affect the healing processes by causing an adverse inflammatory response[2]. To overcome these challenges, surface modification techniques as Plasma Electrolytic Oxidation (PEO) can be exploited to produce thick conversion coatings and reduce Mg susceptibility to corrosion while supporting bone healing at the implantation site[3]. In our work, we focused on the development and tuning of different phosphate-based PEO coatings on AZ31 Mg alloy, to improve bone cell activity while increasing corrosion resistance, for prospective application in bone defect repair.

METHODS: The AZ31 Mg samples were PEO treated in pulsed DC conditions, using different electrolytes made of KOH and either Na_3PO_4 (P1), $Na_5P_3O_{10}$ (P3) or $Na_6(PO_3)_6$ (P6), with or without the addition of $Ca(OH)_2$ (P6-Ca). The morphology, chemical and phase composition of the coatings were then assessed via SEM-EDS and XRD analyses, while their thickness was measured with an eddy current probe. The samples' corrosion properties were evaluated by potentiodynamic polarization (PDP) tests in simulated body fluid (SBF) at 37°C.

RESULTS: The coatings produced in P6 exhibit a multilayered surface (**Fig. 1**) with big but partially occluded pores, compared to the typical volcano-like structure obtained in P1 and P3.

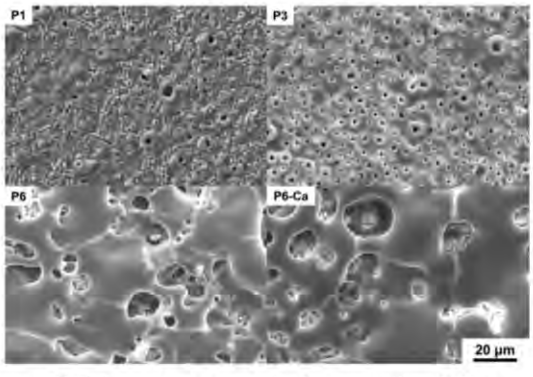

Fig. 1: SEM surface morphology of the PEO coatings formed in the different electrolytes.

Both the thickness of the oxide and the amorphous phosphate content of the coatings follow the trend P6>P3>P1. The PDP tests (**Fig. 2**) highlighted an up to 100-fold decrease in corrosion rate as compared to untreated AZ31 Mg for P6 and P6-Ca samples, as well as a bigger passivation region for these sample groups.

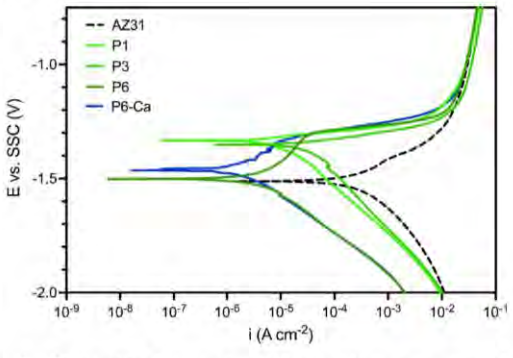

Fig. 2: Potentiodynamic polarization curves of the PEO coatings formed in the different electrolytes.

DISCUSSION & CONCLUSIONS: An observed progressive increase in amorphous phase content of the coatings with the complexity of the phosphate group is shown by the XRD data. This aspect, together with the increase in surface pore occlusion, is potentially beneficial in terms of corrosion control, as confirmed by the PDP results, showing optimal conditions for a longer-term retention of the base material's mechanical properties. Moreover, the presence of calcium in the P6-Ca coating demonstrated not to hinder these good corrosion performances, while representing a potentially beneficial addition to improve bone cell activity.
Ongoing studies are focusing on the *in vitro* evaluation of the cytocompatibility, cell response and cell mediated corrosion behaviour of the PEO coated samples, to confirm their promising properties as candidate for applications in bone fixation and repair.

REFERENCES: [1] P.C. Banerjee et al (2019) *Materials (Basel)* **12**:1–21. [2] M.D. Costantino et al (2020) *Acta Biomater* **101**:598–608. [3] G.P. Wirtz et al (1991) *Mater Manuf Process* **6**:87–115.

Magnetic field influence on corrosion behaviour of pure Fe in Hanks´ solution

I. Limón[1], N. Abu-Warda[1], V. Utrilla[1], M. Lieblich[2], B. Torres[1], J.Rams[1], M. Multigner[1]

[1]*Dpto Ciencia e Ingeniería de Materiales, ESCET, Universidad Rey Juan Carlos, c/Tulipán s/n, Móstoles, Madrid 28933, Spain,* [2]CENIM-CSIC, Madrid 28040, Spain,

INTRODUCTION: Synchronization of healing process with degradation of the implant would be the final goal of degradable biomaterials. Magnetic fields have been previously proposed for accelerating the degradation rate of ferrous materials in Hanks´ solution[1]. The effect of magnetic fields of relatively low intensity and under pseudo-phisiological conditions of corrosion process remains unclear. The present study is focused on understanding the role that the magnetic field plays for accelerating the corrosion of Fe in modified Hanks´ solution at 37 ºC.

METHODS: Pure ferromagnetic iron (99.8% Fe) rolled and treated at 650ºC/1h. Electrochemical experiments were carried out in a three electrode configuration adapted to be placed inside a cooper coil for magnetic field generation. 1 hour and 14 days static in-vitro tests have been performed at 37ºC in modified Hanks´ solution under two continuous magnetic field conditions (14 mT) parallel and perpendicular to the working electrode surface and without magnetic field. Three samples were tested in each condition. Anodic potentiodynamic polarisation curves were performed from -0,1 V to 1,2 vs OCP with a scan rate of 1 mV/s. Corrosion rate was evaluated in the Tafel region. Surface and corrosion products were characterized by profilometry, scanning electron microscopy and X-ray diffraction techniques.

RESULTS: Potentiodynamic polarization results show that the free corrosion potential (E_{corr}) does not change by the presence of the magnetic field, but the corrosion current density (i_{corr}) reaches higher values in the samples tested with magnetic field (Table 1), both after 1 hour and 14 days immersion. The active-passive transition is clearly visible for both field conditions after 1 hour immersion, but the passivation capacity is lost after 14 days.(Fig. 1).

Table 1. Fe corrosion potential and current density after 1 hour and 14 days immersion, without (H0) and with magnetic field (HDC) parallel to the electrode surface.

	FeH0_1h	FeHDC_1h	FeH0_14d	FeHDC_14d
Ecorr (V)	-0,685	-0,657	-0,712	-0,709
icorr (mV/cm²)	7,8E-06	9,2 E-06	3,4 E-06	4,4 E-06

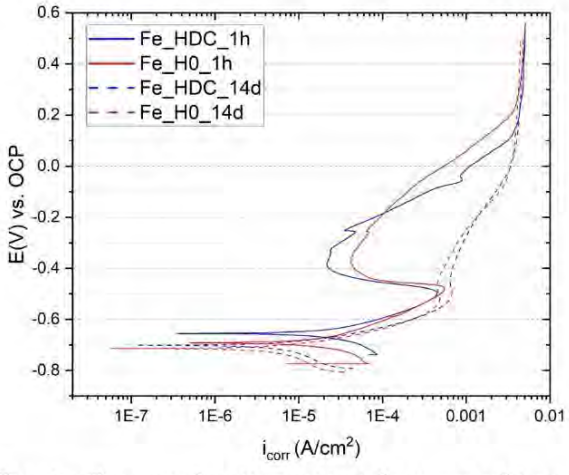

Fig. 1. Current density–potential curves of iron in modified Hanks´ solution without and with applied magnetic field parallel to the electrode surface (scan rate of 1 mV/s).

Furthermore, the magnetic field does not affect the composition of the corrosion products but modifies the morphology of the layer, producing more cracks and poorer attachment to the surface.

DISCUSSION & CONCLUSIONS: A 14 mT magnetic field applied on Fe immersed in modified Hanks´ solution does not induce corrosion mechanisms others than those that exist in the absence of the magnetic field. However, it produces a less adhere and more cracked layer of corrosion products that could be related with the observed increase of the corrosion current density. These results suggest that magnetic fields could be used for accelerating the biodegradation of Fe.

REFERENCES:

[1]M.Multigner et al. (2019). 11th Biometals Abstract book Corr-13.

ACKNOWLEDGEMENTS: Financial support of Spanish MICINN: PID2021-123891OB-I00 PID2019-104351GB-C21 and PID2021-124341OB-C21 and student I. Lucena.

15th Biometal
AUGUST 21 TO 27, 2023
Grand Hôtel San Michele, Cetraro, CS, Italy

Magnetic fields: A new method to modify the corrosion rate of biodegradable metals?

Irene Limón[1], Sandra C. Cifuentes[1], Ana L. Ramírez-Ledesma[2], Julio A. Juarez-Islas [3], Belén Torres[1], Joaquín Rams[1], Marta Multigner[1]

[1] Dpto Ciencia e Ingeniería de Materiales, ESCET, Universidad Rey Juan Carlos, c/Tulipán s/n, Móstoles, Madrid 28933, Spain.

[2] Facultad de Química, [3] Instituto de Investigaciones en Materiales, Universidad Nacional Autónoma de México, Ciudad de México, México.

INTRODUCTION: It is our aim to comprehend the mechanisms and actions of magnetic fields to corrosion and degradation of biodegradable metals. In previous results we have demonstrated that AC and DC magnetic fields greatly influence the degradation rate of ferromagnetic samples (Fe and FeMn)[1]. In this work we explore the effect of magnetic fields on the degradation of a not magnetic biodegradable metal, Zinc. Zn is a diamagnetic metal with no unpaired electrons in its atomic structure. Its corrosion products (ZnO and Zn^{2+} ions) are also diamagnetic. However, under the effect of a very strong magnet zinc gets influenced.

METHODS:

We study the effect of AC and DC magnetic fields on the degradation behaviour of cold worked Zn during 2 months in Hank´s solution. Rectangular zinc samples (14 mm x 7 mm x 2 mm) were ground and polished up to 1 um diamond paste. In vitro tests have been performed during 60 days at 37 ºC in modified pseudo-physiological Hanks´ solution under three different conditions: continuous (H_{DC}), alternate (H_{AC}) and no applied magnetic field. Systems were adjusted to obtain H_{DC} and rms H_{AC} of 10000 A/m. Each sample was suspended with a nylon thread in a centrifuge plastic tube containing 50 mL of the medium. Studies were performed in triplicate. The experimental set-up is shown in Figure 1. The corrosion rate was evaluated through weight loss. Surface changes were characterized by profilometry and scanning electron microscopy. Corrosion products were characterized by ICP, FTIR and X-ray diffraction techniques.

RESULTS: Figure 2 shows the mass loss of pure Zn and Fe samples immersed in Hanks´ solution for 60 days under the three different conditions (H0, H_{AC} and H_{DC}). The mean values of mass loss show that DC magnetic fields accelerate the corrosion rate of pure Zn. Samples in the H0 condition experience a mass loss of 0,33% while samples in H_{DC} condition experience a mass loss of 0,50%. The mass loss of samples in H_{AC} condition is similar to H0 samples (0,37%). The mass loss of iron is increased under both, continuous and direct magnetic field. The mass loss under H0 condition was 2,5% while under H_{AC} and H_{DC} was 3,7% and 4,3% respectively.

Fig. 1: Experimental set-up (a) Sample in the tube and the cylindrical copper coil (b) H_{AC} configuration. Coils connected to an autotransformer (c) H_{DC} configuration. Coils connected to a DC power supply.

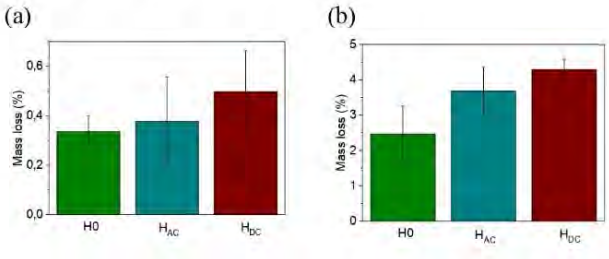

Fig. 2: (a) Weight loss of pure zinc (b) Weight loss of pure iron after 60 days of immersion in modified Hank´s solution

DISCUSSION & CONCLUSIONS: Results of Zn mass loss under continuous, alternate and no applied magnetic field show that DC magnetic fields do influence the degradation of this diamagnetic biodegradable metal. Comparing Zn and Fe mass loss results lead to understand that the effect of magnetic fields on the acceleration of corrosion rate is stronger on a ferromagnetic metal (Fe) than on a diamagnetic metal (Zn), mainly due to the reinforcing effect of the ferromagnetic material in the surrounding magnetic field.

REFERENCES: [1]M.Multigner et al. (2019). 11th Biometals Abstract book Corr-13. I. Limón et al. (2022) 14th Biometals

ACKNOWLEDGEMENTS: This work was funded by PID2021-123891OB-I00 and PID2021-124341OB-C21.

In Vitro

Friday, August 25th, 2023

Resorbable molybdenum for temporary cardiac pacing leads

C. Redlich[1], M. Prieto[2], A. Schauer[3], C. Guder[1], G. Poehle[1], T. Weissgaerber[1,4], V. Adams[3], U. Kappert[5], A. El-Armouche[6], A. Linke[2], M. Wagner[2]

[1] Fraunhofer Institute for Manufacturing Technology and Advanced Materials IFAM, Branch Lab Dresden
[2] Clinic for Internal Medicine and Cardiology, Heart Center Dresden, Technische Universität Dresden
[3] Laboratory of Experimental and Molecular Cardiology, Heart Center Dresden, Technische Universität Dresden
[4] Chair of Powder Metallurgy, Institute of Materials Science, Technische Universität Dresden
[5] Clinic for Cardiac Surgery, Heart Center Dresden, Technische Universität Dresden
[6] Institute of Pharmacology and Toxicology, Technische Universität Dresden

INTRODUCTION: Postoperative cardiac arrhythmias are routinely treated with temporary pacing leads made of stainless steel that are implanted at the time of heart surgery. However, manually extracting the pacing leads can result in complications since the wires sometimes resist extraction due to tissue in-growth. On the other hand, if the leads are cut and left in the body, there is a risk of infection and migration and in some cases revision surgery is required. We investigate the novel approach of using biodegradable temporary pacing leads that can remain in the body and are fully resorbed after a defined time (Figure 1a). This approach is based on the use of molybdenum (Mo), whose uniform degradation in-vivo and good biocompatibility were demonstrated by the project partners earlier [1,2].

METHODS: Braided leads were manufactured from 40 µm Mo wires and electrically insulated by dip-coating with absorbable biopolymers (Figure 1a). In-vitro degradation testing of demonstrators by immersion in modified Kokubo's SBF at 37 °C, pH 7.4 for 28 days was performed. Furthermore, apoptosis and necrosis assays for human cardiac fibroblasts (HCF) and cardiac myocyte cell lines (HCM) towards Mo ions were conducted. Pacing protocols for Mo demonstrators in comparison to commercially available stainless steel leads were established in an ex-vivo Langendorff model in preparation of the proof-of-principle test in an in-vivo rat model.

RESULTS: Manufacturing of demonstrator leads with a 4×4 wire configuration and coating first with a bulk-eroding biopolymer for better handling and secondly with a surface-eroding biopolymer for electrical insulation was successful. Dissolution rates of 30 µg/cm²·d for uncoated leads are similar to Mo material tested in recent studies [1,2], whilst dissolution of Mo in polymer-coated leads was strongly reduced. Pacing thresholds and performance parameters as well as electrical parameters like impedance and sensing amplitude of resorbable pacing leads were found to be at least equivalent to stainless steel leads. No significant induction of apoptosis or necrosis towards HCF and HCM cell lines was observed up to the highest tested concentration of 200 mg/L of Mo.

DISCUSSION & CONCLUSIONS: The results of the in-vitro tests with pacing leads made of Mo and biopolymers show the desired temporary electrical insulation and delay of the onset of degradation. The Mo leads also show equivalency in the ex-vivo pacing protocols in the Langendorff model. Sensing and pacing as well as degradation and biosafety are currently tested for up to 12 months in an in-vivo rat model.

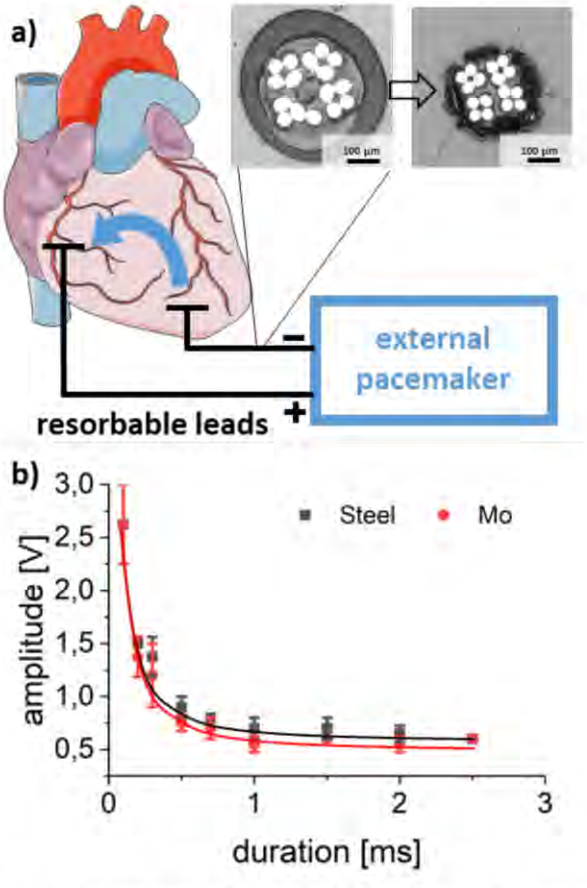

Fig. 1: Schematic of resorbable epicardial pacing leads (a), pacing threshold curve of Mo lead compared to stainless steel lead (b).

REFERENCES:

[1] C. Redlich et al., *Metals* **2021**, 11, 761
[2] A. Schauer et al., *Materials* **2021**, 14, 7776.

ACKNOWLEGDEMENT: This work was financially supported by Else Kröner Fresenius Zentrum (EKFZ) for Digital Health.

Personalized skeletal fixation with resorbable metal components

D Dean,[1] L Olivas[1,2], A Chmielewska[1], D Cho[1], B Panton,[1] T Avey,[1] and A Luo[1]

[1] *Department of Materials Science and Engineering, The Ohio State University, Columbus, OH.*

[2] *Escuela de Ingeniería y Ciencias, Tecnologico de Monterrey, Monterrey, Nuevo Leon, MEXICO*

INTRODUCTION: Standard of care skeletal fixation and replacement devices predominantly utilize highly stiff Ti-6Al-4V (i.e., 116 GPa). It is well documented that these devices can lead to bone resorption, device loosening, and/or fatigue failure. While rigidity may be helpful during post-surgical healing, it will be disruptive if previously developed corridors of dense cortical bone (stiffness ~20 GPa) no longer receive a load once healing is complete. By combining a less stiff NiTi (i.e., 48 GPa) shell and a resorbable Mg alloy porous core (Figure 1), the risk of post-healing stress shielding may be dramatically reduced.

METHODS: Our multimaterial device combining 3D printed, superelastic NiTi shell with a porous, resorbable Mg-1.2Zn-0.5Ca-0.5Mn core (Fig 1) can be prepared entirely at the point of care, as is done in our sheep mandibular graft fixation device model. Our fixation device's Mg alloy core's pore geometry uses Schoen's gyroid (equation 1)[1]:

$$\sin x \cos y + \sin y \cos z + \sin z \cos x = 0 \qquad (1)$$

Schoen's gyroid allows us to specify strut diameter, pore diameter, and porosity.

The in-progress validation study reported here will verify that our 3D printed fixation devices performance matches our computer simulation of patient outcome. In our current validation study specimens (9 frozen sheep crania) were 3D CT-scanned. The resulting 3D images of the sheep crania were used to design mandibular graft fixation devices. We harvest the mandible from these specimens to run mechanical tests after implanting a bone graft and attaching our multi-material graft fixation device to each mandible.

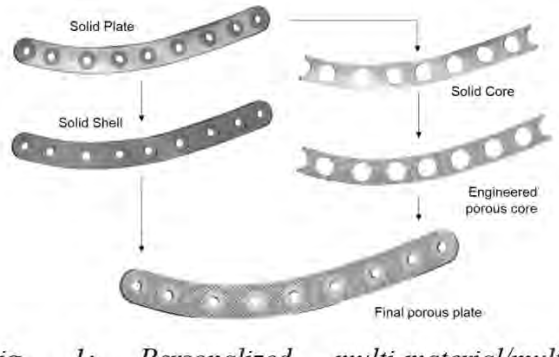

Fig. 1: Personalized multi-material/multi-component mandibular graft fixation devices. Pore geometry (i.e., strut diameter, pore diameter) and solid regions can be personalized to fit flush against the host mandible and graft bone surface.

Simultaneously we are testing non-personalized fixation devices and small coupons per the ISO 13485 (good manufacturing practices),[2] and ASTM F382 (fixation plate validation) guidelines.[3]

RESULTS:

We have computationally assessed, via Finite Element Analysis (FEA), the effect of varying the pore diameter. Once the strut and pore diameter are selected, the apparent density (porosity ⟨ρ⟩) will affect the mechanical properties of 3D printed NiTi or Mg alloy gyroid structures. As seen in Table 1, the apparent elastic modulus decreases with decreasing apparent density (higher pore size).

Table 1. Apparent elastic modulus for porous NiTi structures as a function of varying pore size

Strut size, (μm)	Pore size, (μm)	Apparent density, ⟨ρ⟩, %	Normalized Apparent Elastic Modulus, ⟨E⟩/E
300	50	97	0.829
	150	74	0.619
	300	50	0.260
	600	25	0.052
	900	14	0.015
	1200	8	0.004

DISCUSSION & CONCLUSIONS:

Mechanical analysis and design of a multimaterial, NiTi+Mg alloy fixation device shows promise for avoiding stress shielding-induced bone loss and cyclic loading-induced fatigue failure. Stiffness during the healing pattern can be controlled by varying porosity. Long term stability would derive from resorption of the Mg alloy component.

REFERENCES: [1]Gyroid; [2]Lee S.B., et al. (2022). Journal of Korean Society for Quality Management 50.3: 503-515.; [3]Mohammed, A.A.A.R. (2022). British Journal of Oral and Maxillofacial Surgery 60(6):785-90.

ACKNOWLEDGEMENTS: This research was supported by grants from the State of Ohio's Third Frontier Accelerator program and The Ohio State University James Comprehensive Cancer Center Cancer Engineering Center and Biomedical Device Initiative.

15th Biometal
AUGUST 21 TO 27, 2023
Grand Hôtel San Michele, Cetraro, CS, Italy

Additive manufacturing of biodegradable Mg1%Y-based ureteral stents: Understanding the corrosion under simulated urinary tract environment

M Pacheco[1,2], CJ Hassila[3], F D'Elia[3], C Persson[3], E Lima[4], AA Barros[1,2], RL Reis[1,2]

[1]3B's Research Group—Research Institute on Biomaterials, Biodegradables and Biomimetics, University of Minho, Guimarães, Portugal. [2]ICVS/3B's-PT Government Associate Laboratory, Braga/Guimarães, Portugal [3]Division of Biomedical Engineering, Department of Materials Science and Engineering, Uppsala University, Uppsala, Sweden [4]School of Health Sciences, Life and Health Sciences Research Institute (ICVS), University of Minho, Braga, Portugal

INTRODUCTION: Biodegradable metals have been gaining popularity in the biomedical field, especially for cardiovascular stents and bone implant research. Its utilization in urology is still in its infancy, but the few studies available point out some essential advantages. A biodegradable metallic ureteral stent will have a longer corrosion time than the current biodegradable polymeric ones, is expected to be anti-bacterial (a fundamental characteristic given the frequency of urinary infection deriving from stenting), and avoids the second surgery for stent removal[1,2]. Herein Mg1Y alloy is investigated as a ureteral stent material. Ureteral stent prototypes (meshed tubes) were produced by additive manufacturing (AM) through laser powder bed fusion (LPBF), and the corrosion of these structures under urinary tract environment was studied.

METHODS: Meshed tubes of 5 mm height, 2.33 mm external diameter, and 1.82 mm internal diameter were produced by LPBF, using previously optimized parameters for thin structures. The modulated laser mode was used with a scanning speed of 50 mm/s, laser power of 50W, 0.01 MHz laser modulation frequency, and 75 µs laser modulation width. The samples were placed inside a dynamic system with a constant fresh artificial urine solution (AUS) flow at 37 °C. XRD was employed for corrosion layer analysis. In addition, the cytotoxic effect of the Mg1Y samples was evaluated using L929 and G/G cell lines. Further studies on the corrosion layer (Raman, XPS, SEM-EDS) and corrosion rate (ICP and mass loss) are ongoing.

RESULTS: The surface of the samples was covered by a whitish corrosion layer (Fig. 1). The corrosion layer composition appeared to be a mixture of products from the metal corrosion and components precipitated from the AUS. The fragments released during degradation were in different shapes, and the dimensions (diameter) varied between 0.3 - 1.3 mm, which we considered small enough not to cause a problem during degradation in the patient. The samples showed no toxicity for L929 or mouse bladder cells.

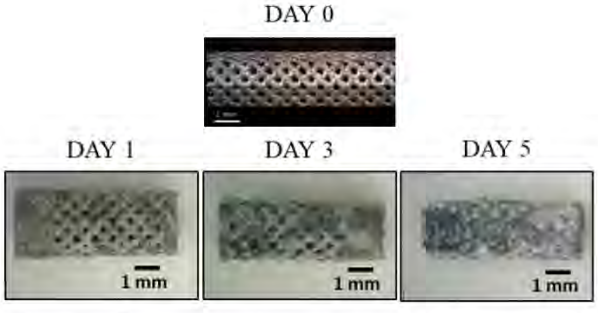

Fig. 1: Representative pictures of the samples before at day 0 and after 1-, 3- and 5-days immersion in the simulated dynamic conditions.

DISCUSSION & CONCLUSIONS: This is the first time that Mg1Y-based urinary stent prototypes produced by AM are characterized under urinary tract environment. This alloy was selected based on previous studies where it outperformed comparing with other Mg alloys[3]. The corrosion layer slightly grows along the time and the corrosion evolution is visible comparing day 1, 3 and 5 days (Fig.1). The fragments generated during corrosion, which started to being noticeable at day 5, did not appear large enough to create stent obstruction and no sharp ends were visible, but future studies will be conducted. Mg1Y ureteral stents produced by AM seem to be a promising research topic for future biodegradable ureteral stents.

REFERENCES:

[1] D. Tie, N. Hort, M. Chen, R. Guan, S. Ulasevich, E.V. Skorb, D. Zhao, Y. Liu, P. Holt-Torres, H. Liu (2022) *Bioact. Mater.* 7:254-262. [2] J.Y. Lock, E. Wyatt, S. Upadhyayula, V.A. Whall, V.I. Nuñez, H.L. Vulley (2014) *J. Biomed Mater. Res. – Part A.* 102:781-792. [3] D. Mei, C. Wang, M. Nienaber, M. Pacheco, A. Barros, S. Neves, et al. (2021) *Corros. Sci.* 189.

ACKNOWLEDGEMENTS: The authors are grateful to FCT, through the PhD Scholarship SFRH/BD/145285/2019, and the project NORTE-01-0247-FEDER-047112 as well as VINNOVA through Competence Centre AM4Life (2019-00029).

15th Biometal
AUGUST 21 TO 27, 2023
Grand Hôtel San Michele, Cetraro, CS, Italy

Exploring the biodegradability and biocompatibility of candidate metallic intravascular stent materials using microCT and CECT.

L Leyssens[1,2], N Lapraille[1], G Pyka[1,2], P Jacques[1], S Horman[2], J Goldman[3], G Kerckhofs[1,2,4,5]

[1] iMMC, UCLouvain, Belgium. [2] IREC, UCLouvain. [3] Dpt. Biomedical Engineering, Michigan Tech, USA. [4] Dpt. Materials Engineering, KU Leuven, Belgium. [5] Prometheus, KU Leuven.

INTRODUCTION: During the last two decades, biodegradable metals have been studied in an effort to replace permanent intravascular stents. The material with ideal degradation rate and behavior, mechanical properties, and biocompatibility has not yet been found. We evaluated the *in vitro* degradation and surface properties and the *in vivo* behavior of different biodegradable metals using microfocus X-ray computed tomography (microCT) and contrast-enhanced microCT (CECT). Wires were used to mimic a single stent strut.

METHODS: For all experiments, Co-Cr alloy (biostable reference), Fe, Zn, and Zn-Ag-Cu-Mn-Zr alloy (Zn alloy) [1] wires (diameter - 250 µm) were used. *In vitro immersion* – Wires were immersed in Hanks' solution for 1, 4, or 7 days. Wires were imaged with microCT prior to and after immersion. Based on the 3D images, degradation rate (based on volume loss), degradation mode, and surface roughness (using surface profile evaluation [2]) were determined. *In vivo implantation* – Wires were imaged with microCT prior to implantation. Then, they were implanted in the rat aorta. Rats were euthanized after 7, 24, or 84 days and the aorta implanted with the wire was harvested [3]. The samples were fixed in 4% formaldehyde. They were first imaged with microCT to visualize the wire. They were then stained with isotonic Lugol's iodine solution (1:1 dilution in Sorenson's buffer) for 17 hours and imaged with CECT. Degradation rate and degradation mode were evaluated.

RESULTS: The microCT images of the wires from the *in vitro* and *in vivo* experiments show consistent results. Fe shows only surface corrosion and low variation in roughness. Zn exhibits heterogeneous pitting corrosion and a large increase in roughness. The Zn alloy corrodes more homogeneously with less pitting compared to pure Zn. However, the formation of internal dendrites is observed (Fig. 1). The Zn alloy shows the lowest increase in roughness across all time points. In terms of corrosion rate, the pure Zn degrades faster than pure Fe. The newly developed Zn alloy has a degradation rate that is close to that of the pure Zn, which is considered a good compromise between Fe and Mg, which degrades too fast. In a next step, the CECT-based images from the *in vivo* implantations will be used to identify the formation of neointima to determine biocompatibility of the materials by evaluating the neointimal activation (Fig. 2).

Fig. 1: MicroCT-based images of degradation behavior of Zn alloy. Grey at time point 0 and orange after 7d of immersion. Scalebar = 50 µm.

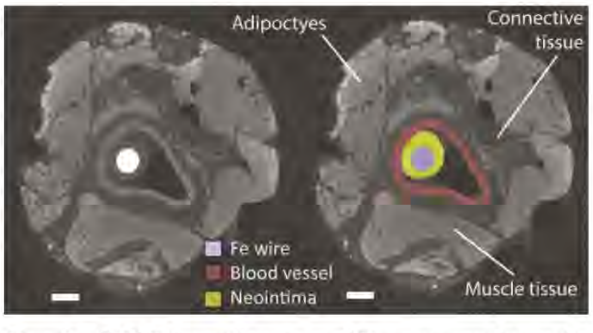

Fig. 2: CECT-based image of Fe wire implanted in the rat aorta and identification of the neointima at 24d - time point. Scalebar = 300 µm.

DISCUSSION & CONCLUSIONS: This study proposes a novel microCT- and CECT-based technique for evaluating alloys for intravascular stent applications. This technique provides new insights into the *in vitro* and *in vivo* behavior of biodegradable alloys. The results could potentially inform the development of more effective biodegradable materials for medical devices.

REFERENCES: [1] A.A. Oliver (2020) *Bio Mater.* **3**:6779-6789, [2] G. Kerckhofs (2013) *Adv. Eng. Mater.* **15**:153-158 [3] R.J. Guillory II (2019), **11**:19884-19893

ACKNOWLEDGEMENTS: This template was modified with kind permission from eCM Journal.

15th Biometal
AUGUST 21 TO 27, 2023
Grand Hôtel San Michele, Cetraro, CS, Italy

How plastic deformations affects performance of absorbable zinc alloys? A focus on biological behaviour

A Jarzębska[1], D Wojtas[1,4], M Wróbel[1], K Trembecka-Wójciga[1], M Bugajska[1], A Bigos[1], Ł Maj[1], M Bieda[1], J Kawałko[2], S Przybysz[3], J Skiba[3], R Schirhagl[4], A Mzyk[1,4]

[1] Institute of Metallurgy and Materials Science, Polish Academy of Sciences, Krakow, Poland, [2] Academic Centre for Materials and Nanotechnology AGH University of Science and Technology, Krakow, Poland, [3] Institute of High Pressure Physics, Polish Academy of Sciences, Warszawa, Poland, [4] University of Groningen, University Medical Center Groningen, Groningen, Netherlands

INTRODUCTION: So far, pure Zn has not been a preferred material for producing absorbable implants due to its insufficient mechanical properties. Solution to this problem is the implementation of plastic deformation processes, often supported by alloying additions. The application of hydrostatic extrusion has been particularly beneficial in improving the strength of Zn-based materials. Refined microstructure and the presence of structural defects are the key factors responsible for this enhancement. However, such microstructure can also affect the corrosion and biological behaviour of Zn-based materials. Thus, it is crucial to investigate the microstructure and correlate it with the properties. While methods for study the modification of microstructural, mechanical, and corrosion properties altered by plastic deformation are well-established and the results are straightforward, the literature findings present inconsistencies in the case of biological properties. Therefore, in this study a novel method of diamond magnetometry was applied to support the data about the biological performance of absorbable Zn alloys.

METHODS: In order to study the effect of plastic deformation on microstructure and the properties of Zn-based materials, hydrostatically extruded (HSE) pure Zn, Zn-Mg and Zn-Mg-Cu alloys were compared to their hot extruded (HE) counterparts. Microstructural characterization of the studied Zn-based materials was carried out by using the electron backscattered diffraction (EBSD) technique. Mechanical properties were assessed based on a series of static tensile tests. Information regarding corrosion properties were acquired by performing immersion and electrochemical tests. Biological studies, encompassing indirect contact cytotoxicity assays and confocal laser scanning microscopy (CLSM) studies, were also performed. In order to obtain additional insight into biological properties of the examined materials, the novel technique of diamond magnetometry was used. The method served as a tool enabling the analysis of early cell response.

RESULTS: Studies confirmed great grain refinement caused by HSE as roughly 20 times smaller grain size was obtained for HSE-treated materials as compared to their HE counterparts. Significant improvement in the mechanical properties was also observed. The highest values of YS = 361 MPa, UTS = 430 MPa and E = 21% were achieved for Zn-Mg alloy after HSE. In comparison to HE-treated materials, lower corrosion rates were evaluated for materials subjected to HSE. MTT assay as well as confocal studies did not reveal any significant differences between the HSE- and HE-treated materials. However, diamond magnetometry indicated that the production of free radicals was more pronounced in cells exposed to extracts produced from the materials after HSE.

DISCUSSION & CONCLUSIONS: Plastic deformation via HSE caused substantial great grain refinement, which positively affected the mechanical properties of Zn-based materials. Such microstructural changes improved their corrosion resistance as well. Based on the data obtained by using diamond magnetometry it can be stated that plastic deformation also influenced biological properties of the studied Zn alloys. The generation of free radicals was more pronounced for the HSE-treated materials, what indicates the state of oxidative stress, induced possibly by higher intracellular Zn levels. However, such a tendency was observed only during the early stages of incubation of cells with Zn-bearing media. Diamond magnetometry method could be effectively used for the assessment of material cytotoxicity.

ACKNOWLEDGEMENTS: This work was financially supported by the National Centre for Research and Development, project no. LIDER/54/0229/L-11/19/NCBR/2020

15th Biometal
AUGUST 21 TO 27, 2023
Grand Hôtel San Michele, Cetraro, CS, Italy

Highly biocompatible Mg–Ca alloy with enhanced bioactivity towards bone regeneration

N De Berardinis[1], A Rich[2], C Persson[1], G Hulsart Billström[3,1], JF Löffler[2]

[1] Division of Biomedical Engineering, Department of Materials Science and Engineering, Uppsala University, Sweden. [2] Laboratory of Metal Physics and Technology, Department of Materials, ETH Zurich, Switzerland. [3] Department of Medical Cell Biology, Uppsala University, Sweden.

INTRODUCTION: While rare-earth element (REE) containing Mg-based alloys (such as WE43) are clinically used as biodegradable implants due to their high strength and suitable degradation rate[1], Mg–Ca alloys have arisen as REE-free alternatives with similar properties.[2, 3] A novel alloy developed at ETH Zurich, X0 (MgCa0.45, in wt.%), has shown promise as a suitable implant material for bone-fracture fixation.[2] To better understand and evaluate this alloy, *in vitro* biocompatibility and cellular interactions need to be verified. This study assesses the biocompatibility and bioactivity of a pre-osteoblastic cell line (MC3T3-E1) cultured in the same environment as X0 and WE43 samples via transwell inserts.

METHODS: The Mg-alloy X0 was compared against WE43, which contains about 4 wt.% Y and 3 wt.% REE, and against cells alone, using the pre-osteoblastic cell line MC3T3-E1 (ATCC) over a period of 21 days with four time points: days 3, 7, 14 and 21. One day prior to the start of the experiment, the cells were seeded in four 12-well plates and allowed to adhere and grow for 24 h. The media used was αMEM, containing osteoinductive compounds such as ascorbic acid, dexamethasone, and β-glycerophosphate. The next day, the materials were placed in triplicates into the plates via transwell inserts. From then on, the media were replaced every three days. For each time point, the materials were removed from the plate and the media were replaced with PrestoBlue™ to quantify the cellular metabolism. After that, the cells were lysed, and LDH (Lactate Dehydrogenase) and ALP (Alkaline Phosphatase) assays were performed on the cell lysates to assess the proliferation and differentiation, respectively. For the data analysis, a two-way ANOVA test with Bonferroni post hoc correction was performed.

RESULTS: The differentiation results show remarkable bioactivity of both materials in terms of maturation of pre-osteoblasts into mature osteoblasts, the most active cellular stage with regard to bone deposition. Although no statistical significance was found between the groups for either material, after 21 days, cells cultured together with X0 showed a trend towards increased ALP production and differentiation compared to the cells cultured with WE43. The proliferation results confirm the *in vitro* biocompatibility of both materials, with X0 showing a considerable (statistically significant) improvement over WE43. Moreover, time was a significant factor for the proliferation but not for the differentiation.

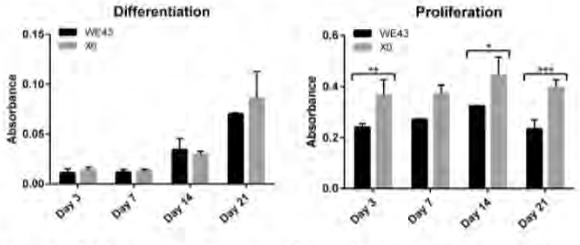

Fig. 1: Differentiation and proliferation measures of X0 versus WE43. A two-way ANOVA statistical test with Bonferroni post hoc correction was performed for both datasets ($p < 0,05$; ** $p < 0,01$; *** $p < 0,001$).*

DISCUSSION & CONCLUSIONS: Our results suggest that the X0 Mg-alloy is superior to WE43 in creating an environment favourable to cell thriving. The enhanced cell proliferation and differentiation is expected to generate improved tissue regeneration. In addition, potential biological problems that might arise from REEs[4] can be avoided. For these reasons, X0 is a good candidate for further *in vivo* follow-up studies, required to confirm the *in vitro* findings in a more complex and natural environment.

REFERENCES: [1]H.S. Han, et al. (2019) Mater Today 23:57-71. [2]L. Berger, et al., 14th Biometal Conf. (Aug. 24-29, 2022), Europ. Cells and Materials (2023), in press. [3]T. Akhmetshina, et al., 14th Biometal Conf. (Aug. 24-29, 2022), Europ. Cells and Materials (2023), in press. [4]F. Amerstorfer, et al. (2016) Acta Biomater. 42:440-450.

ACKNOWLEDGEMENTS: This project has received funding from the European Union's Horizon 2020 under the Marie Skłodowska-Curie grant agreement No. 956004, a BioTrib ETN project. We also gratefully acknowledge funding from the Swedish Research Council (grant no. 2021-04708) and the Swiss National Science Foundation (SNF Sinergia, grant no. CRSII5- 180367).

15th Biometal
AUGUST 21 TO 27, 2023
Grand Hôtel San Michele, Cetraro, CS, Italy

Insights into Mg degradation with X-ray ptychographic computed tomography

T. Akhmetshina[1], RE. Schäublin[1], AM. Rich[1], W. Rubin[1], NW. Phillips[2], L. Berger[1], JF. Löffler[1]

[1]*Laboratory of Metal Physics and Technology, Department of Materials, ETH Zurich, Switzerland*

[2]*Paul Scherrer Institute, 5232 Villigen PSI, Switzerland*

INTRODUCTION: Rapid and yet not well-understood degradation of magnesium alloys is delaying their clinical application. Magnesium is usually alloyed with various elements, among which rare-earth (RE) elements are believed to improve corrosion resistance. Despite potential harmful effects, such RE-containing alloys are often used for biodegradable implants. In this work we compare the degradation behavior of a medical-grade WE43 (Mg–Nd–Y–Zr) and X0 (Mg–Ca) alloys via X-ray ptychographic computed tomography. The results explain the commonly reported high corrosion resistance of WE43 in in-vivo studies, and reveal unexpected details of its degradation evolution. Our findings show a higher corrosion resistance of X0 compared to WE43.

METHODS: The X0 (Mg-0.45Ca, wt.%) alloy[1,2] was prepared from ultrahigh-purity (XHP) Mg (99.999%, ETH Zurich) and Ca (99.5 wt.%, from ABCR GmbH). Medical-grade WE43 (Mg-4Y-2.3Nd-0.5Zr, in wt.%) was obtained from Luxfer MEL Technologies (Manchester, UK). Both alloys were hot-extruded[2] and the microstructure was analyzed via scanning and transmission electron microscopy (SEM, TEM, EDX). Samples for tomography were shaped to pillars of 5 µm in diameter using focused ion beam (FIB) milling. X-ray ptychographic tomography (PXCT) measurements were performed at the cSAXS beamline at the Swiss Light Source (SLS). The samples were scanned in the pristine state (no corrosion), and after 1, 2, 4 and 8 hours of immersion in simulated body fluid (SBF) at 37 °C (Fig. 1).

RESULTS: The precipitates in WE43 were found as intermetallics isostructural to Mg_5Gd (β phase), with average composition $Mg_{86.3}Y_{7.7}Nd_{5.3}Zr_{0.7}$. In X0, the precipitates are made of the Mg_2Ca Laves phase. After reconstruction of the ptychographic scans, the average isotropic resolution was estimated to be 55 nm, and the best achieved resolution was 23 nm. Thanks to the high surface-to-volume ratio of the pillars, we were able to image complete degradation of the Mg alloys in the given beam time. The WE43 pillar was fully converted into corrosion products already after 2 hours of immersion in SBF, while for the X0 pillar the Mg matrix nearly completely dissolved only after 4 hours.

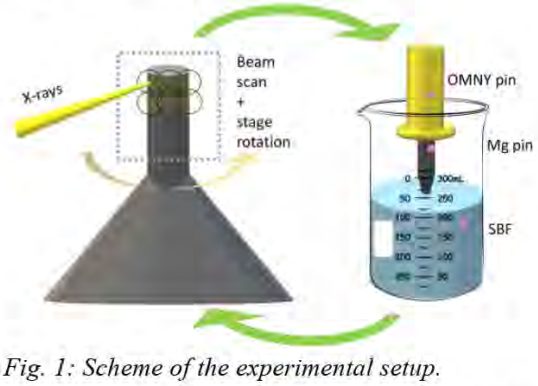

Fig. 1: Scheme of the experimental setup.

Importantly, the precipitates in WE43 remained well embedded in the corrosion products, and some RE elements were re-distributed in the corrosion products, forming a thin rim. The overall shape of the WE43 pillar was retained, while the X0 pillar showed a layer-by-layer degradation.

DISCUSSION & CONCLUSIONS: The high resolution and phase sensitivity of the method allowed us to image in 3D a complete process of Mg-alloy corrosion with nanoscale resolution and non-destructively. With the 3D electron density maps we were able to detect RE precipitates that remained in the fully corroded WE43 pillar, which would not have been possible with classical absorption contrast and low resolution. Our findings clearly reveal different degradation mechanisms for RE-containing and RE-free Mg alloys, whereas in the former case the non-degraded RE elements may be problematic in biodegradable implant applications.

REFERENCES: [1]L. Berger, et al., 14th Biometal Conf. (Aug. 2022), Europ. Cells and Materials (2023), in press. [2]T. Akhmetshina, et al., 14th Biometal Conf. (Aug. 2022), Europ. Cells and Materials (2023), in press.

ACKNOWLEDGEMENTS: The authors gratefully acknowledge financial support from the Swiss National Science Foundation (SNF Sinergia, Grant No. CRSII5-180367). They also thank the Paul Scherrer Institute for the allocation of beamtime at the SLS and ScopeM at ETH Zurich for the access to its facilities.

The hydrogen released from biodegradable Mg to regulate CAFs reducing drug resistance in gallbladder cancer

Rui Zan[1], Xiaonong Zhang[2*], Houbao Liu[1], Tao Suo[1*]

[1] *Department of General Surgery, Zhongshan Hospital, Fudan University, Shanghai, China.*

2 State Key Laboratory of Metal Matrix Composites, School of Materials Science and Engineering, Shanghai Jiao Tong University, China

INTRODUCTION: Gallbladder cancer, a malignant tumor located in the biliary tract, has an overall 5-year survival rate of less than 5% [1]. Unfortunately, drug resistance is a significant hurdle in the effective treatment of this cancer. Tumor stromal cells, specifically cancer-associated fibroblasts (CAFs), create a drug barrier that hampers chemotherapy and secrete cytokines that improve the tumor cells' anti-apoptotic ability [2, 3]. Interestingly, our previous study showed that the evolution of hydrogen gas (H_2) from magnesium (Mg) induced apoptosis in tumor cells during the degradable process [4]. Nonetheless, it is still unclear whether hydrogen can target CAFs as a therapeutic strategy to overcome drug resistance in gallbladder cancer. Thus, we extracted CAFs from human gallbladder cancer tissues and evaluated the effect of H_2 on CAFs using a 3D co-culture system with gallbladder cells.

METHODS: For 3D co-culture spheroid formation, cells (10000 SGC-996 or 5000 SGC-996 cells mixed with 5000 CAFs/well) were seeded onto a round bottom ultralow attachment 96-well microplate. SGC-996/CAFs spheroids were cultured in DMEM/F12 culture medium with 10% fetal bovine serum and incubated at 37°C under a humidified atmosphere with 5% CO_2. The spheroid cells were observed of α-SMA and Collagen I distribution after H_2 treatment for 48 h.

RESULTS: The secretion of gallbladder CAFs (G-CAFs) was found to increase the cell viability of SGC-996 gallbladder cancer cells. Fig. 1a demonstrates that the conditioned medium (CM) of CAFs improved the resistance of SGC-996 cells to the chemotherapy drug oxaliplatin. Moreover, during the formation of the 3D co-culture, CAFs promoted the density of the spheroids by decreasing their diameter. This promoted the shielding effect of the drug barrier on oxaliplatin and facilitated crosstalk between CAFs and SGC-996 cells. However, treatment with H_2 broke the extracellular barrier, and oxaliplatin-induced apoptosis in SGC-996 cells by activating the p53 signaling pathway.

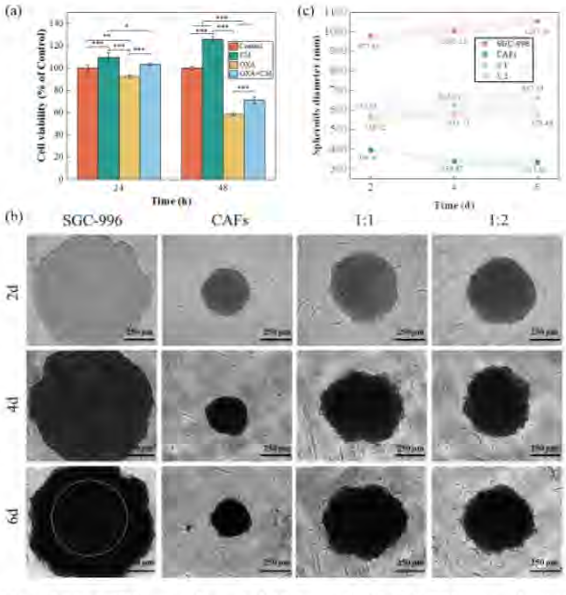

Fig.1 (a) The cell viability of SGC-996 cells after CM of CAFs treatment. (b) The spheroid cells and (c) the diameter of the different spheroid cells.

DISCUSSION & CONCLUSIONS: To sum up, our findings suggest that G-CAFs contribute to drug resistance in SGC-996 cells. However, by regulating the G-CAFs, the released H_2 from Mg decreased drug resistance in gallbladder cancer.

REFERENCES: [1]J.C. Roa, P. García, V.K. Kapoor, et al (2022) Nature Reviews Disease Primers 8(1) 69. [2]P.E. Saw, J. Chen, E. Song, (2022) Trends in Cancer 8(7) 527-555. [3]S. Rizzolio, S. Giordano, S. Corso, (2022) Journal of Experimental & Clinical Cancer Research 41(1) 319. [4]R. Zan, H. Wang, W. Cai, et al (2022) Bioactive Materials 9 385-396.

ACKNOWLEDGEMENTS: The authors are grateful for support from the Science and Technology Commission of Shanghai Municipality (20DZ2254500).

Critical assessment of direct contact cytotoxicity assay based on the *in vitro* studies on biodegradable Zn-Ag-Mg alloys

M. Watroba[1], M. Banzhaf [2], J. Michler[1], J. Schwiedrzik[1], P. Bała[3], Aldo R. Boccaccini[4]

[1] Empa Swiss Federal Laboratories for Materials Science and Technology, Laboratory for Mechanics of Materials and Nanostructures, Thun, Switzerland, [2] University of Birmingham, Institute of Microbiology and Infection and School of Biosciences, Birmingham, UK, [3]AGH University of Science and Technology, Academic Centre for Materials and Nanotechnology, Krakow, Poland,[4] University of Erlangen-Nuremberg, Institute of Biomaterials, Erlangen,Germany

INTRODUCTION: Zn, which demonstrates an optimal corrosion rate between Mg- and Fe-based alloys, has been reported to have excellent biocompatibility[1]. Therefore, modifying Zn's unsatisfactory mechanical properties via alloying should not worsen its biological response. As sufficient strength, ductility, and corrosion behavior required for load-bearing implants have already been obtained in plastically deformed Zn-3Ag-0.5Mg[2], the effect of simultaneous Ag and Mg additions on *in vitro* cytocompatibility and antibacterial properties was studied in relation to Zn and Zn-3Ag. *In vitro* cytotoxicity assessment is an essential step in developing new implant biomaterials. However, commonly used water-soluble tetrazolium salt-based (WST) cytotoxicity assay has limitations for direct tests on Zn-based materials, which may give misleading results. This aspect was the first time highlighted for Zn in the current studies.

METHODS: The samples of pure Zn, Zn-3Ag, and Zn-3Ag-0.5Mg (wt %) alloys were fabricated by hot extrusion at 200˚C and subsequent room temperature cold rolling. Materials were carefully characterized via SEM, XRF, and XRD. The in vitro cytocompatibility evaluation was performed using direct and indirect methods on human osteosarcoma MG-63 cells. All samples were prepared as flat polished disks, ultrasonically cleaned, and sterilized before the tests. Cell viability and cytotoxicity of the MG-63 cells were quantified via WST-assay and LDH-assay, respectively. These measurements were supported by SEM imaging of fixed cells on the disks and fluorescence imaging of live-dead stained cells in the extracts. In addition, the antibacterial activity of the Zn-based samples was determined using *S. aureus* and *E. coli* bacteria strains by turbidity assay and agar diffusion tests.

RESULTS: Direct cell culture on samples and indirect extract-based tests showed almost no significant differences between the tested Zn-based materials. The diluted extracts of Zn, Zn-3Ag, and Zn-3Ag-0.5Mg showed no cytotoxicity towards MG-63 cells at a concentration of ≤12.5%. Ion release measurements showed that the cytotoxic effect was observed only at high Zn^{2+} concentrations and when in direct contact with metallic samples. The highest LD_{50} (lethal dose killing 50% of cells) of 13.4 mg/L of Zn^{2+} ions was determined for the Zn-3Ag-0.5Mg. Similar antibacterial activity against both *S. aureus* and *E. coli* was observed for Zn and Zn alloys[3].

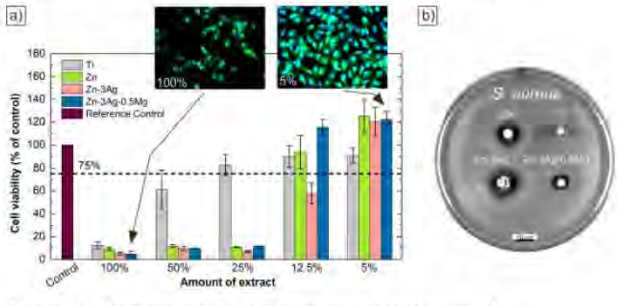

Fig. 1: Extract-based cytotoxicity (a) and antibacterial activity (b) evaluation of Zn, Zn-3Ag, and Zn-3Ag-0.5Mg materials.

DISCUSSION & CONCLUSIONS: Changes in the chemical and phase composition in the fabricated Zn alloys caused by alloying with Ag and Mg additions do not distinctly affect cell viability and antibacterial activity. The antibacterial effect is attributed mainly to the released Zn^{2+} ions exhibiting bactericidal properties. The discrepancies noticed between the WST-assay and microscopic observations are most probably attributed to the interference of Zn^{2+} ions with tetrazolium salt, favoring its transformation into formazan and giving quantitative false-positive cell viability results. Therefore, a more suitable cytotoxicity assay should be chosen for Zn-based samples, or an additional qualitative technique should be used to verify obtained quantitative results.

REFERENCES: [1] PK Bowen et al (2013) *Adv Mater.* **25**:2577- 2582 [2] M. Wątroba et al (2021)

Coating of a biodegradable magnesium alloy for rapid action against S. aureus after ultraviolet exposition

P Tamurejo-Alonso[1], ML González-Martín[2,3], MA Pacha-Olivenza[1,3]

[1] Department of Biomedical Sciences, Faculty of Medicine and University Institute of Biosanitary Research of Extremadura (INUBE). [2] Department of Applied Physics, Faculty of Science and University Institute of Biosanitary Research of Extremadura (INUBE). [3] Network Research Center on Bioengineering, Biomaterials and Nanomedicine (CIBER-BBN), Badajoz, Spain. [3]

INTRODUCTION: One of the reasons for implant failure is bacterial colonisation of the implant surface and the consequent formation of biofilms. The advantage of Mg alloys is that the Mg^{2+} ions resulting from their degradation affect the viability of bacteria. This bactericidal behaviour is a synergistic effect between the pH, which causes an increase in the alkalinity of the medium, and the Mg^{2+} cation, which interacts with the microbial cell wall affecting the integrity of the membrane, leading to leakage of proteins and intracellular constituents. However, the high degradation rate of magnesium and its alloys compromises the mechanical properties of the implant. Therefore, the electrodeposition technique can be used to produce coatings that provide an increased supply of Mg^{2+} ions. In addition, coatings can be supplemented with ZnO, which can reduce corrosion. ZnO is a trace element with photocatalytic capacity. Its antibacterial effect is related to the production of reactive oxygen species (ROS) by UV irradiation that can penetrate cells and thus inhibit or kill microorganisms. In previous studies we demonstrated the ability of a $Mg_3(PO_4)_2$, ZnO and hydroxyapatite coating on AZ31 to reduce the viability of bacteria in their initial adhesion phase[1]. Our current objective to demonstrate that this coated surface also exhibits antibacterial properties even after the formation of a mature biofilm on its surface. For this, we will relate these results with the release of Mg^{2+} ions and the alkalinization of the medium.

METHODS: $Mg_3(PO_4)_2$ and ZnO were co-deposited with hydroxyapatite on AZ31 discs by electrodeposition. One set of samples was not subjected to any additional treatment, while a second set of samples was exposed to a UV source for 24 h. The strain used for the bacterial tests was *Staphylococcus aureus* ATCC25923. The number of viable bacteria in biofilm cultures on the surfaces was determined by ATP quantification. BacTiter-Glo Microbial Cell Viability Assay (Promega Corporation, Madison, WI, USA) was used according to the manufacturer's instructions. Relative light units (LRU) were measured with a luminometer (Microplate Fluorescent Reader FLX 800, Bio-Tek Instruments, USA). The release of Mg^{2+} ions from samples (ICP-Ms) and the variation of pH with time were also measured.

RESULTS: The release of Mg^{2+} ions started immediately after contact with body fluids. The pH increased with increasing contact time. Viability of bacteria in biofilm on coated surface after being exposed to a UV-C source reached an extremely low, nearly null, level.

DISCUSSION & CONCLUSIONS: The damage to the bacteria is due to the combined action of magnesium ions attached to the cell, favored by the alkalinization of the medium, which promotes the loss of membrane integrity. This membrane damage is responsible for the leakage of components from inside the bacteria, but also allows a more efficient action of the ROS generated by the ZnO excitation, which penetrate inside the cells, thus causing total damage to cell viability. As a result, the coatings produce a 90% reduction in the bacteria's ability to make the biofilm. This research can bring great benefits in the field of implantable devices in the human body.

REFERENCES: [1]Purificación Tamurejo-Alonso, M. Luisa González-Martín, Miguel A. Pacha-Olivenza, Coating of a biodegradable magnesium alloy for rapid action against *S. aureus* after ultraviolet exposition, Applied Surface Science, Volume 613, 2023, 156006, ISSN 0169-4332, https://doi.org/10.1016/j.apsusc.2022.156006

ACKNOWLEDGEMENTS: Authors are grateful to the Junta de Extremadura and FEDER (Fondo Europeo de Desarrollo Regional "Una manera de hacer Europa"), for financial help (RTI2018-096862-B-100 and GR18153). Also, authors acknowledge to NANBIOSIS and SACSS–SAIUEX.

Fatigue behaviour of biodegradable Zn-0.3Li alloy

Guannan Li[1], Dandan Xia[2], Yan Cheng[3], Yufeng Zheng[1, 3]

[1] School of Materials Science and Engineering, Peking University, Beijing 100871, China. [2] Department of Dental Materials, Peking University School and Hospital of Stomatology, Beijing, China. [3] Academy for Advanced Interdisciplinary Studies, Peking University, Beijing, China.

INTRODUCTION: Metallic implants such as bone fixation devices are subjected to dynamic loadings during service. Thus, corrosion fatigue behaviours are critical for judging their feasibility for applications. For biodegradable metals, Gu et al. investigated the corrosion fatigue behaviours of as-cast AZ91D and as-extruded WE43 alloys [1]. The corrosion fatigue strength was calculated to be 20MPa and 40 MPa, respectively. Cracks were found to derive from localized corrosion pits. However, no such research has ever been conducted on Zn-Li alloys, which are considered promising candidates for load-bearing applications due to their extraordinary mechanical properties [2]. In this paper, the fatigue behavior of biodegradable Zn-Li binary alloy will be studied for the first time.

METHODS: The nominal composition of the investigated material was Zn-0.3wt.%Li. The as-cast ingots were homogenized at 300°C for 1.5 hours in a nitrogen atmosphere. The ingots were then kept at 200°C for 10 minutes followed by extrusion to a diameter of 10 mm with a speed of 1 mm/s (the extrusion ratio was 16:1), and air cooling to ambient temperature. Fatigue specimens with a circular cross-section were machined and loaded parallel to the extrusion direction sinusoidally with a frequency of 10 Hz and R=-1.

RESULTS: As shown in Figure 1a, the material exhibited obvious tension-compression asymmetry. The compressive yield strength was higher than the tensile one, and the alloy showed continuous work hardening when compressed. The fatigue strength of Zn-0.3wt.%Li alloy in air was calculated to be 87.8 MPa when the expected duration was 10^7 cycles. The fracture surface was rather flat (Figure 1c) while the observed step proved that two crack sources were propagating at the same time. Fractography revealed that fatigue cracks originated from sample surface (Figure 1d) and propagated in a transgranular manner (Figure 1e). These results demonstrated the feasibility of this alloy for load-bearing applications.

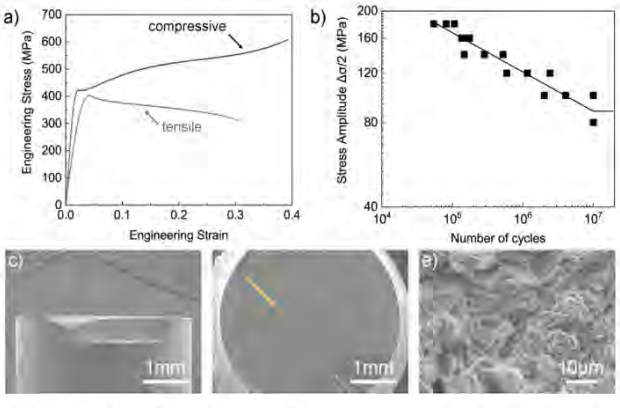

Fig. 1: (a) Tensile and compressive stress-strain curves of Zn-0.3wt.%Li alloy. (b) S-N curve of the alloy fatigued in air. (c-e) Sideview (c), fractography (d), and magnified propagation zone (e) of a specimen fractured at Δσ/2=100 MPa in air. (Yellow arrows designated the crack propagation directions)

DISCUSSION & CONCLUSIONS: Zn-0.3wt.%Li alloy showed higher strength and fracture elongation during compression test. The work softening phenomenon was also absent during compression. During fully reversed tension-compression fatigue test, the material showed higher fatigue strength compared to Mg alloys reported in literature [1]. Such an improvement in fatigue strength was normally considered to result from higher monotonic strength. Fatigue cracks originated from extrusions/intrusions at surface and propagated transgranularly in Zn-0.3wt.%Li. Above results demonstrated the feasibility of this alloy for load-bearing applications.

REFERENCES: [1] X.N. Gu, W.R. Zhou, Y.F. Zheng, Y. Cheng, S.C. Wei, S.P. Zhong, T.F. Xi, L.J. Chen (2010) *Acta Biomater* **6**: 4605-4613 [2] H.T. Yang, B. Jia, Z.C. Zhang, X.H. Qu, G.N. Li, W.J. Lin, D.H. Zhu, K.R. Dai, Y.F. Zheng (2020) *Nat. Commun.* **11**: 401

ACKNOWLEDGEMENTS: This work was supported by National Natural Science Foundation of China (Grant No. 51931001, 52271243).

Design and antimicrobial performance of HT-Ag-PL composite coatings on magnesium alloys

Tao Liang, Haobo Pan, Ying Zhao*

Shenzhen Institute of Advanced Technology, Chinese Academy of Sciences Shenzhen, China

INTRODUCTION: Biodegradable magnesium alloys have received increasing attention due to their outstanding biological performance and mechanical properties[1]. However, rapid degradation and potential surgery infection limits their clinical applications. In this work, a multifunctional composite coating was constructed via hydrothermal treatment, ion exchange, and self-assembly. The *in vitro* degradation and antibacterial performance were systematically researched.

METHODS: As-cast WE43 magnesium alloys was cut into 10×10×5 mm^3 block and mechanically ground using up to 2000 grit SiC paper. Then the samples were hydrothermal treated in 0.2 M K_2HPO_4 solution at 120 ℃, and then immersed in 0.2 mM $AgNO_3$ solution for ion exchange. Afterwards, the samples were immersed in PEGylated lysozyme emulsion for self-assembly. The immersion test and electrochemical measurements were used to determine the degradation resistance. *In vitro* antibacterial performance against *S. aureus* and *E. coli* was evaluated by spread plating method, Dead/Live staining, SEM, ONPG, and ATP assay.

RESULTS: As shown in Fig. 1a and b, the *pH* value and Mg^{2+} concentration for HT-Ag-PL sample after immersion in PBS for 1, 3, and 7 d is lower than that of the untreated sample. Compared with the untreated sample, the HT-Ag-PL sample exhibited nobler open circuit potential, smaller corrosion current density, larger diameter of the capacitive arc and impedance modulus. Above results suggest that HT-Ag-PL composite coating diminishes the degradation rate of WE43.

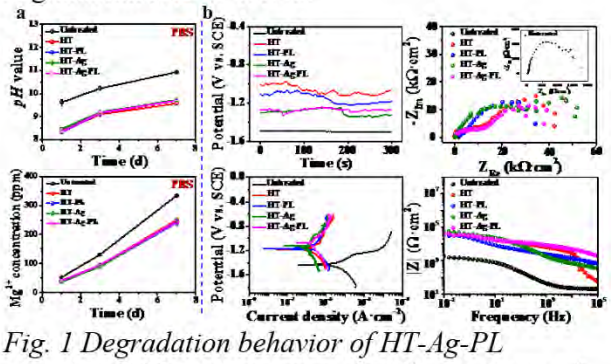

Fig. 1 Degradation behavior of HT-Ag-PL samples: (a) Immersion test; (b) Electrochemical measurements.

As exhibited in Fig. 2, it was difficult to observe *S. aureus* and *E. coli* on the HT-Ag-PL samples. But lots of live bacteria were found on the untreated samples. And the morphology of bacteria on the untreated sample were normal with intact spherical and rod structures, respectively. Antibacterial rates of HT-Ag-PL sample against *S. aureus* and *E. coli* are 100% and 99.6%, respectively, and they are significantly higher than that of the untreated sample. In addition, higher level of β-galactosidase and ATP expression were found in HT-Ag-PL sample compared to the untreated sample.

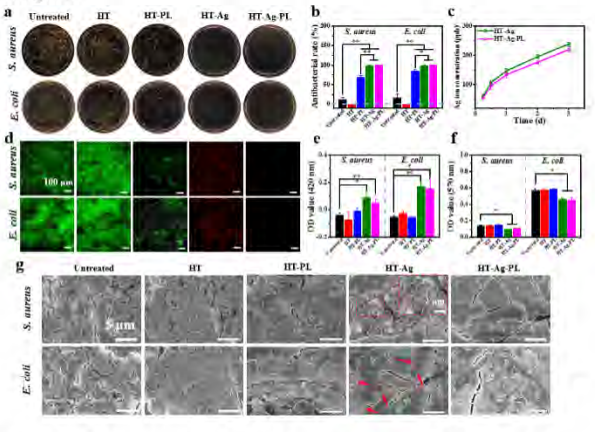

Fig. 2: Antibacterial performance of HT-Ag-PL sample against S. aureus and E. coli: (a) Image of the colony; (b) Antibacterial rate; (c) Released Ag^+ concentration; (d) Live/Dead images; (d) ONPG assay; (e) ATP assay; (f) SEM images.

DISCUSSION & CONCLUSIONS: Improved antibacterial property of HT-Ag-PL sample was attributed to the PEG chains of the coatings to inhibite bacteria adhesion and the released Ag ions to kill bacteria. The Ag ions induced higher level of β-galactosidase and ATP expression, and resulted in bacterial membrane rupture and finally bacterial death.

REFERENCES: 1. Liang T, Zhao Y, et al., Bioactive Materials 6 (2021)3049

ACKNOWLEDGEMENTS: This study was financially supported by the Natural Science Foundation of Guangdong Province (2022A1515011339).

Effect of Zn, Mg, and Ca in solution and released from 3D-printed scaffolds on musculoskeletal cells

B. Limones-Ahijón [1], P.J. Díaz-Payno [1], V. Sevostianova [1], G. Domínguez [1], M. Li [1], S. Pöstges [2], A. Kopp [2], J. Molina-Aldareguía [1,3] and J. Patterson [1]

[1] IMDEA Materials Institute, 28906 Getafe, Madrid, Spain; [2] Meotec GmbH, 52068 Aachen, Germany; [3] Universidad Politécnica de Madrid, 28040 Madrid, Spain

INTRODUCTION: Zinc (Zn) and magnesium (Mg) are biodegradable metals that have gained interest for use in 3D printed scaffolds in tissue engineering[1]. Meanwhile, calcium (Ca)-based materials offer advantages such as biocompatibility and osteoconductivity facilitating bone repair[2]. Further, Ca and Mg have been shown to play a role in cardiomyocyte signalling and in cardiovascular disease[3,4]. Nevertheless, additional research is warranted to elucidate the underlying molecular and cellular mechanisms involved. The aim of this study is to characterize the cytotoxicity elicited by different concentrations of Ca, Mg and Zn ions and the compatibility of 3D printed biodegradable metal scaffolds towards different musculoskeletal cells for eventual applications in bone and cardiac regeneration.

METHODS: Scaffolds made of either Zn1Mg and WE43 alloys were 3D printed by Laser Powder Bed Fusion. $CaCl_2$ and $MgCl_2$ were prepared in the cell culture medium for each cell type at 1 mM, 10 mM, and 50 mM, while $ZnCl_2$ and $ZnSO_4$ were prepared at 0.1 mM, 0.25 mM, and 0.5 mM. Scaffolds were incubated in the appropriate cell media for 24 h to prepare extracts for an indirect test._Human osteosarcoma cells (SaOS-2), rat myoblasts (H9c2[2-1]), mouse myoblasts (C2C12) and mouse fibroblasts (MC3T3-E1) cells were obtained from CLS and cultured following the manufacturer's guidance. SaOS-2 cells were seeded on the surface of the scaffolds as a direct test of cytocompatibility. A Presto blue assay was performed to evaluate the metabolic activity of all cell types in the presence of the different ions and also for the direct and indirect tests. To evaluate the cell death, the Click-iT™ Plus TUNEL Assay was performed._The scaffolds with cells were prepared for SEM analysis (Apreo 2S LoVac-Field Emission SEM) by fixing them with 4% PFA and subsequently drying them with ethanol in distilled water and HMDS in ethanol with increasing concentrations. Staining of the fixed cells was also conducted using DAPI and Phalloidin to facilitate the visualization under a confocal microscope (Olympus FV3000).

RESULTS: MC3T3 cells showed less sensitivity to ion types, while all cell types exhibited decreased metabolic activity when exposed to ≥ 0.25 mM Zn. SaOS-2 cells displayed a decline in metabolic activity over time when cultured in medium supplemented with ≥ 10 mM $CaCl_2$, and C2C12 cells experienced an overall decrease in metabolic activity with no recovery at 50 mM $MgCl_2$. SaOS-2 cells exposed to 100% extracts demonstrated a significant decrease in metabolic activity after 72 h, while cells exposed to lower percentages (50, 30 and 10% in fresh culture medium) showed metabolic activity levels similar to the positive control. The direct assay showed a reduction of the metabolic activity for all the specimens, including the positive control, at 48 h, which began to recover after 72 h. SEM and DAPI/Phalloidin staining confirmed the SaOS-2 attachment to the scaffold's surface (Fig 1).

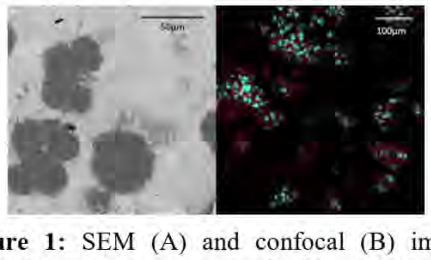

Figure 1: SEM (A) and confocal (B) images of SaOS-2 cells cultured on the Zn1Mg scaffolds.

DISCUSSION & CONCLUSIONS: The results demonstrate that the ion concentration is key for the cytocompatibility of Ca, Mg and Zn derived materials. Zn1Mg scaffolds showed good cell viability but seem to affect the cell morphology.

REFERENCES

1. Qin, Y. et al. *Acta Biomater*. 98, 3–22 (2019); 2. Samavedi, S. et al. *Acta Biomater*. 9, 8037–8045 (2013); 3. Laurant, P. & Touyz, R. M. *J. Hypertens*. 18, 1177 (2000); 4. Louch, W. E. et al. *Physiol.* 593, 1047–1063 (2015).

ACKNOWLEDGEMENTS: Funding from the European Union's Horizon Europe research and innovation programme under grant agreement No. 101047008 (BIOMET4D) and the biomedicine call of the Community of Madrid (CARDIOBOOST-CM; ref. P2022/BMD-7245).

In Vivo

Saturday, August 26th 2023

Bioresorbable flow diverters for the treatment of intracranial aneurysms

AA Oliver[1,2], C Bilgin[1], AJ Vercnocke[1], KD Carlson[2], R Kadirvel[1,3], RJ Guillory II[4], AJ Griebel[5], JE Schaffer[5], D Dragomir-Daescu[2], DF Kallmes[1]

[1]Radiology, [2]Physiology and Biomedical Engineering, and [3]Neurosurgery, Mayo Clinic, Rochester, MN. [4]Biomedical Engineering, Michigan Technological University, Houghton, MI. [5]Fort Wayne Metals, Fort Wayne, IN

INTRODUCTION: Flow diverters (FDs) are miniature braided stents used to treat intracranial aneurysms. Bioresorbable FDs (BRFDs) have been proposed as the next generation of FD technology [1]. BRFDs aim to serve their temporary function of occluding and healing the aneurysm and then safely dissolve into the body, mitigating complications associated with the permanent presence of conventional FDs. In this work, we prototype BRFDs out of magnesium (MgBRFD) and iron (FeBRFD) alloys and compare them on the bench. The FeBRFDs are investigated in vivo.

METHODS: The MgBRFDs and FeBRFDs were constructed from WE22 (>95% Mg, the rest rare earth elements by wt%) and FeMnN (35% Mn, 0.15% N, balance Fe by wt%) wires, respectively. Twenty-five percent of the wires in each device were polyimide coated tantalum to impart radiopacity [2]. All wire components were manufactured by Fort Wayne Metals. The devices were deployed within flow loops mimicking the physiological environment and serial MicroCT imaging was used to evaluate resorption over time in vitro (Fig. 2) [2]. The FeBRFDs were deployed in the rabbit elastase-induced aneurysm model [3]. Digital subtraction angiography images were taken before and immediately after FeBRFD deployment across the aneurysm neck (Fig. 3).

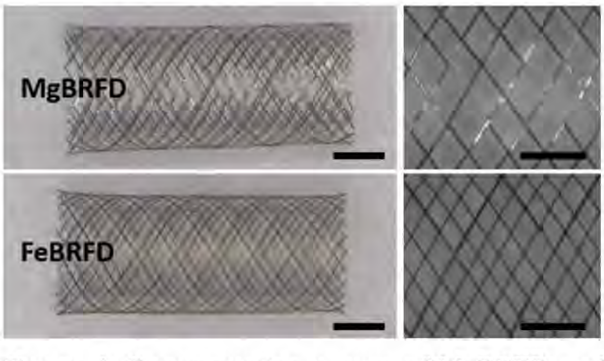

Figure 1. Representative images of MgBRFD and FeBRFD. Scale bars are 2 mm (left column) and 1 mm (right column)

RESULTS: The higher strength and anticipated slower resorption rate of the iron alloy facilitated the use of smaller diameter wires, which allowed us to incorporate more wires into the braid (Ø25 µm x 48 wires for FeBRFD vs Ø50 µm x 32 wires for MgBRFD) (Fig. 1). The FeBRFD wire diameter, wire count, and device radial strength (data not shown) were in the range of FDA-approved FDs.

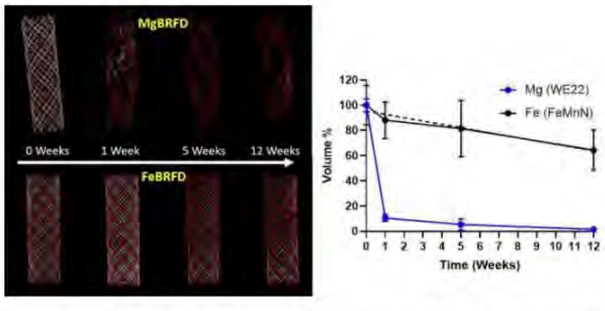

Figure 2. Left) 3D renderings: white represents bioresorbable wires and red tantalum for both devices. Right) Bioresorbable wire volume reduction over time.

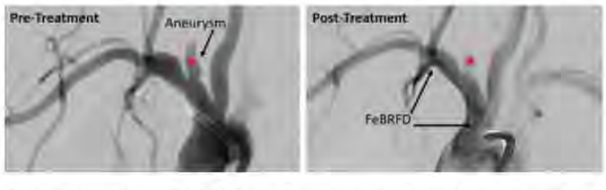

Figure 3. Rabbit elastase-induced aneurysm (asterisk) pre- and immediately post-treatment with an FeBRFD.

DISCUSSION & CONCLUSIONS: These data suggest that Fe alloys are well suited for the BRFD application due to their high strength and slow resorption rate. The ideal resorption rate needs to be determined for the BRFD application. Ongoing work is investigating FeBRFD aneurysm occlusion efficacy, resorption, and biocompatibility in vivo.

REFERENCES: [1]A. Oliver, K. Carlson, C. Bilgin, et al (2023) *J Neurointerv Surg* **15.2:** 178-182. [2]A. Oliver, C. Bilgin, A. Vercnocke, et al (2022) *J Neurosurg* **1:** 1-7. [3]T. Altes, H. Cloft, J. Short, et al (2000) *Am J Roentgenol* **174.2:** 349-354.

ACKNOWLEDGEMENTS: This work was partially funded by NIH grant # R01 NS076491 and the Mayo Clinic Radiology Department. Alexander Oliver is supported by the American Heart Association grant # 23PRE1012781.

15th Biometal
AUGUST 21 TO 27, 2023
Grand Hôtel San Michele, Cetraro, CS, Italy

ex vivo thrombosis study of pure biodegradable metals and clinical cardiovascular alloys for vascular stent applications

DEJ Anderson[1], H Vu[1], J Johnson[1], JE Aslan[1], J Goldman[2], MT Hinds[1]

[1] Department of Biomedical Engineering, *Oregon Health & Science University, Portland, OR, USA.*
[2] Department of Biomedical Engineering, *Michigan Technological University, Houghton, MI, USA.*

INTRODUCTION: Biodegradable metals present an excellent opportunity for cardiovascular devices, such as stents. However, little work has examined the thrombogenicity of the metals in the absence of anticoagulants or antiplatelet therapies. While these therapies are effective in preventing biomaterial thrombosis, they present risks to patients, including an increased risk of bleeding. This work used a strict non-human primate *ex vivo* thrombosis model to quantify thrombosis on pure metals (Mg, Zn, Fe, and Mo) as well as commonly used clinical alloys [NiTi, CoCr, and stainless steel (SS)]. Our goal was to thoroughly evaluate thrombosis, including platelet attachment, fibrin accumulation, and platelet markers on metal wires exposed to whole, flowing blood.

METHODS: Pure and alloyed metal wires (0.25mm diameter) were wrapped into 4mm inner diameter, 2cm length coils and placed into an exteriorized arteriovenous shunt loop. In brief, coils were exposed to whole, non-anticoagulated blood from a single non-human primate and blood flow was controlled at 100mL/min for 1hr. Dynamic platelet and endpoint fibrin attachment were quantified using radioisotopes, ^{111}In and ^{125}I, respectively (n=4). Boundary layer blood draws from downstream of the metals allowed for quantification of platelet and inflammation markers with fluorescence activated cell sorting (FACS) and quantification of metal ions with inductively coupled plasma mass spectrometry (ICP-MS). Wires were fixed for scanning electron microscopy (SEM) to assess thrombus quality (n=2).

RESULTS: Platelet and fibrin accumulation (Fig. 1) on the metal wires was significantly lower for Mg than other metals or alloys. However, analysis of the downstream blood samples showed no significant change in platelet-leukocyte interactions, p-selectin, or lactadherin from FACS analysis, suggesting the activation of platelets and inflammation was consistent across all metal types. ICP-MS data showed no significant changes in metal ion concentrations for any element tested (Fe, Zn, Mo, Mg, Cu, Mn) in the pure metal coils, indicating a lack of significant, detectable metal degradation during the 1hr test.

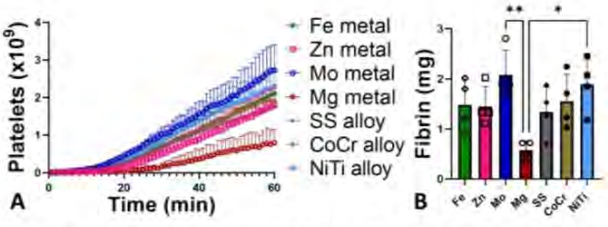

Fig. 1: Platelet (A) and fibrin (B) quantification of pure and alloyed metal coils during 1hr exposure to flowing whole blood without anticoagulants. Platelet data were analysed with a 1-way repeated measures ANOVA. Fibrin data were analysed with a 1-way ANOVA. ($p<0.05$, ** $p<0.01$)*

SEM (Fig. 2) showed considerable thrombus components, including platelets, neutrophils, red blood cells, and fibrin fibers on all wires, but with no obvious differences between metal types.

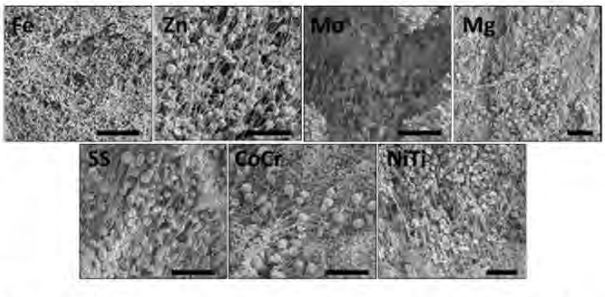

Fig. 2: SEM images from wires exposed to whole flowing blood showed thrombus elements on all samples. Scale bar = 25µm.

DISCUSSION & CONCLUSIONS: All pure and alloyed metal coils showed considerable platelet and fibrin accumulation suggesting the necessity of antiplatelet or anticoagulant therapies with clinical use and the corresponding bleeding risk that accompanies those medications. Future work will consider surface modifications to decrease thrombosis.

ACKNOWLEDGEMENTS: This work was supported by NIH grants R01HL130274, R01HL144113, R01HL101972, R01HL151367, and R01HL168696. We gratefully acknowledge the veterinary staff at the Oregon National Primate Research Center, supported by P51OD011092.

Osteosynthesis with bioabsorbable magnesium screws and pins - experiences and learnings from our first 1,000 cases

A Kopp[1], M Müther[1], C Ptock[1], J Seitz[2], A Aksu[3], F Reinauer[3], M Gertig[2], C Coppers[2], K Reuss[2]

[1] *Meotec GmbH, Aachen, DE.* [2] *Medical Magnesium GmbH, Aachen, DE, KLS Martin, Gebrüder Martin GmbH & Co. KG, Tuttlingen, DE*

INTRODUCTION: Medical magnesium alloys have found its way into daily clinical routine. In form of bioabsorbable screws, pins and prospectively plates they are used for osteosynthesis of long and facial bones as well as fixation of osteochondral fragments among others.

METHODS: Commercially available CE-marked mm.X screws and pins (Medical Magnesium GmbH, Aachen), namely

- **mm.IF**: interference screw in Ø 5-11 mm and L 19-35 mm for soft tissue fixation
- **mm.CS**: Herbert style compression screw in Ø 2.8/3.5/5.0 mm and L 10–34/40/60 mm
- **mm.PIP**: interphalangeal arthrodesis pin in L 1.7/2.1 mm, W 3.8 mm and 0/10/20° (angle)

were manufactured from bioabsorbable magnesium alloy WE43MEO (Meotec GmbH, Aachen) by SWISS type turning, successively treated by PEO surface modification (Kermasorb®) and clinically applied for surveillance.

RESULTS:

The implants were widely applied in different medical indications in elective and trauma surgery.

The findings will be discussed in terms of clinical performance, absorption kinetics and gas formation.

Treated clinical indications comprised:

- Elective forefoot surgery (hallux valgus correction, hammertoe correction),
- traumatic joint near fractures including osteochondral shear fractures (OC and OCD refixation,
- fractures of the elbow and upper limb and
- ligament reconstruction techniques (e.g. ACL) including avulsion fractures.

Patients were surgically treated with mm.X bioabsorbable magnesium implants at clinical centers in different locations in Germany and Switzerland. The patients were routinely followed up for different time points. *Figure 1* shows a successful osteochondral refixation to restore the anatomical biomechanics of a patient's knee after traumatic injury at 12 weeks postoperative care.

Figure 1: Postoperative (A, B) and 3 months follow-up (C, D) x-rays showing the refixed osteo-chondral flake using canulated mm.CS 2.8 mm compression screws.

DISCUSSION & CONCLUSIONS: The overall clinical performance of tested bioabsorbable magnesium screws under surveillance shows highly satisfactory clinical and functional results.

No implant related serious adverse events were observed within our first 1,000 cases: In two applications mm.IF screws however damaged sutures during insertion. No delayed healing and no non-union has been observed so far. All fractures consolidated well and no early mechanical implant failure has been reported to the manufacturer. In nearly all patients no larger (>2mm²) gas accumulations were visible in the surrounding bone or soft tissue.

Although clinically irrelevant, a very limited number of 5-10 out of 1.000 patients revealed prominent radiolucent areas (most likely gas accumulations) in radiographic imaging. This phenomena still needs to be monitored to fully understand influencing factors.

In our experience, when potential application of magnesium devices is chosen consciously based on case data and target indications, full compliance with clinical expectations can be met.

Extension to further clinical fields of surgery is advised on step-by-step basis and needs to be challenged by both, the medical device manufacturer and surgeon as well as to be kept within the regulatory boundaries.

15th Biometal
AUGUST 21 TO 27, 2023
Grand Hôtel San Michele, Cetraro, CS, Italy

From dynamic *in vivo* to multimodal *ex vivo*: exploring comprehensive approaches in preclinical research of magnesium implants for fracture repair

Yu Sun[1], Heike Helmholz[1], Regine Willumeit-Römer[1]

[1] *Institute of Metallic Biomaterials, Helmholtz-Zentrum Hereon, Geesthacht, Germany*

INTRODUCTION: For developing biodegradable metallic materials in fracture fixation devices, *in vivo* tests remain the most effective way to reproduce the orchestrated process of bone healing and implant degradation. However, deficient experimental design and sample analysis can hardly provide effective support for clinical translation [1]. The authors explored the feasibility of establishing research pipelines in a preclinical trial, to facilitate dynamic monitoring of fracture healing and implant degradation comparable to clinical practice, as well as subsequent multimodal *ex vivo* sample analyses at multiple levels.

METHODS: Sprague-Dawley rats underwent external fixation of femoral fractures, and intramedullary implantation of magnesium (Mg) pins before bone reduction [2]. *In vivo* micro-CT were conducted directly after surgery and at postoperative week 12, to evaluate fracture union and implant degradation. Bone samples underwent tissue preparation and sectioning after *ex vivo* micro-CT, for histochemical staining, immunohistochemistry (IHC) and micro-X-ray fluorescence spectrometry (µXRF), to access the feasibility of multimodal sample analysis [3].

RESULTS: The animals resumed full weight-bearing activities early after surgery, and no subcutaneous air cavity or wound infection were detected during the follow-up. *In vivo* degradation was lower than *in vitro* test results. The removal of fixation devices didn't involve tissue damage at the fracture site, supporting the conduction of *ex vivo* CT scan, histochemistry, IHC and µXRF in well preserved samples. Histochemical and IHC staining revealed typical endochondral ossification process for fracture repair, and mapping of bone mineral elements Ca and P was realized in tissue sections, demonstrating µXRF as a promising method for future research of tissue regeneration and novel biomaterials (Fig.1).

DISCUSSION & CONCLUSIONS: The surgical model, which is close to clinical fracture management, allowed the dynamic monitoring of fracture healing and implant degradation. Further tests in *ex vivo* samples supported multimodal analyses at the tissue, cellular, molecular, and elemental levels. Given the scalability of the model, it supports relevant studies of trauma, inflammation or infection in the musculoskeletal system, providing quality evidence for translation of degradable Mg-based and other biomaterials.

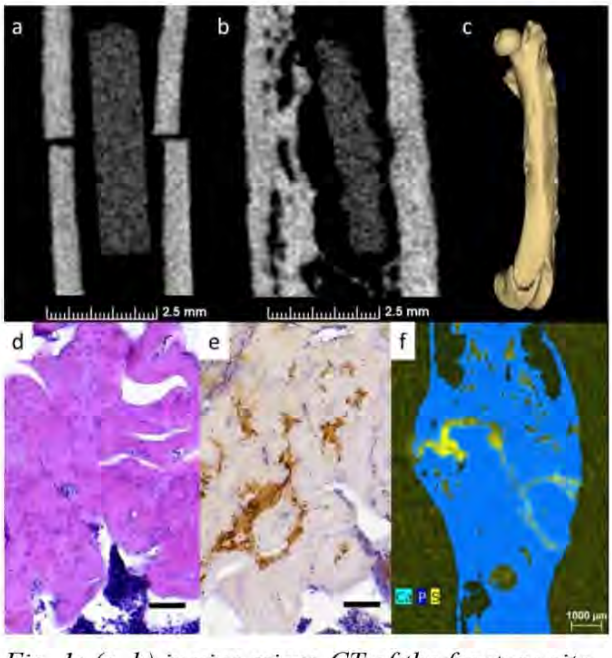

Fig. 1: (a, b) in vivo micro-CT of the fracture site directly after surgery and at week 12; (c) 3D rendering of ex vivo micro-CT scans showing fracture union; (d, e) H&E and IHC (collagen type-X) staining of fracture site (scale bar: 60µm); (f) elemental mapping for Ca, P and S.

REFERENCES: [1] M. Peric, I. Dumic-Cule, D. Grcevic, et al (2015) *Bone* **70**: 73-86. [2] Y. Sun, H. Helmholz, R. Willumeit-Römer, et al (2022) *Biomater Sci* **10**: 1532-1543. [3] H. Helmholz, B. Luthringer-Feyerabend, R. Willumeit-Römer (2019) *JAAS* **34**: 356-365.

ACKNOWLEDGEMENTS: Dr. Björn Wiese, Dr. Thomas Ebel, Monika Luczak (Helmholtz-Zentrum hereon); The Central Animal Facility (ZTH) and Molecular Imaging North Competence Center (MOIN CC, Section Biomedical Imaging) at UKSH, Kiel University.

15th Biometal
AUGUST 21 TO 27, 2023
Grand Hôtel San Michele, Cetraro, CS, Italy

3D micro- and nanoscale analysis of bone morphology surrounding Mg-10Gd and Ti implants

S. Sefa[1], D.C.F. Wieland[1], R. Willumeit-Römer[1], B. Zeller-Plumhoff[1]

[1] *Institute of Metallic Biomaterials, Helmholtz-Zentrum Hereon, Geesthacht, DE*

INTRODUCTION: Bone implants interact with their surrounding tissue and can affect the bone function across several orders of magnitude. Biodegradable magnesium-10wt.% gadolinium (Mg-10Gd) implants, have shown good osseointegration in rat bone, in terms of bone volume fraction and bone-to-implant contact, and suitably low degradation rates [1]. At the same time, studies of the bone crystal structure found indications of incorporation of Mg into bone and differences in bone remodelling compared to Ti [2]. In this study, we aim to assess the microstructure of bone to bridge the knowledge gap between morphological structure on the µm-mm level and the crystal structure on the Å-nm level, by studying the lacuno-canalicular network (LCN) of rat bone surrounding Mg-10Gd and Ti implants between 4 and 20 weeks post-implantation. The LCN houses the osteocytes and orchestrates the remodelling and mineralization of bone.

METHODS: Mg-10Gd and Ti screws (length 4 mm, Ø 2 mm, M2 thread and 0.5 x 0.5 mm slotted screw head) were implanted into Sprague-Dawley rats for 4, 8, 10, 12 and 20 weeks. Following sacrifice of the animal, the bone surrounding the implants was explanted. Samples at 4, 8 and 12 weeks were imaged in 3D using high-resolution micro computed tomography (µCT) at 5 µm voxel resolution to extract the lacunar and vascular density. Samples at 10 and 20 weeks were further processed to extract small (Ø 50 µm) samples near the implant interface for 3D transmission X-ray microscopy (TXM) and the LCN morphology was determined.

RESULTS: The µCT analysis shows that the lacunar density (Fig. 1A) was significantly higher ($p<0.05$) for Ti than Mg-10Gd at all time points. Using TXM, we visualized (Fig. 1B&C) that for both materials, the lacunae were aligned parallel to the implant surface, with the canaliculi running perpendicular to them but with enlarged surface area and less order for Mg-10Gd (Fig. 1C) compared to Ti (Fig. 1B). In terms of quantifiable LCN morphology, no significant differences were found between Mg-10Gd and Ti, though LCN porosity (volume fraction of the LCN in bone, Fig. 1D) and canaliculi surface area and junction density (not shown) appeared higher for Mg-10Gd at 10 weeks.

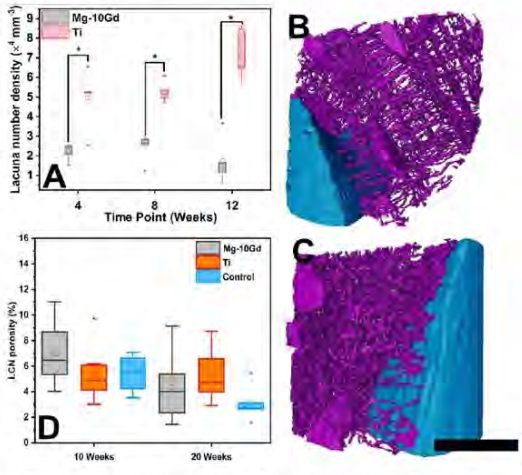

Fig. 1: (A) Lacunar number density at 4, 8 and 12 weeks for Mg-10Gd (grey) and Ti (red). (B&C) volume rendering of LCN (purple) attaching to implant surface (blue) to Ti (B) and Mg-10Gd (C) at 10 weeks, scale bar is 10 µm (D) LCN porosity at 10 and 20 weeks.

DISCUSSION & CONCLUSIONS: Our results indicate that the degradation of Mg-10Gd influences the lacunar density rather than the morphology of the LCN. The differences in density suggests a higher degree of remodelling in the bone surround Ti implants, which could be related to the differences in mechanical properties of the implant material. The observed trends for the LCN morphology may suggest a tendency for the LCN to regulate the increased mass transport required for the biodegradable Mg-10Gd implants. Since different time points had to be assessed for µCT and TXM due to technical reasons, additional future studies should be conducted to study the LCN morphology surrounding Mg-based implants at additional healing times.

REFERENCES: [1] D. Krüger et al., Bioactive Materials (2022), [2] B. Zeller-Plumhoff et al., Acta Biomaterialia (2020)

ACKNOWLEDGEMENTS: We acknowledge funding by the German Ministry for Education and Research (05K16CGA, 05K16CGB).

Magnesium-containing biomimetic hydrogel facilitates in-situ cartilage regeneration under OA

Han Wu[1], Jinhui Zhao[2], Guangyin Yuan[1], Wenjiang Ding[1], Weitao Jia[2*], Jia Pei[1*]

[1] *National Engineering Research Center of Light Alloy Net Forming and State Key Laboratory of Metal Matrix Composites, Shanghai Jiao Tong University, Shanghai, 200240, China.*

[2] *Department of Orthopedic Surgery, Shanghai Jiao Tong University Affiliated Sixth People's Hospital, Shanghai 200233, China.*

INTRODUCTION: Osteoarthritis (OA) is a prevalent type of arthritis associated with pain and loss of joint function[1]. In pathological situations, the abnormal level of reactive oxygen species (ROS) produced by chondrocytes or macrophages is known to lead to cartilage degradation and damage. Worse still, cartilage is highly differentiated tissue lacking blood vessels, leading to a limited ability for intrinsic regeneration, while the current treatments are difficult to achieve desirable therapeutic effects.

Mg has been extensively studied in the cardiovascular, orthopedic, and dental implant fields[2]. Our previous study has shown the potential of appropriate amount of Mg^{2+} in inhibiting the inflammatory response and promoting the chondrogenic differentiation of stem cells[3]. In addition, another degradation product, H_2 has also long been demonstrated to have anti-inflammatory effects[4]. Nevertheless, there is few reports on cartilage regeneration under OA by using Mg-based biomaterials, as controlling the rapid degradation of Mg to achieve favorable microenvironment remains a great obstacle.

METHODS: We fabricated a biomimetic GM/LPFEG composite hydrogel with coated Mg powders and nanofibers, and characterized the physicochemical properties of the hydrogel. Next, we assessed the in vitro anti-inflammatory properties and cytocompatibility of the hydrogel. Finally, we evaluated the effect of the hydrogel on cartilage regeneration in vivo under OA with the underlying mechanisms investigated.

RESULTS: The as-prepared biomimetic Mg-containing hydrogel continuously released Mg^{2+} and H_2, synergistically inhibiting inflammation. The hydrogel also facilitated the adhesion, proliferation, and chondrogenic differentiation of hBMSCs, attributed to biomimetic nanofibers and appropriate amount of Mg^{2+} released. Moreover, the in vivo study indicated that the hydrogel exhibited satisfactory cartilage regeneration in a rat OA model.

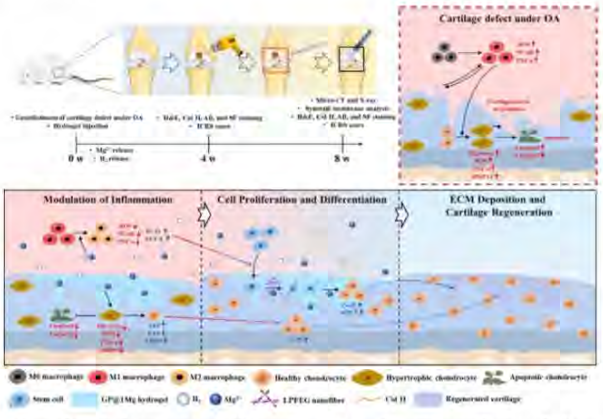

Fig. 1: Schematic illustration of surgical modeling and the Mg-containing hydrogel treatment for in-situ cartilage regeneration under OA.

DISCUSSION & CONCLUSIONS: The sustained release of Mg^{2+} and H_2 synergistically inhibits inflammation, providing an optimal micro-environment for cell proliferation and chondrogenic differentiation, thereby promoting the reconstruction of cartilage matrix and achieving cartilage regeneration under OA conditions. Collectively, our study first reported the potential of Mg-based biomaterials for cartilage regeneration under OA and unveiled the synergistic anti-inflammatory mechanism of Mg^{2+} and H_2, which thus may shed light on developing Mg-based biomaterials that benefit patients with cartilage defect under OA.

REFERENCES: [1] H. Kwon, W.E. Brown, C.A. Lee, et al (2019) *Nat. Rev. Rheumatol* **15**:550-570. [2] J.L. Wang, J.K. Xu, C. Hopkins, et al (2020) *Adv. Sci.* **7**:1902443. [3] J.H. Zhao, H. Wu, L.T. Wang, et al (2022) *Biomater. Adv.* **134**:112719. [4] I. Ohsawa, M. Ishikawa, K. Takahashi, et al (2007) *Nat. Med.* **13**:688-694.

ACKNOWLEDGEMENTS: This work was supported by National Key Research and Development Program of China (2021YFE0204900), and the National Science Fund for Excellent Young Scholars (52222108).

15th Biometal
AUGUST 21 TO 27, 2023
Grand Hôtel San Michele, Cetraro, CS, Italy

Measurements of strain, temperature, and pH on magnesium and titanium plates *in vivo* during fracture healing in sheep

AM Rich[1], W Rubin[1], S Rickli[2], T Akhmetshina[1], L Berger[1], K Nuss[3], B von Rechenberg[3], B Schaller[4], JF Löffler[1]

[1] *Laboratory of Metal Physics and Technology, ETH Zurich, CH.* [2] *Department of Information Technology and Electrical Engineering, ETH Zurich, CH.* [3] *Musculoskeletal Research Unit, University of Zurich, CH.* [4] *Inselspital, Bern University Hospital, CH.*

INTRODUCTION: While it is known that mechanical and environmental parameters (temperature, pH) affect magnesium degradation,[1,2] little is currently known about the exact *in vivo* conditions[3]. Limited mechanical loading data exists, though this has strong implications for implant design and fracture healing[4]. To address these shortcomings, we developed a fully-implantable measurement system to record temperature, pH, and strain *in vivo*. The measurements were performed on magnesium and titanium plates, fixating bilateral zygomatic arch fractures in three female alpine sheep for 8 weeks.

METHODS: A battery-powered embedded system was fabricated using discreet electronic components mounted on a printed circuit board (PCB) and a stretchable polyurethane cable. Four semiconductor strain gauges and a miniature pH sensor were mounted on plates made of plasma electrolytic oxidation (PEO)-treated Mg alloy (X0, MgCa0.45, in wt.%) and grade-2 titanium. Two digital temperature sensors were soldered to the cable, with one placed above the fracture and the other 2-3 cm away (reference sensor). Coatings of polyurethane and Parylene-C provided a biocompatible and waterproof seal. Surgically, a completely mobile fracture on the zygomatic-arch bone about 1 cm in length was created bilaterally. The assemblies were implanted in the sheep, screwing the plate onto the bone and placing the sensor case subcutaneously. Data was collected autonomously from the sensors for 8 weeks, recording 10 s every hour, then downloaded and analyzed following sacrifice of the animals.

RESULTS: Coating failure limited the lifetime of the recordings to between 1-5 days. Temperature and pH measurements are shown in *Table 1*; some sensors recorded longer than others, resulting in differences in sample size. *Fig. 1* shows strain readings from Mg and Ti plates, recorded simultaneously during one 10 s measurement period. This data was recorded 6 hours after implantation, presumably while the animal was chewing.

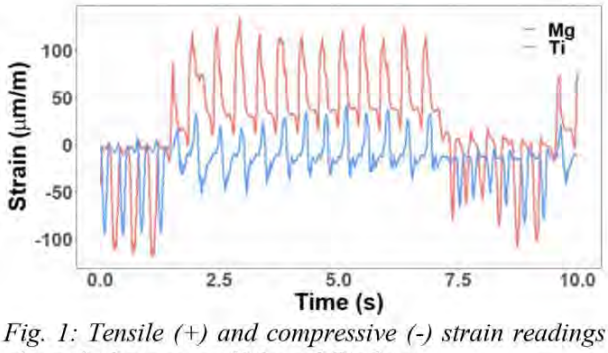

Fig. 1: Tensile (+) and compressive (-) strain readings along the long axis of Mg and Ti plates.

Table 1. Average temperature grouped by sensor location and implant material; pH grouped by implant material. Results shown as mean ± SD (sample size).

	Fracture (°C)	Reference (°C)	pH
Mg	37.3 ± 0.9 (149)	37.9 ± 0.7 (550)	7.4 ± 0.9 (88)
Ti	37.9 ± 0.9 (167)	38.2 ± 0.6 (1068)	6.6 ± 0.4 (21)

DISCUSSION & CONCLUSIONS: No strong trend can be seen regarding temperature, indicating no localized temperature increase during fracture healing. The pH above the Mg plates shows a trend towards higher pH compared to Ti, though not higher than expected for normal blood pH. Continued investigation of the data will reveal if degradation time also affects pH. Strain readings allow determination of static plate loading during implantation (not shown), as well as dynamic loading that the plates experience during chewing. More advanced protective coating options are currently being investigated. These results show that it is possible to record environmental and mechanical factors that may affect biodegradable implants *in vivo* continuously, enhancing the understanding of these alloys and allowing for improvements in clinical applications.

REFERENCES: [1]J. Gonzalez et al (2021) *Adv. Healthcare Mater.* **10**: 2100053. [2]C Wang et al (2022) *Corr. Sci.* **197**: 110059. [3]A.H.M Sanchez, et al (2015) *Acta Biomater.* **13**: 16-31. [4]L. Claes (2021) *J. Biomech.* **115**: 110148.

ACKNOWLEDGEMENTS: The authors gratefully acknowledge the Swiss National Science Foundation for funding this research (grant number CRSII5-180367).

The novel magnesium alloy suture anchor promotes fibrocartilaginous enthesis regeneration in rabbit rotator cuff repair

LL Tan[1], W Zhang[1], Q Zhang[2]

[1] *Institute of Metals Research, Chinese Academy of Sciences, Shen Yang, China.* [2] *PLA General Hospital, the Fourth Medical Centre, Bei Jing, China*

INTRODUCTION: The fibrocartilaginous enthesis regeneration has been a challenge for tendon-to-bone healing after rotator cuff repair. Although biologically based strategies including the use of growth factors and stem cell therapy and related tissue engineering strategies are employed to augment the healing of tendon-to-bone [1]. The biomaterials used to achieve mechanical stability are indispensable. magnesium alloys are bioactive materials with good biosafety, mechanical properties and osteogenic activity [2]. In this study, a novel magnesium alloy anchor was used to repair rotator cuff tear in rabbit model. In vivo degradation of anchor, tendon bone interface, etc. were studied. Magnesium alloy anchor showed promotion of tendon-bone interface healing and bone tissue remodeling.

METHODS: The novel magnesium alloy anchor and compared PLLA anchor were used to repair the severed supraspinatus tendon in rabbit model. The supraspinatus tendon-humerus complexes were harvested for micro-CT and histological analysis, including both undecalcified Goldner staining and decalcified HE, Masson and Safranin O/fast green staining. The qPCR and western blot were analyzed for tendon bone interface. The biomechanical test was used to evaluate the strength of the healing interface.

RESULTS: The open structure of the magnesium alloy anchor exhibited in-growth of bone (Fig. 1) and the anchor provides adequate fixation during the healing process. The mature fibrocartilage enthesis regeneration and the obvious tendon bone embedded structure were observed in the magnesium alloy anchor group (Fig. 2).

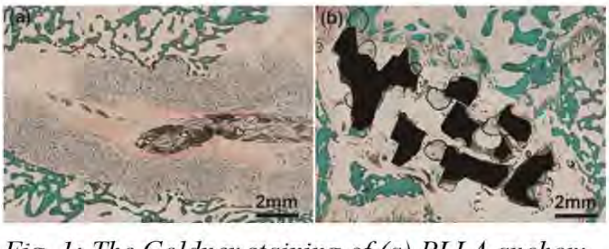

Fig. 1: The Goldner staining of (a) PLLA anchor; (b) magnesium alloy vented anchor.

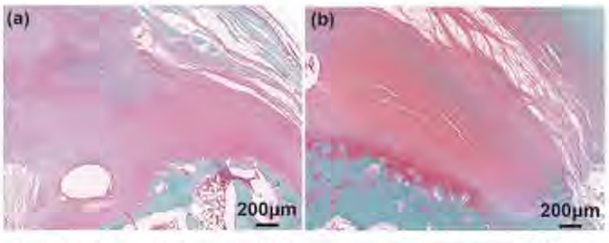

Fig. 1: The Safranin O/fast green staining of the tendon-to-bone interface for (a) PLLA anchor; (b) magnesium alloy vented anchor.

DISCUSSION & CONCLUSIONS: Magnesium alloy vented anchor provides open channel for the growth of bone tissue and promotes the remodeling of surrounding bone tissue. During the degradation of anchor, the design of anchor head suture fixation revealed relatively ideal anchoring effect. The potential mechanisms for this enhancement are related to magnesium ions regulating the cellular functions involved in osteogenic activity, indirectly stimulate the release of TGF-β1 and the secretion of platelet-derived growth factor [3], and bone marrow mesenchymal cells were recruited at the tendon-bone interface. In addition, magnesium ions promote the differentiation of macrophages to M2 type, upregulating the level of growth factors such as BMP-2, and thus promote the expression of fibrochondrogenic transcription factors such as SOX-9 [4]. Enthesis regeneration close to the native structure improves the bioconjugation of tendon bone.

REFERENCES: [1] Gulotta LV, Kovacevic D, Ying L, et al (2008) *Am J Sports Med*. **7**: 1290-7. [2] Wang JL, Xu JK, Hopkins C, et al (2020) *Adv. Sci*. **7**: 1902443. [3] Chen Z, Mao X, Tan L, et al (2014) *Biomaterials*. **35**: 8553-8665. [4] Cheng PF, Han P, Zhao CL, et al (2016) *Biomaterials* **81**: 14-26.

ACKNOWLEDGEMENTS: This work was supported by The National Key Research and Development Program of China (No. 2020YFC1107501), National Natural Science Foundation of China (No. 51971222), STS program (No.20201600200042) and DongGuan Innovative Research Team Program.

Biocompatibility of bioabsorbable metallic molybdenum

M.P. Kwesiga[1], A.L. Canull[2], R. J. Guillory[2]

[1]Biomedical Sciences, Grand Valley State University, USA [2]Biomedical Engineering, Michigan Technological University, USA

INTRODUCTION: Molybdenum (Mo) has emerged as a strong bioabsorbable metal candidate given its excellent mechanical properties and adequate degradation profile [1,2]. Studies have shown that Mo could incur cytotoxic effects specifically in the kidneys, which would ultimately hinder a favourable host response to the degrading material and vice versa [1,3]. Here, we assessed the biocompatibility of Mo in the short and long-term using an in vitro and in vivo approach to confirm its safety for clinical applications, with a particular focus on kidney compatibility in a murine subcutaneous implant model.

METHODS: L929 fibroblast cells were cultured in medium containing varying concentrations of molybdate salt ($MoNa_2O_4 \cdot 2H_2O$). An XTT viability assay was conducted to determine the cytotoxic effect of Mo. In vivo studies using C5BL/6 mice were also performed. Mo foils (34±2 mm^2) were implanted in the subcutaneous tissue of mice aged 4 months for 2, 8 and 16 weeks. Kidney function was assessed using histological analysis to determine the glomerulus to bowman capsule ratio (G/B), proteinuria and caspase 8 expression.

RESULTS: The in vitro cell culture studies showed that concentrations below 1.5 mM of Mo had no cytotoxic effect on L929 fibroblast cells as per ISO standards (above 75% cell viability). The histological analysis performed on kidney sections showed no significant differencs in the G/B ratio for mice implanted with Mo foils from 2 weeks to 16 weeks. Physiological kidney function was further determined by proteinuria, the results showed increases in high molecular weight protein content from 2 to 16 weeks in control mice and Mo implanted mice. Caspase 8 protein expression in kidney tissue samples was absent in both the control mice and Mo implanted mice.

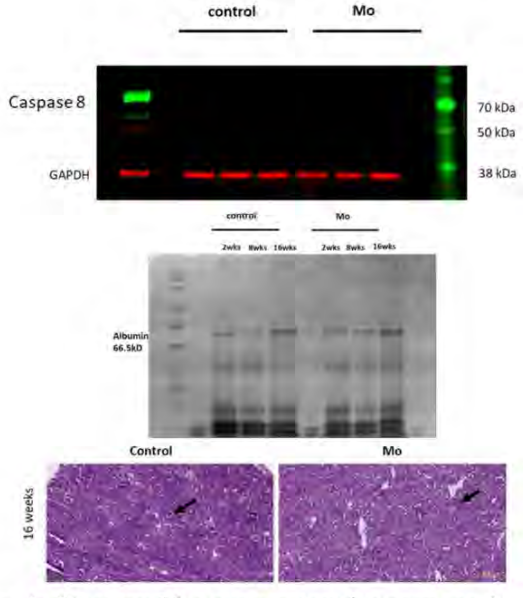

Fig. 1: Western blot expression for caspase 8, protein in kidney mice samples without and with Mo implants for 2, 8 and 16 weeks .H&E of kidneys from mice with implanted with steel (control) or Mo.

	2 weeks	8 weeks	16 weeks
Control	0.58±0.10	0.68±0.08	0.72±0.06
Mo	0.57±0.10	0.66±0.10	0.74±0.06

Table 1. G/B ratio calculated in control and Mo implanted mice at 2, 8 and 16 weeks.

DISCUSSION & CONCLUSIONS: Our work showed no cytotoxic effect below 1.5mM for L929 cell cultures. Moreover, we also tested for kidney injury, which has been reported to be a possible adverse side effect to Mo degradation products. The data showed intact kidney function comparable to mice without Mo implants. Age related degenerative changes were observed in both control and Mo mice. The results obtained from our study support the biosafety of Mo implants.

REFERENCES: [1] Sikora-Jasinska, Malgorzata, et al. *Bioactive Materials* 14 (2022) [2]A Schauer et al., Materials (2021) [3]Bompart, Guy, et al. *Toxicology letters* 52.3 (1990)

In vivo and in vitro biocorrosion of iron molybdenum composite bioabsorbable wires

AJ Griebel[1], P Maier[2], B Clausius[2], JE Schaffer[1] R Guillory II[3]

[1] Fort Wayne Metals [2]University of Applied Sciences Stralsund, Germany [3] Michigan Technological University, USA

INTRODUCTION: Efforts in material development within the past decade have been mainly focused on balloon expandable absorbable vascular scaffolds, leading to multiple developed devices reaching clinical trials[1]. Braided vascular devices, made from very thin wires ranging from 20-50 µm or less can also benefit from bioresorption functionality[2].

The use of classic bioabsorbable materials in wire form presents some challenges. Magnesium (Mg) will degrade too quickly in small wire sizes. Iron (Fe) could benefit from better radiopacity and is prone to fragmentation. Zinc (Zn) is not elastic enough to achieve appropriate wall apposition. The concept of drawn filled tubed (DFT®) composite absorbable wires was introduced in 2012 and displayed favourable properties such as tunability in mechanical and degradation performance[3]. Recently, molybdenum (Mo) was introduced as a potential absorbable metal material and is a favourable DFT composite candidate due to its high ductility, radiopacity, and galvanic pairings. Here, we explore the in vivo biocorrosion performance of multiple Fe-Mo DFT composite wires in a murine arterial implant model.

METHODS: Three different Fe-Mo DFT composite configurations (Fig. 1) were constructed using an FeMnN alloy and pure Mo, and drawn using standard wire drawing methods to a final diameter of 100 µm. Wires were implanted into the abdominal aorta of adult C57Bl6 mice for 1, 3, and 6 months. Explanted wires were evaluated using standard metallographic procedures, SEM/EDS/BSE, and µCT. Wires were also immersed in DMEM to evaluate in vitro biocorrosion progression.

RESULTS: All three configurations of the DFT Fe-Mo composite wires displayed degradation at 1 and 3 months upon gross inspection. The biocorrosion was mostly localized towards the ends of the implants, and at 3 months the second and third configuration displayed biocorrosion activity also in the center luminal portion of the wire. We focused on the third configuration for the shown data in Fig. 2, with the two most leftmost panels showing the in vivo implants and the right-handed panel displaying SEM-EDS mapping of 5 day in vitro corroded specimens.

Fig. 1: Three different Fe-Mo DFT configurations used in this study.

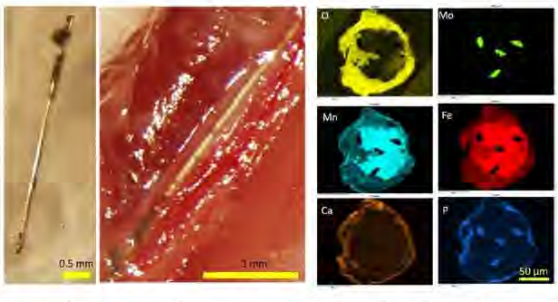

Fig. 2: 3 month implant of the third configuration from figure 1, showing moderate corrosion at the ends of the wire. Third panel displays SEM-EDS of 5 day in vitro DMEM immersed samples

DISCUSSION & CONCLUSIONS: Biocorrosion activity was observed for all three configurations at 1 month and continued for 3 months. Evaluations have shown that the Mo-core increases the corrosion rate of the surrounding Fe material and can thus increase the relatively low corrosion rate. 6 month data will be collected soon, and compared to the already extracted timepoints.

REFERENCES: [1]Dean J. Kereiakes et al. (2016) Bioresorbable Vascular Scaffolds for Coronary Revascularization, Circulation, 134:168–182. [2]A Griebel and J Schaffer (2015) Expanding Magnesium's Reach through Cold Drawing, Proceedings of 72nd Annual International Magnesium Association Conference [3] JE Schaffer et al. (2012) Metallurgical and Materials Transactions B

local release of magnesium and cgrp accelerates bone repair in calvarial defects with or without periosteum

D Hong[1,5,6], SH Zaky[3,5,6], K Liu[3,5], J Gao[2,5], G Hung[1,5,6], N Lacin[3,5], R Chong[5], L Lukashova[5], K Verdelis[3,4,5,6], G Intini[2,3,5,6], C Sfeir[1,2,3,5,6]

[1]Department of Bioengineering, University of Pittsburgh, Pittsburgh, PA USA
[2]Department of Periodontics and Preventive Dentistry, School of Dental Medicine, University of Pittsburgh, Pittsburgh, PA USA
[3]Department of Oral and Craniofacial Sciences, School of Dental Medicine, University of Pittsburgh, Pittsburgh, PA USA
[4]Department of Endodontics, School of Dental Medicine, University of Pittsburgh, Pittsburgh, PA USA
[5]Center for Craniofacial Regeneration, School of Dental Medicine, University of Pittsburgh, Pittsburgh, PA USA
[6]McGowan Institute for Regenerative Medicine, University of Pittsburgh, PA USA

INTRODUCTION: Degradable biomaterials, such as magnesium (Mg), represent promising and lower-risk alternatives to current devices that are fabricated primarily using permanent and inert metals, such as titanium and surgical stainless steel. (1) Mg has been shown to facilitate the process of bone repair by stimulating the local production of calcitonin gene-related peptide (CGRP). (2) Formation of new bone around Mg-based implants below the periosteum raises the possibility that Mg can stimulate osteogenesis of the periosteum and thus induce cell differentiation and local bone regeneration. In this study, we investigated the therapeutic effects of the local release of Mg and CGRP in the bone repair process.

METHODS: We electrospun Mg metal nanopowder and CGRP into PLGA nanofibers, and implanted in male and female rat calvaria defect models with or without periosteum. After one month, samples were harvested and analyzed using microCT and histology.

RESULTS: Our results indicated that the direct release of Mg and CGRP are able to induce new bone formation from rat calvarial periosteum, higher from female rats than that from males. CGRP+ and Mg+ periosteum groups generated a greater volume of new bone compared to control groups (empty defect and PLGA scaffold only). Our µCT analysis showed that the periosteum plays a critical role in bone regeneration. Higher new bone volume has been observed when the periosteum was sutured above the defect.

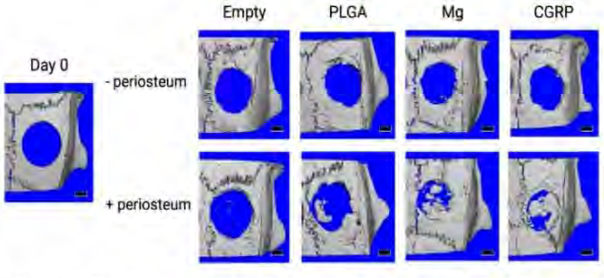

Fig. 1: Representative microCT images of 3D reconstructed male rat calvaria defect after 1 month (Scale bar = 1 µm)

DISCUSSION & CONCLUSIONS: In this study, we assessed the osteogenic effect of Mg and CGRP on rat calvaria defects. We showed that the periosteum is critical in bone regeneration. Local release of Mg and CGRP effectively induced new bone formation. Our results also suggest that new bone formation can be sex-dependent, as we observed higher new bone volume in general from female compared to male rats. Furthermore, we have developed novel electrospun PLGA scaffolds that release Mg metal powder and CGRP and promote bone repair, suggesting the therapeutic potential of this biomaterial to facilitate the repair of cranial injuries.

REFERENCES: [1] Chaya A, Yoshizawa S, Verdelis K, et al. In vivo study of magnesium plate and screw degradation and bone fracture healing. *Acta Biomater*. 2015;18:262-269. [2] Zhang Y, Xu J, Ruan YC, et al. Implant-derived magnesium induces local neuronal production of CGRP to improve bone-fracture healing in rats. *Nat Med*. 2016;22(10):1160-1169.

ACKNOWLEDGEMENTS: This study was supported by the University of Pittsburgh's Center for Craniofacial Regeneration and NSF ERC RMB (grant 0812348),

Lithium-induced optimization mechanism for an ultrathin-strut biodegradable Zn-based vascular scaffold

Hongtao Yangs[1, 2], Yufeng Zheng[1, *]

[1] *School of Materials Science and Engineering, Peking University, Beijing, 100871, China*

[2] *School of Engineering Medicine, Beihang University, Beijing, 100191, China*

INTRODUCTION: To reduce incidences of in-stent restenosis and thrombosis, the use of a thinner-strut stent has been clinically proven to be effective. Therefore, the contemporary trend is towards the use of ultrathin-strut (≤70 μm) designs for durable stents. However, stents made from biodegradable platforms have failed to achieve intergenerational breakthroughs due to their excessively thick struts. Here, microalloying was used to create an ultrathin-strut (65 μm) Zn scaffold with modified biodegradation behavior and improved biofunction, by adding Li.

METHODS: The main purpose of this study was to investigate the fundamental impact of Li on the mechanical performance, biodegradation behavior, and biological effects of biodegradable Zn-based scaffolds. The microstructure of Zn-0.1Li micro-tubes was examined by the electron backscattered diffraction (EBSD) and the transmission election microscope (TEM). Zn-0.1Li scaffolds were implanted into the coronary arteries of Barna pigs. Degradation of the Zn-0.1Li scaffold was studied by a multistage analysis. Micro-CT was used to observe the degradation profile of scaffolds at a macro-level. The microscopic appearance of the scaffold and analysis of corresponding degradation products were performed by SEM, TEM and time of flight - secondary ion mass spectrometry (TOF-SIMS). Six Barna pigs (mean weight, 30 kg) were purchased from Songlian Experimental Animal Farm (Shanghai, China). Each pig was implanted with two Zn-0.1Li scaffolds. All surgical procedures were conducted according to the ARRIVE guidelines (Animal Research: Reporting of In Vivo Experiments) and approved by the Animal Ethics Committees of Shanghai Children's Medical Center, Shanghai Jiaotong University.

RESULTS: The scaffold backbone consists of an ultrafine-grained Zn matrix (average grain diameter 2.28 μm) with uniformly distributed nanoscale Li-containing phases (Fig. 1). Grain refinement and precipitation strengthening enable it to achieve twice the radial strength with only 40% of the strut thickness of the pure Zn scaffold. Adding Li altered the thermodynamic formation pathways of products during scaffold biodegradation, creating an alkaline microenvironment. Li_2CO_3 may actively stabilize this microenvironment due to its higher solubility and better buffering capability than Zn products. The co-release of ionic zinc and lithium enhances the beneficial differential effects on activities of endothelial cells and smooth muscle cells, resulting in good endothelialization and limited intimal hyperplasia in porcine coronary arteries.

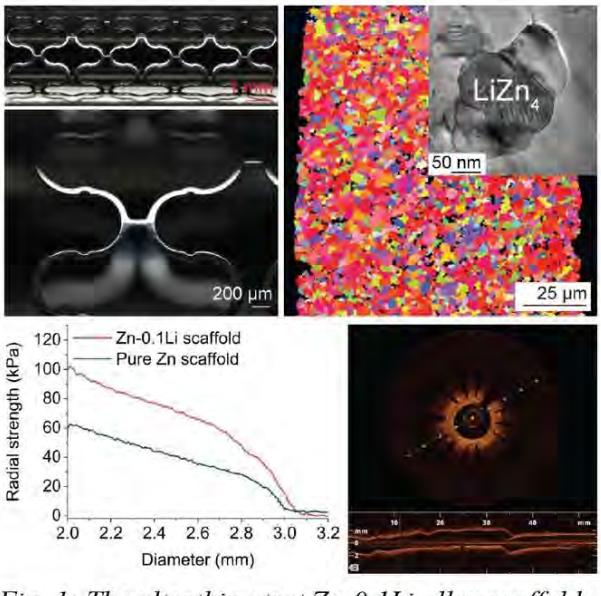

Fig. 1: The ultrathin-strut Zn-0.1Li alloy scaffold with its microstructure, radial strength, and OCT image of scaffolded porcine coronary artery at 12 months.

DISCUSSION & CONCLUSIONS: These findings provide a systematic exploration and validation of a next-generation biodegradable vascular scaffold with comparable mechanical performance to durable metallic stents and potential biofunctions to advance vessel healing.

15th Biometal
AUGUST 21 TO 27, 2023
Grand Hôtel San Michele, Cetraro, CS, Italy

Influence of subchondral implantation of small magnesium cylinder on cartilage and bone in an OA-rabbit model

Nina Angrisani[1], Christin von der Ahe[1], Regine Willumeit-Römer[2], Henning Windhagen[1], Verena Scheper[3], Björn Wiese[2], Bavya Mavila[2], Heike Helmholz[2], Janin Reifenrath[1]

[1]Hannover Medical School, Clinic for Orthopedic Surgery, NIFE, Hannover, D. [2] Helmholtz-Zentrum Hereon, Institute of Metallic Biomaterials, Geesthacht, D. [3]Hannover Medical School, Department of Otolaryngology, NIFE, Hannover, D.

INTRODUCTION: Osteoarthritis still lacks a regenerative therapy and causes severe problems in patients including pain and gait disorders, which often results in total joint replacement as a common ultimate treatment to reduce pain. In the pathological process, different aspects of the joint are involved, including the subchondral bone, the cartilage and synovial structures. Considering the subchondral bone, remodelling processes result in sclerotic bone, which is mechanically less solid and implements cystic lesions. Cartilage is degenerated or even lost. Resulting pain is associated with new growth of vessels in the bone and in the cartilaginous area, accompanied by nerve structures, which are assumed to induce pain. To influence regeneration and repair, microspudding is a common used first therapeutic technique and induces remodelling processes in the subchondral bone and migration of bone marrow stem cells in the chondral defect area. The hypothesis of the current study was to influence bone remodelling, cartilage structure and pain by additional subchondral implantation of degradable magnesium cylinders (Mg and WE43) in the subchondral bone.

METHODS: The *in vivo* study was performed in a rabbit osteoarthritis model, with anterior crucial ligament transection in combination with an incision into the medial meniscus 12 weeks prior to therapeutic approach (NZW rabbits, authorized according to the German Animal Welfare act, registration number 33.9-42502-04-18/2774). Pure magnesium and WE43 cylinder (0.5 x 1.0 mm), produced by extrusion moulding and following cutting/clipping were used. Animals were randomly divided into three groups which received either 20 drill holes (0.5 mm ø, five into each half of the femoral and tibial part of the knee) or 20 drill holes which were additionally filled with one cylinder each, as described in Angrisani et al. 2021[1]. During the postoperative follow up, subjective lameness evaluation was performed by a score and additional objective lameness evaluation by a pressure sensor mat. µ-Computed tomographical (CT) scans were performed immediately after 2nd surgery as well as after 4 and 8 weeks to detect bone changes and cylinder degradation. After euthanasia femoral samples were taken and processed for histological evaluation. Slides were stained with Safranin-O and scored according to OARSI and immunohistochemistry was performed to detect CD271 positive cells and vessels.

RESULTS: Lameness evaluation in the first postoperative week showed moderate lameness and improved during the postoperative follow up period. There were large interindividual differences between single animals and no significant differences between the three groups. µ-CT evaluation showed significant differences between cylinder and drill groups. Calculated degradation rate based on volume loss of WE-cylinders was 3.5 mm/y. Detection of Mg cylinders was not able due to similar density compared to bone and insufficient resolution of the used *in vivo* µ-CT. The condition of the cartilage evaluated by scoring according to OARSI did not show differences between groups, but differences in CD271 staining of vessels and cells.

DISCUSSION & CONCLUSIONS:

Although no impact on pain associated lameness could be observed between groups, impact on CD271 positive cells and vessels could be shown due to Mg and WE43 application, which is assumed to influence pain in OA.

REFERENCES: [1]Angrisani et al., Eur Cell Mater. 2021 Sep 28;41:179-195. doi: 10.22203/eCM.v042a14.

ACKNOWLEDGEMENTS: This work is funded by the German Research Foundation (DFG, project number 404534760).

15th Biometal
AUGUST 21 TO 27, 2023
Grand Hôtel San Michele, Cetraro, CS, Italy

In vivo assessment of magnesium-based biodegradable screw-plate implants in a large-animal cranio-maxillofacial defect model

W Rubin[1], T Akhmetshina[1], AM Rich[1], J Ross[2], D Toneatti[3], K Nuss[2], B Schaller[3], JF Löffler[1]

[1] *Laboratory of Metal Physics and Technology, Department of Materials, ETH Zurich, Zurich, CH.* [2] *Musculoskeletal Research Unit (MSRU), University of Zurich, Zurich, CH.* [3] *Department of Cranio-Maxillofacial Surgery of the University Hospital, Inselspital Bern, Bern, CH.*

INTRODUCTION: Biodegradable metallic alloys (BMAs) offer a promising alternative to permanent metallic implant materials for potential clinical use in traumatology. Lean magnesium–calcium-based alloys have been the subject of numerous studies in pre-clinical settings.[1-3] However, *in vivo* investigations on multi-component implants commonly used in clinical practice, such as screw-plate constructs, are limited, despite they are highly relevant for broad and flexible clinical applications to fully utilize the benefits of BMAs. To deepen our understanding and characterize the post-operative performance of such BMAs, we present first results of a large-animal study conducted with screw-plate implants.

METHODS: Twelve female Swiss alpine sheep were used in this study and assigned to two implantation durations of two and six months. Each animal received fully mobilized bone defects located at the calvarial and zygomatic arc regions, mechanically non- and mildly loaded cranio-maxillofacial areas, and stabilized by two different types of screw-plate implants: (i) Specifically designed plasma electrolytic oxidation (PEO)-coated Mg–Ca (X0) alloy implants, and (ii) standard titanium-based implants as reference. Post-operative follow-up and analysis included radiographic, histological, and hematological examinations. Study parameters consider bone response, fracture-gap consolidation, gas-cavity formation, blood analysis, and implant-retention potential.

RESULTS: Bone fracture-gap consolidation was delayed in the whole study population and was not radiographically detectable before six to eight and eight weeks for the Ti and Mg group, respectively. Bone-density reduction near the Mg screws was found radiographically from the second week on and confirmed by histomorphometry. In contrast, based on histology, the Mg group had twice the bone-implant contact (BIC) compared to titanium in both defect areas (*Fig. 1*). In accordance, new bone formation was higher in the Mg group, peaked for both materials in weeks four and six whereas the mildly loaded defect exhibited a generally higher bone formation activity. Equally for both defects of the Mg group the largest gas-cavity volumes occurred in weeks two and four. Both implantation sites did not differ in their gas-cavity volumes when normalized to the implant surfaces. The degradation rate was 0.24 mm/year, based on mass loss after six months of implantation. Hematological examinations showed occasionally slightly exceeding normal blood parameter ranges. For the mechanically mildly loaded defect, screw loosening occurred without leading to critical fragment dislocations.

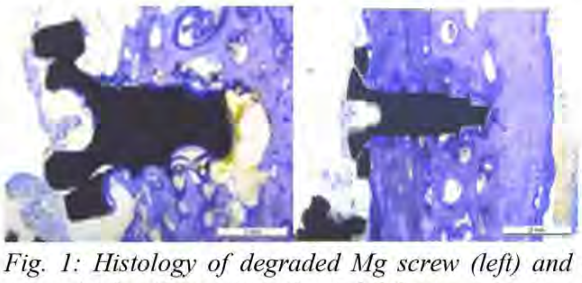

Fig. 1: Histology of degraded Mg screw (left) and Ti screw (right) (6 months, calvarial defect).

DISCUSSION & CONCLUSIONS: The delayed fracture consolidation did not affect fragment retention for both materials and groups. In general, the Ti implants revealed a stable fixation and unhindered bone formation in their surroundings. The PEO-coated bio-degrading Mg samples showed high gas formation in the early stages as well as continuous bone-tissue resorption surrounding the implants was present. The bone loss around the screws resulted in compromised anchoring, leading to occasional screw loosening and non-critical fragment dislocations in the mildly loaded area, which did not adversely impact mastication behavior. The BIC measured directly on the screw surface was considerably higher than for the Ti reference material. The hematological findings, despite a few random parameter outliers, exhibited non-critical results emphasizing the good biocompatibility of the X0 material.

REFERENCES: [1]R. Marek et al. (2023) Biomater. Adv. 150:213417. [2]P. Holweg et al. (2020) Acta Biomater. 113:646-659. [3]J. Hofstetter et al. (2014) JOM 66:566-572.

ACKNOWLEDGEMENTS: The authors gratefully acknowledge financial support from the Swiss National Science Foundation (SNF Sinergia, Grant No. CRSII5-180367) They also thank the Department of Health Sciences and Technology at ETH Zurich for its support in radiography.

Biosafety and efficacy evaluation of a biodegradable Zn-Cu-Mn-based stent in porcine Coronary Artery

Y Qian[1,2], JL Niu[1],JM Jiang[1],J Pei[1], JZ Zhu[2,*], GY Yuan[1,*]

[1]School of Materials Science and Engineering, Shanghai Jiao Tong University, Shanghai 200240, China.[2]Cardiovascular Department, Ruijin Hospital, Shanghai JiaoTong University School of Medicine, Shanghai, China

INTRODUCTION: Zn-based alloys are promising materials for biodegradable cardiovascular stents due to their good mechanical properties, degradation rate and biosafety. In this work, a novel patented Zn-Cu-Mn-based stent was implanted into porcine coronary arteries to observe the biosafety and efficacy in vivo.

METHODS: Experimental stent (Zn-Cu-Mn alloy) and commercial Co-Cr DES (Firebird2) as control group were implanted in porcine coronary arteries. Coronary angiography and OCT examination were performed, and the volume changes of scaffolds were detected by micro CT. Endothelialization was observed by SEM. Inflammation, thrombus, endothelialization and other indicators were examined by pathological exmaination.

RESULTS: Concentrations(Fig1.a) of Zn,Cu,and Mn fluctuated at different time points are all in the normal range. Angiography(Fig1.b) showed restenosis in the stent of 1m experimental group, and attenuated with time within 6 months. Blood vessels in the 12, 18m groups recovered natural curvature, suggesting partial absorption of the stent. Intimal hyperplasia was obvious in the 1m OCT groups (Fig1.c).There were no significant differences in the average lumen area, thickness and area of the new intima in later time point groups compared with the control group. Micro CT (Fig1.d) results revealed about 50% volume of the scaffolds were degraded in the 12m experimental group. SEM examination showed complete endothelial coverage of the stents in the 1, 3 and 6m groups.

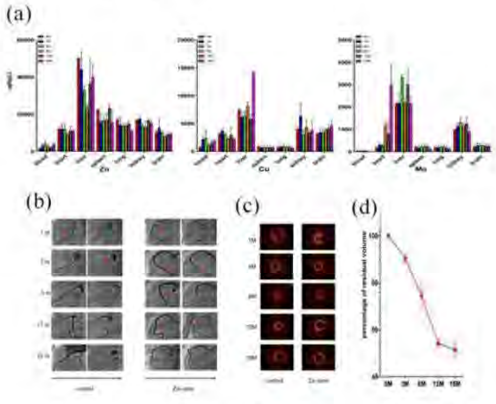

Fig1: (a)Zn,Cu,Mn element concentrations,(b,c)coronary angiography and OCT results followed-up after stent implantation,(d)percentages of residual volume of the stent calculated by microCT results.

DISCUSSION & CONCLUSIONS: The results confirmed the biosafety and efficacy of these Zn-Cu-Mn-based stents in vivo for promising application. The early inflammatory reaction was thought inducing the restenosis in scaffolds. Therefore, the combination of degradable coating materials with drug carried may be an improved method to inhibit intimal hyperplasia.

REFERENCES: [1]J Jiang, H Huang, G Yuan, et al(2022) *J Acta Biomater*,151:647-660.[2]J Jiang, Y Qian, G Yuan, et al(2022) *J Mater Sci Eng C* 112652.

ACKNOWLEDGEMENTS: This work is financially supported by the National Key Research and Development Program of China (2018YFE0115400), the National Natural Science Foundation of China (51971134, 52101290).

15th Biometal
AUGUST 21 TO 27, 2023
Grand Hôtel San Michele, Cetraro, CS, Italy

Improved fracture healing and concurrent bone-inhibitory effects from intramedullary magnesium implants: observations in a rat femoral model

Yu Sun[1], Heike Helmholz[1], Regine Willumeit-Römer[1]

[1] *Institute of Metallic Biomaterials, Helmholtz-Zentrum Hereon, Geesthacht, Germany*

INTRODUCTION: The clinical application of magnesium (Mg)-based implants for the treatment of bone fractures has been well supported by *in vitro* and *in vivo* tests [1,2]. However, there are also rational concerns for potential adverse effects on bone repair from the long-term retention of Mg and its alloys, due to the continuous release of Mg ions and related degradation products in the surgical area [3]. Moreover, *in vivo* studies are still warranted to validate the beneficial therapeutic effects of Mg implants in surgical models involving standardized fixation devices [4]. With these concerns, the authors analyzed the results from a preliminary study of Mg implantation in a rat femoral fracture model.

METHODS: External fixation devices (RatExFix, RISystem AG) were applied in Sprague-Dawley rats for the bone stabilization after osteotomy in femoral shafts. The experimental group underwent intramedullary implantation of Mg pins (1.2 mm in diameter, 5.0 mm in length) before fracture reduction, and the control group underwent fracture fixation without Mg implants. The animals' general status and local tissue reactions at the incision site were closely monitored during a 12-week follow-up. Imaging data from Micro-CT scans was analyzed for qualitative assessment of bone union and quantitative evaluation of mineralization.

RESULTS: Fixators were well tolerated in both groups after surgery, and guaranteed anatomical alignment and rotational stability of the surgical femora during follow-up (n = 7 per group). All animals in the Mg group achieved bone union at the postoperative week 12 (Fig.1a), while two non-union cases were detected in the control group (Fig.1b), showing the bone-promoting effects from Mg implants. However, the bone tissue volume in the trabecular area of distal metaphysis was lower in the Mg group compared to the control group, leading to osteoporotic-like changes associated with the local Mg implants (Fig.1c, 1d).

DISCUSSION & CONCLUSIONS: Results from this surgical model validated the beneficial application of Mg implants in promoting fracture union. However, the concurrent bone-inhibitory effects in the distal trabecular area indicated the necessity of comprehensive analyses in future research of bioactive materials for bone implants. In addition, further preclinical trials are needed to identify candidate Mg-based materials with tailored degradation properties, for controlling the potential adverse reactions without compromising the treatment outcomes.

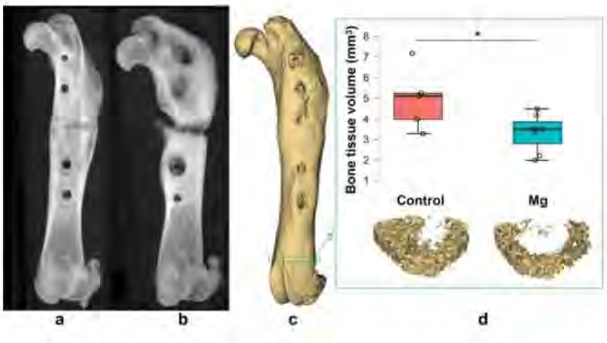

*Fig. 1: (a) 2D image reconstructed from CT scans showing fracture union at postoperative week 12 (Mg group); (b) fracture non-union at post-operative week 12 (control group) (c) 3D view of the surgical femur and distal metaphyseal region (green dotted box); (d) comparison of tissue mineral volume in the distal trabecular areas with 3D rendering (mean ± SD, 4.96 ± 1.48 vs. 3.32 ± 0.93 mm³, respectively; * P < 0.05, two-sided t-test).*

REFERENCES: [1] D. Zhao , F. Witte, F. Lu, et al (2017) *Biomaterials* **112**: 287-302. [2] Y. Zhang, J. Xu, Y.C. Ruan, et al (2016) *Nat Med* **22**: 1160-1169. [3] W. Qiao, K.H.M. Wong, J. Shen, et al (2021) *Nat Commun* **12**: 2885. [4] Y. Sun, H. Helmholz, R. Willumeit-Römer, et al (2022) *Biomater Sci* **10**: 1532-1543.

ACKNOWLEDGEMENTS: The authors express sincere thanks to: Dr. Björn Wiese, Dr. Thomas Ebel, Monika Luczak (Helmholtz-Zentrum hereon); The Central Animal Facility (ZTH) and Molecular Imaging North Competence Center (MOIN CC, Section Biomedical Imaging) at UKSH, Kiel University.

Vascular biocompatibility of Mg-Li-Y wires in the murine aorta

W He[1], K MacLeod[2], D Bow[3], M Steckel[3] , R Guillory II[1]

[1] Michigan Technological University [2]University of Strathclyde, [3]MedAlliance Ltd

INTRODUCTION: Magnesium materials have continuously been improved for bioresorbable vascular scaffolds via alloying, and material processing[1]. It is critical to evaluate vascular biocompatibility during material development, since vascular healing and resultant tissue stabilization (neointima formation) are critical to device efficacy. Here, we evaluate two novel Mg-Li-Y alloys for vascular biocompatibility and biodegradation characteristics in a murine wire implantation model.

METHODS: Mg-4Li-0.5Y (0.5Y) and Mg-4Li-2Y (2Y) alloy wires with diameters ranging from 125µm-150 µm were manufactured via standard processes. Using a well-documented wire implantation model[1], we implanted (2Y) and (0.5Y) wires within the aorta of C57Bl/6 mice for 7 (n=3), 14 (n=3), and 28 (n=3) days. Arterial sections were collected and processed for multiple imaging modalities. Frozen sections were either dehydrated in a series of ethanol baths, formalin fixed, or imaged natively (n >20 sections per sample). We evaluated the tissue sections for macrophage presence and phenotype (CD68, F4/80, iNOS), vascular cell presence and activation (alpha-SMA, vWF, CD31, VCAM), and cellular death (CC3). Samples were also prepared metallographically and imaged with SEM/EDX/BSE in order to quantify biodegradation at each time point.

RESULTS: Initial gross histological analysis shows stable neointima development with mild progression up to 28 days for the 2Y system. Upon further examination with immunofluorescent labelling, a mild amount of inflammatory cell infiltrates can be seen at 7 days (CD68+F4/80+), with no apparent smooth muscle cell proliferation(a-sma-). There is a lowly confluent endothelium (vWF+) layer surrounding the neointima. At 14 days, smooth muscle cell presence is apparent within the neointima, coupled with a reduced number of inflammatory infiltrates and a stabilized highly confluent endothelial cell layer. At 28 days, inflammatory macrophages increase in presence near the tissue material interface, smooth muscle cell proliferation subsides, and the endothelium remains confluent surrounding the neointima (Fig.1).

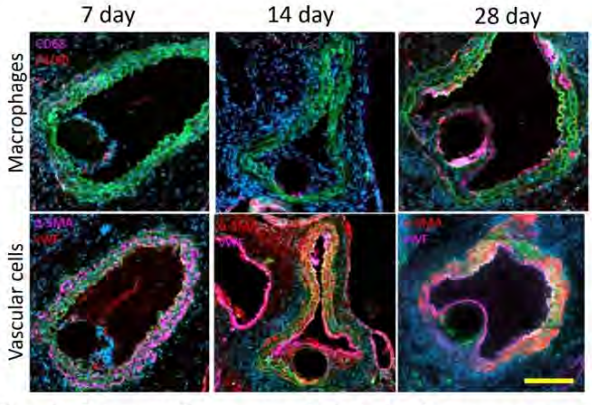

Fig. 1: Immunoflourescently labelled cryo-sections of the 2Y alloy system explanted at 7, 14, and 28 days. Top row denotes macrohpae staining using CD68 and F4/80, bottom row denotes vascular cell identification with vWF and a-SMA. Scale bar is 100 µm

DISCUSSION & CONCLUSIONS: We demonstrate for the first time the biocompatibility and biodegradation properties of the Mg-y-Li system in a murine vascular implant model. Detailed histological analysis for the 2Y system reveals a normal immunological and vascular reaction towards a bioresorbable material, wherein stabilization of the neointima takes place within 1 month. The neointima is characterized by inflammatory cells near the interface at the later time point, due to the increase in biodegradation (data not shown). The ability of the neointima to maintain a confluent endothelial cell layer during the normal initial and chronic inflammatory response demonstrates the tissue stability and biocompatibility of the 2Y material up to 28 days.

REFERENCES: [1]Oliver, Alexander A., et al. "Recent advances and directions in the development of bioabsorbable metallic cardiovascular stents: insights from recent human and in vivo studies." *Acta Biomaterialia* 127 (2021): 1-23.

Degradable magnesium and its surface modification as tumor embolic agent for transcatheter arterial chemoembolization

Xinbao Kang[1], Wenhui Wang[1], Xiaonong Zhang[1,2,*]

[1] *State Key Laboratory of Metal Matrix Composites, School of Materials Science and Engineering, Shanghai Jiao Tong University, Shanghai 200240, China.* [2] *Suzhou Origin Medical Technology Co. Ltd., Suzhou 215513, China.*

INTRODUCTION: Transcatheter arterial chemoembolization (TACE) is an effective method for traditional cancer treatment. Currently, various embolic agents block the blood vessels in the TACE operation. Our work explored the feasibility of applying degradable Mg to TACE. The degradation behavior of Mg particles and PLLA modified Mg particles used as embolic agents in contrast media was studied.

Fig. 1: Effect of degradable Mg particles as embolic agents in TACE. The degradation products of Mg can inhibit tumor, and the embolization of particles can block tumor blood supply.

METHODS: The ratio of embolic agent to contrast agent added to three beaker is 1g: 15mL. The corrosion rate of the degradable Mg particles in the contrast medium was characterized by measuring the change in pH of the contrast medium with immersion time. A small amount of Mg particles was taken out from the beaker at a particular time. After drying, the corrosion morphology was photographed by the scanning electron microscope with EDS (SEM, Rise). Two groups of samples soaked in the contrast medium were selected for testing.

RESULTS: The degradation behavior of Mg and PLLA-modified Mg in the contrast agent indicates that the corrosion mechanism in the contrast agent is different from that in simulated body fluid. Mg reacts with water in the contrast agent to generate $Mg(OH)_2$ and first releases H_2. Due to the viscosity of the contrast agent, the generated Mg(OH)2 will be evenly attached to the surface of the Mg particles to form a passive film. With the progress of corrosion, the water in the contrast medium gradually decreased, and the $Mg(OH)_2$ shell cracked due to Cl^- attacking. Subsequently, ioversol in the contrast agent decomposes due to light or other conditions and slowly releases element I, which exists in the solution as ion. These released I^- may dissolve the $Mg(OH)_2$ shell on the surface of the Mg particles and further react to form MgI_2. The mechanism at this stage is similar to the dissolution of $Mg(OH)_2$ by Cl^-.

After surface modification, the PLLA coating on the surface of the Mg particles is corroded by the contrast agent. The generated small molecule lactic acid will combine with amino butanol in the contrast agent and adhere to the surface. When PLLA is corroded and the Mg surface is exposed to the contrast agent, the corrosion reaction of Mg and water occurs, forming a $Mg(OH)_2$ shell and releasing H_2. Subsequently, the corrosion reaction continued. However, as the adsorption process of anion to the Mg matrix is hindered by the PLLA coating, the $Mg(OH)_2$ film's dissolution by I^- is weakened, and the degradation rate is slowed down.

DISCUSSION & CONCLUSIONS: Unmodified pure Mg has a high degradation rate because the contrast agent can decrease the protectiveness of the degradation layer. At the same time, the consumption of I will also lead to a decrease in the effectiveness of the contrast agent itself, which means that a pure Mg is not suitable for TACE. The PLLA-modified Mg can sustain a slow degradation rate within at least 48 h in contrast medium, which effectively reduces the consumption of I and also forms a suitable microenvironment with Mg^{2+} and H_2 release. These findings contribute to broadening the clinical application of biodegradable Mg in the future.

REFERENCES: [1] X.B. Kang, Y.G. Wang, H.T. Li, et al (2023) *J Crystals* **13** (2):194.

ACKNOWLEDGEMENTS: This research was funded by Changshu Science and Technology Program (Industrial) Project (No.CG202107).

Tissue plasminogen activator-loaded magnetoacoustic discoidal polymeric particles for thrombolysis

Wonseok Choi[1,2], Hyeyoun Cho[2], Inchan Youn[1,3], Jaehong Key[2], Sungmin Han[1,3,*]

[1] *Biomedical Research Division, Korea Insititute of Science and Technology (KIST), Republic of Korea*
[2] *Department of Biomedical Engineering, Yonsei University, Republic of Korea*
[3] *Divison of Bio-Medical Science & Technology, KIST School, Republic of Korea*

INTRODUCTION: Thrombosis is a blockage of a blood vessel caused by an undesirably expressed blood clot. Recombinant tissue plasminogen activator (rtPA) is one of the available thrombolytic agents in the clinical field. However, the potentially dangerous nature of the drug has limited its utilization, such as rigid restrictions on time-delayed administration and the perilous potential for hemorrhagic transformation. Recent advances in nanomedicine have granted drug delivery systems the ability to transfer types of protein drugs. Thus, we hypothesized that these limitations of the drug could be managed by particles synthesized through a top-down fabrication method. In this work, we developed rtPA-loaded magnetoacoustic discoidal polymeric particles capable of physically targeting and controlling drug release by magnetic and acoustic stimuli, respectively. More detailed characteristics of the magnetoacoustic particles are presented in this abstract.

METHODS: The fabrication of magnetoacoustic particles has been conducted by a lithography-based top-down fabrication method, well described elsewhere[1,2]. The overall components of magnetoacoustic particles, such as superparamagnetic iron oxide nanoparticles (SPIONs), rtPA, and poly(lactic-co-glycolic) acid (PLGA), have been loaded into the hydrophilic disposable poly(vinyl alcohol) (PVA) film. The PVA film loaded with the overall materials was dissolved into distilled water to release the magnetoacoustic particles in the distilled water. The particles were purified using μm-sized pore filtration and subsequently subjected to freeze-drying. The formulations were characterized by energy-dispersive X-ray spectroscopy (EDS), scanning electron microscopy (SEM), microscopic imaging, and recruiting potential toward an external magnet.

RESULTS: The shape of synthesized magnetoacoustic particles was a disc, which was the same as the silicon master template utilized in our top-down fabrication (**Fig. 1a-b**). The EDS analysis indicated the presence of sulfur (S) and iron (Fe) elements in the formulation, although only a small amount of both elements were detected in the spectrum (**Table 1**). The recruiting of particles toward the vertical magnetic field successfully occurred along with time (**Fig. 1c**).

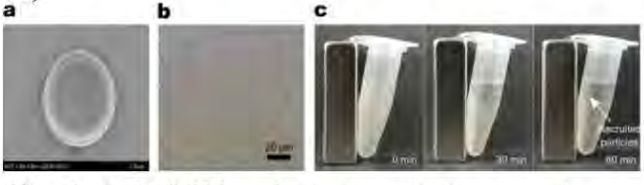

***Fig. 1**: **(a,b)** SEM and microscopic images of magnetoacoustic particles. **(c)** Recruiting particles toward the external magnet along with time.*

***Table 1**. Quantitative results of EDS analysis of magnetoacoustic particles (n=3)*

Element	Line series	Wt%(mean±SD)
Carbon (C)	K	81.3±3.2
Oxygen (O)	K	16.4±2.8
Iron (Fe)	K	1.7±0.6
Sulfur (S)	L	0.8±0.2

DISCUSSION & CONCLUSIONS: Our preliminary results suggest incorporating SPIONs and rtPA into the polymeric structure using a top-down procedure is feasible. The magnetoacoustic particles can be applied to time-sensitive thrombotic diseases, such as ischemic stroke, coronary infarction, and pulmonary embolism, using a physically targeted and controlled release mechanism.

REFERENCES:

[1] Key, J. *et al.* Soft discoidal polymeric nanoconstructs resist macrophage uptake and enhance vascular targeting in tumors. *ACS nano* **9**, 11628-11641 (2015).

[2] Park, J. Y. *et al.* Biodegradable micro-sized discoidal polymeric particles for lung-targeted delivery system. *Biomaterials* **218**, 119331 (2019).

ACKNOWLEDGEMENTS: This work was supported by the Technology Innovation Program (20014477) funded by the Ministry of Trade, Industry & Energy (MOTIE, Korea)

15th Biometal
AUGUST 21 TO 27, 2023
Grand Hôtel San Michele, Cetraro, CS, Italy

Novel in-situ elemental imaging of bioabsorbable metal vascular implants

K MacRenaris PhD [1], W He PhD[2], A Gillette PhD [4] T O'Halloran PhD [1], R Guillory II PhD[4]
[1]Quantitative Bio-Elemental Analysis and Mapping Center (QBEAM) in the Michigan State University Elemental Health Institute [2]Michigan Technological University [3]Morgridge Research Institute [4]Medical College of Wisconsin

I. Introduction

A major challenge in understanding bioabsorbable metal biocompatibility is the lack of information regarding in situ local implant derived metals, and their subsequent cellular/ tissue fate and concentration. In collaboration with the QBEAM (Quantitative Bio Element Analysis and Mapping) facility located within the Elemental Health Institute at Michigan State University, we sought to describe in a qualitative and semi-quantitative fashion, the local distribution and concentration of Mg implant derived metals within vascular tissue.

II. Methods

A. *Wire implantation*

WE22 wires (manufactured by Fort Wayne Metals, 100µm diameter) were implanted into the abdominal aorta of three, 6-month-old APOE-/- transgenic mice (Charles River Laboratories) using methods previously described elsewhere. Implants were extracted at 30 day time points.

B. *Sample preperation and elemental imaging*

The vascular tissue containing the wire was collected after euthanasia by cutting the proximal and distal ends of the aorta-vena cava bundle. The tissue was placed into cryomolds and surrounded by OCT media and snap frozen in liquid nitrogen. Samples were cryo-sectioned with a HM525 cryomicrotome at -20 °C, and warm collected onto Histobond slides. After the warm collection, samples were immediately frozen and stored at -80 °C for further processing. Cryo-sections were warmed to room temperature and immediately exposed to -20 °C cold 200 proof ethanol for 30 seconds. Sections were dried in a fume hood overnight. Tissue sections were scanned with a custom LA-ICP-TOF-MS system at the QBEAM center (2 µm - 4µm circular laser spot size), and scans were calibrated against concurrently scanned custom mixed element spiked gelatin standards.

III. Results & Discssussion

The explanted wire- artery samples were evaluated for implant derived metal distribution via elemental imaging via LA-ICP-TOF-MS. Mg was found distributed in the adventitial portion of the artery, away from the original implant location. Y and Nd, alloying elements in WE22 were found distributed within the neointima and sparsely in the adventitial portion of the artery as well. We semi-quantitatively describe a decreasing gradient of Mg (max values >/= 2000 ppm) and Y/ Nd (max values >/=20ppm) away from the implant interface.

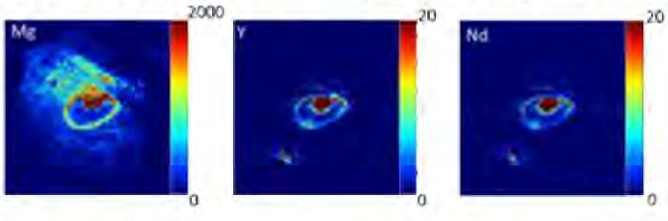

Fig.1. Semi-quantitative LA-ICP-TOF-MS scans of tissue sections containing WE22 wire implanted within the abdominal aorta of APOE-/- mice for 30 days. Maps for Mg, Y, and Nd are shown, with heat bar scale in ppm.

While our semi-quantitative scans have given insight into element distribution surrounding bioabsorbable wires in vascular implants, more work is needed to further characterize the elemental maps. Critically, multiple cross sections will need to be evaluated to determine precise concentration values of elements within the tissue. Additionally, the speciation of the observed elements is not determined with this technique. Future work must clarify the species in relation to the element present, to differentiate the variety of corrosion products from implant derived cations bound to tissue/ proteins.

IV. Conclusions

We have successfully demonstrated the feasibility of measuring the local in situ elemental distribution within soft tissues with high resolution and high sensitivity. More work is needed to further explore the information provided by semi-quantitative elemental mapping.

Acknowledgments

We would like to thank Fort Wayne Metals for providing the WE22 wire used in this study We would like to thank Dr. Erico Freitas for his assistance in obtaining S-TEM images and spectra, and the ACMAL facility at MTU. This work was partially funded by R15HL16722

the important role of degradable magnesium metal in mediating subperiosteal osteogenesis through the bone immune microenvironment

LW Chen[1], JH Zhu[1], JM Han[1], CB GUO[1]

[1] *Peking University School and Hospital of Stomatology*

INTRODUCTION: Biodegradable magnesium metal has a positive effect in promoting bone formation, but the underlying mechanism is still unclear. This study aims to further explore the important role of magnesium metal in promoting subperiosteal osteogenesis through the bone immune microenvironment.

METHODS: In this study, MgZn alloy nails were implanted in the distal femur of mice to induce subperiosteal osteogenesis. The increase of the bone volume was confirmed by Micro-CT and HE and Masson's staining. The changes in the bone immune microenvironment were analyzed through a combination of transcriptome and proteomic analysis and confirmed by immunofluorescence, flow cytometry, and RT-PCR. Periosteum stripping and macrophage depletion were conducted to confirm the critical effect of macrophages and periosteum stem cells.

Moreover, the co-culture of magnesium alloy and macrophages in vitro was used to confirm the immunoregulatory effect of magnesium alloy. Finally, the osteogenic role of periosteum stem cells induced by macrophage-conditioned medium stimulated by magnesium alloy was identified.

RESULTS: Micro-CT and Histological staining confirmed that the cortical bone volume was significantly increased after magnesium alloy implantation. Immunofluorescence and flow cytometry results showed a significant increase of F4/80+ macrophages and CD51+ periosteal osteoblasts, with no significant changes in the number of lymphoid immune cells. Both the periosteum stripping and macrophage depletion significantly inhibited new bone formation induced by magnesium alloy. Additionally, in vitro studies demonstrated that co-culturing magnesium alloy with macrophages led to an increase in intracellular magnesium ion concentration and induced M2-type polarization, accompanied by the increase of secretion of the anti-inflammatory cytokines. Cultivating periosteum stem cells with macrophage conditioned medium stimulated by magnesium alloy resulted in an elevation of key osteogenic gene expressions such as Postn and RUNX2, thereby enhancing osteogenic differentiation of periosteum stem cells

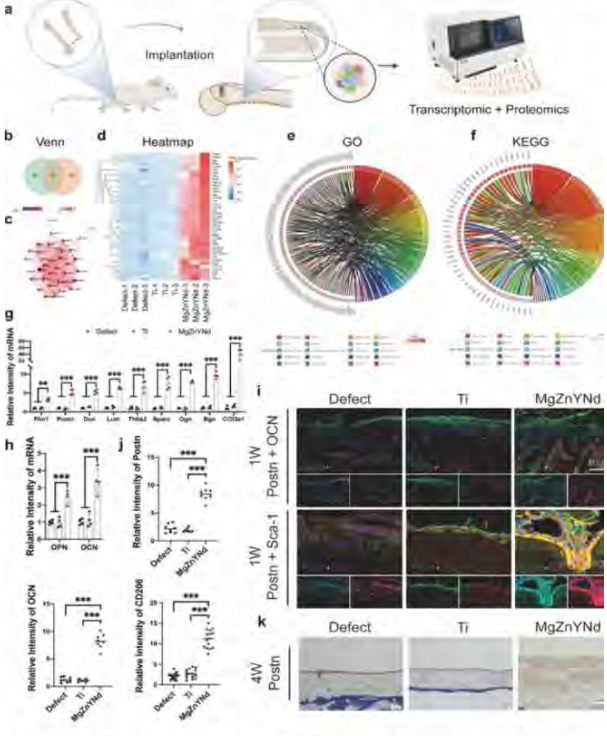

Fig. 1: The combined analysis of transcriptomics and proteomics of osteogenesis microenvironment stimulated by biodegradable magnesium alloy.

DISCUSSION & CONCLUSIONS: Biodegradable magnesium metal can induce obvious subperiosteal osteogenesis. Magnesium led to an increase in macrophage quantity and M2 polarization in the immune microenvironment. After polarization, macrophages may induce significant subperiosteal osteogenesis through the secretion of anti-inflammatory and osteogenic cytokines which promoting the osteogenic differentiation of periosteum-derived stem cells.

REFERENCES: [1] Zhang Y, Xu J, Ruan YC, et al (2016) *Nat Med* 22(10):1160-1169. [2] Qiao W Wong KHM, Shen J, et al (2021) *Nat Commun* **12**(1):2885.

ACKNOWLEDGEMENTS: This work was supported by National Key Research and Development Program of China (2021YFC2400703).

Introducing nanoporous metallic membranes for improved stem cell delivery and function: A collection of in vitro and in vivo studies

TJ Webster[1-5], B Steelman[1], J Davis[1], B Henneman[1], and J Lakey[6]

[1]NanoVault, Minneapolis, MN, USA. [2]School of Health Sciences and Biomedical Engineering, Hebei University of Technology, Tianjin, China. [3]Program in Materials Science, UFPI, Teresina, Brazil. [4]School of Engineering, Saveetha University, Chennai, India. [5]Division of Pre-College and Undergraduate Programs, Brown University, Providence, RI USA. [6]Depeartment of Veterinary Science, University of California at Irvine, Irvine, CA, USA.

INTRODUCTION: Polymer-based capsules have been used as the standard of care for 30+ years for stem cell delivery to the body to treat numerous diseases. However, polymer capsules used for stem cell delivery and function have proven problematic due to a lack of neovascularization bringing nutrients to the cells and removing cellular waste. Likewise, they have been shown to be highly bio-incompatible as they trigger an untoward inflammatory response that clogs the capsule through-pores necessary for cell survival.

METHODS: This study introduces a new classification of materials for improved stem cell delivery and function: biodegradable and non-biodegradable metal nanometer through-porous membranes. In this study, precise complete through nano-sized pores were created in several known medical grade metals (such as Ti, stainless steel, and MgO). Some were further modified to possess a nanoscale topography to promote neovascularization and inhibit inflammation.

Such materials were tested in vitro for the diffusion of insulin and IgG, macrophage response, endothelial cell function, degradation and mechanical stability. Impressively, the optimal through-porous nanometal was tested using a well established sub-cutaneous rat model.

RESULTS: Results of this study demonstrated the ability to create through-pores in any of the aforementioned metals nanometer in size to selectively promote or inhibit insulin or IgG passage, respectively (Figure 1).

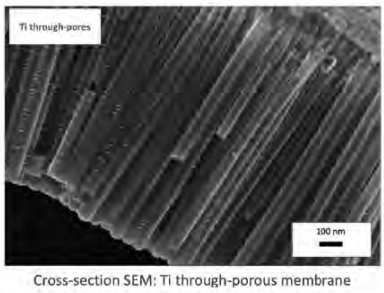

Fig. 1: SEM image of through-porous nanometals.

In vitro, these metals were shown to inhibit inflammation and promote neovascularization. Additionally, we have demonstrated the selective release of insulin analogs (for diabetes applications) while restricting the passage of IgG (which initiate an inflammatory response). Due to their nanoscale pore size, complete inhibition of IgG adsorption and infiltration was measured in "tailored" nanophase porous metal membranes. The size of the nanopores can be precisely controlled to selectively promote or inhibit the passage of numerous biomolecules.

Impressively, in vivo, such through-porous nanometals were shown to significantly improve new blood vessel formation with reduced inflammation imperative for maintaining viable stem cells for delivery and use (Figure 2).

Fig. 2: In vivo increased new blood vessel formation surrounding through-porous nanometals. ViaCyte is an FDA approved polymer stem cell delivery device.

DISCUSSION & CONCLUSIONS: This study introduces a brand new classification of materials, through-porous nanometals, for improved stem cell delivery and function. It demonstrated superiority over traditional polymer stem cell delivery materials through in vitro and in vivo studies.

ACKNOWLEDGEMENTS: This collection of studies was financially supported by NanoVault, Inc.